

DIFFUSION IN CONCENTRATED URANYL NITRATE
SOLUTIONS

By

JOHN BROWNING FINLEY

Bachelor of Science
University of Southwestern Louisiana
Lafayette, Louisiana
1941

Bachelor of Science in Chemical Engineering
University of Southwestern Louisiana
Lafayette, Louisiana
1942

Master of Science
University of Southwestern Louisiana
Lafayette, Louisiana
1960

Submitted to the Faculty of the Graduate School of
the Oklahoma State University
in partial fulfillment of the requirements
for the degree of
DOCTOR OF PHILOSOPHY
May, 1964

OKLAHOMA
STATE UNIVERSITY
LIBRARY

JAN 5 1965

DIFFUSION IN CONCENTRATED URANYL NITRATE
SOLUTIONS

Thesis Approved:

John B. West

Thesis Adviser

R. N. Madsen

K. D. Bell

John E. Moore

J. H. Boyer
Dean of the Graduate School

569544
ii

ACKNOWLEDGEMENT

To Dr. John B. West I shall always extend my warmest admiration for the patience, understanding, and unobtrusive skill he constantly demonstrated in guiding me through the educational preparation and the experimental work that was necessary to make this thesis possible. Dr. R. N. Maddox, Dr. K. J. Bell, Dr. T. E. Moore, and Professor Herbert Scholz, Jr., as members of my advisory committee, are thanked for their frequent encouragement and help when it was needed most.

It is a pleasure to acknowledge the assistance of a number of persons. Professor Paul McCollum, Mr. Buck Brown, and Mr. Richard Tinnell contributed much in the way of electronic know-how that made the analytical work successful. To Mr. Pat Moore, Director of the Operations Division, Continental Oil Company, Ponca City, Oklahoma and members of his staff goes my appreciation for making the IBM 7090 computer available for calculations. The cooperation and mechanical skill of Mr. Eugene McCroskey, of the School of Chemical Engineering, is gratefully acknowledged. Many of my fellow graduate students contributed knowingly or unknowingly to the project. Dale Bush, Robert Robinson, and Lyman Yarborough contributed more than their fair share.

I wish to acknowledge and express my appreciation for the financial support of the Atomic Energy Commission, under Contract AT(11-1)-846, during the three years of graduate study and experimental work.

The greatest debt of gratitude is owed to my wife, Kitty, and

the children. To the children for their endurance and willingness during these lean years and to Kitty for the personal sacrifices she made, for the constant encouragement she gave, and for the many reams of typing she has produced. Always, she was a bright light of hope and cheer in an otherwise dark and dreary world.

TABLE OF CONTENTS

Chapter	Page
I. INTRODUCTION	1
II. THEORY	4
III. EXPERIMENTAL APPARATUS	17
Diffusion Cells	17
Capillaries	21
Scintillation Equipment	23
Constant Temperature Bath	26
IV. EXPERIMENTAL PROCEDURE	29
V. RESULTS AND DISCUSSION	32
Internal Liquid Scintillation	32
Diffusion of Uranyl ion into Water	47
Uranyl Nitrate Diffusing into Nitric Acid	74
Uranium Diffusion into 30% TBP-Amsco	75
VI. CONCLUSIONS AND RECOMMENDATIONS	81
Conclusions	81
Recommendations	83
SELECTED BIBLIOGRAPHY	84
APPENDIX A	88
Experimental Data	89
Analyses of Variance	99
APPENDIX B	115
Calibration of Capillaries and Micro-Syringe	116
Viscosity Determinations of Solutions Used	117
APPENDIX C	122
Calculated Quantities	123
Digital Computer Programs	135
Sample Calculations	139

LIST OF TABLES

Table	Page
I. Integral and Differential Scintillation Spectrum Data for 2 Molar Uranyl Nitrate (Primary Solvent = 50:50 Xylene-Toluene)	40
II. Summary of Uranyl Nitrate Diffusing into Water	48
III. Final Least Means Square Regression Fit of Diffusion Coefficient as a Function of Concentration	54
IV. Comparison of Experimental Calculated Results Uranyl Nitrate Diffusing into Water	59
V. Thermodynamic Correction Factor as a Function of Uranyl Nitrate Concentration (Smoothed values)	62
VI. Thermodynamic-Corrected Integral Diffusion Coefficient as a Function of Uranyl Nitrate Concentration	63
VII. Thermodynamic-Corrected Differential Diffusion Coefficient as a Function of Uranyl Nitrate Concentration	65
VIII. Uranyl Nitrate Concentration Distribution in Capil- lary as a Function of Time (Course Grid Numerical Solution) $C_0 = 2.0$ M	67
IX. Uranyl Nitrate Concentration in Capillary as a Function of Time (Course Grid Numerical Solution) $C_0 = 0.05$ M	69
X. Final Uranyl Nitrate Concentration Distribution in Capillary (Numerical Solution)	71
XI. Summary of Diffusion Data on Uranyl Nitrate Diffusing into Nitric Acid	76
XII. Summary of Experimental Data Uranyl Nitrate Diffusing into Nitric Acid	80
XIII. Differential Scintillation Spectrum Data for Uranyl Nitrate (Primary Solvent-Toluene)	89

Table	Page
XIV. Differential Scintillation Spectrum Data for Uranyl Nitrate (Primary Solvent-Xylene)	90
XV. Differential Scintillation Spectrum Data for Uranyl Nitrate (Primary Solvent 50:50 Xylene-Toluene) .	91
XVI. Differential Scintillation Spectrum Data for Ra D-E-F (Po-210)	92
XVII. Differential Scintillation Spectrum Data for Po-210-U-238 Mixture	93
XVIII. Differential Scintillation Spectrum Data for 1.0 Molar Uranyl Nitrate	95
XIX. Experimental Data-Uranyl Nitrate Diffusing into Water	96
XX. Analysis of Variance Randomized Complete - Block Design Uranyl Nitrate into Water	99
XXI. Analysis of Variance Randomized Complete - Block Design Uranyl Nitrate into Water (Low concentrations) .	100
XXII. Analysis of Variance Randomized Complete - Block Design Uranyl Nitrate Diffusing into 2.0 M Nitric Acid	101
XXIII. Analysis Variance Randomized Complete - Block Design Uranyl Nitrate Diffusing into 1.0 M Nitric Acid	102
XXIV. Analysis of Variance Randomized Complete - Block Design Uranyl Nitrate Diffusing into 0.5 M Nitric Acid	103
XXV. Analysis of Variance Randomized Complete - Block Design Uranyl Nitrate Diffusing into 0.1 M Nitric Acid	104
XXVI. Experimental Data Uranyl Nitrate Diffusing into Nitric Acid	105
XXVII. Experimental Data-Data from Diffusion of Uranyl Nitrate into 30% Tributyl Phosphate-Amsco Mixture . . .	110
XXVIII. Experimental Data-Effect of Strontium on Diffusion of Uranium	112
XXIX. Average Liquid Scintillation Counting Rate as a Function of Uranium Concentration	114

Table	Page
XXX. Calibration of 0.50 mm Bore Capillary Measurements made at 25 °C	116
XXXI. Calibration of 0.75 mm Bore Capillary Measurements made at 25 °C	117
XXXII. Calibration of Hamilton 10 Lambda Micro-Syringe	118
XXXIII. Viscosities of Solutions	119
XXXIV. Data for Least Mean Square Regression of Liquid Scintillation Integral Counting Rate as a Function of Uranium Concentration	123
XXXV. Uranyl Nitrate Activity Coefficients Conversions	127
XXXVI. Thermodynamic Correction Factor as a Function of Uranyl Nitrate Concentration (Coarse Grid)	129
XXXVII. Thermodynamic Correction Factor as a Function of Uranyl Nitrate Concentration (Fine Grid)	130
XXXVIII. Sample of Formal Solution Output Table	138

LIST OF FIGURES

Figure	Page
1. Uranium Decay Schemes	25
2. Differential Scintillation Spectrum for Uranyl Nitrate (Primary Solvent-Toluene)	34
3. Differential Scintillation Spectrum for Uranyl Nitrate (Primary Solvent-Xylene)	35
4. Differential Scintillation Spectrum for Uranyl Nitrate (Primary Solvent 50:50 Xylene-Toluene)	36
5. Differential Scintillation Spectrum for Uranium-U-238 and Radium D-E-F	38
6. Differential Scintillation Spectrum for Uranium and Ra-D-E-F Mixture	39
7. Integral and Differential Scintillation Spectrum of 2.0 M Uranyl Nitrate as a Function of Energy Level (Primary Solvent 50:50 Xylene-Toluene)	41
8. Integral Liquid Scintillation Count Rate as a Linear Function of Uranium Concentration (Lower range)	43
9. Integral Liquid Scintillation Count Rate as a Linear Function of Uranium Concentration (Upper range)	44
10. Integral Diffusion Coefficient of Uranyl Nitrate into Water as a Function of Concentration (Constant D)	50
11. Differential Diffusion Coefficient of Uranyl Nitrate into Water as a Function of Concentration	55
12. Thermodynamic-Corrected Integral Diffusion Coefficient of Uranyl Nitrate into Water as a Function of Concentration	64
13. Thermodynamic-Corrected Differential Diffusion Coefficient of Uranyl Nitrate as a Function of Concentration	66
14. Concentration in Capillary as a Function of Time (Initial Concentration = 2.0 M)	68

Figure	Page
15. Concentration in Capillary as a Function of Time (Initial Concentration = 0.05 M)	70
16. Concentration in Capillary as a Function of Time Fine Grid Numerical Solution (Initial Concentra- tion = 2.0 Molar)	72
17. Integral Diffusion Coefficient of Uranyl Nitrate into Nitric Acid as a Function of Concentration	77
18. Integral Diffusion Coefficient of Uranyl Nitrate into Nitric Acid as a Function of Concentration (Continued)	78
19. Viscosity as a Function of Concentration (Uranyl Nitrate)	121
20. Activity and Activity Coefficient of Uranyl Nitrate as a Function of Molar Concentration	128
21. Thermodynamic-Correction Factor as a Function of Uranyl Nitrate Concentration	131
22. Computer Flow Diagram for Numerical Solution of Fick's Second Law	144

LIST OF PLATES

Plate	Page
I. Capillary Diffusion Cell	18
II. Diffusion Capillaries in Holder	20
III. Diffusion Cells Installed in Constant Temperature Bath	22
IV. Internal Sample Liquid Scintillation Counting Equipment	27

CHAPTER I

INTRODUCTION

In all the mass-transfer operations, molecular diffusion occurs in at least one phase and often in more than one phase. A knowledge of liquid diffusion coefficients is required for the calculation of mass-transfer rates across the liquid films in distillation, extraction, chemical reaction, and mixing. The available diffusivity correlations for dilute solutions of nondissociating solutes are satisfactory when accuracy is not too important (15, 16, 17, 58). However, the existing methods for the correlation of diffusivities in concentrated electrolyte solutions have not been verified experimentally (22).

The science of solutions is very complex. It has evolved its own numerous experimental methods and has required for its clarification many branches of mathematical physics, such as thermodynamics, statistical mechanics, electrostatics, and hydrodynamics. A great deal has been achieved by theory, but this achievement has been by no means enough to warrant the neglect of further experimental investigation. In particular, a complete understanding of the diffusion phenomena occurring with electrolytic solutions has been impeded by the lack of sufficient experimental data with which to test and study the variously proposed correlations.

This thesis presents the results of an experimental investiga-

tion that was initiated to measure and study the molecular diffusion coefficients of a concentrated ionic electrolyte by the capillary cell technique. Robinson and Stokes (47) have reviewed briefly the most widely accepted methods for determining molecular diffusion coefficients in ionic systems. Diaphragm cells, capillary cells, conductimetric diffusion cells, and optical free diffusion cells seem to predominate.

The capillary cell method employs extremely small volumes (i.e. from 4 to 50 μ) which complicates ordinary chemical analyses of the samples. In recent years, the capillary cell technique has received increasing use as a result of the availability of radioisotopes and of sufficiently accurate apparatus for radiometric assays. The method was introduced by Anderson and Saddington (2), and improved by Wang (54, 55, 56, 57) and by Mills and Kennedy (34). It has been used extensively for determining self- and tracer diffusion coefficients of electrolytes. The simplicity of the capillary cell technique coupled with the shorter diffusion times inherent with the method recommended its use in this study.

The decision to use liquid scintillation counting was made after a thorough study of the literature concerning uranium analyses. The internal-sample liquid scintillation would eliminate the self-absorption corrections necessary in alpha-proportional counting. The method would require less sample handling in preparation for counting and the samples could be readied for counting much more rapidly. A routine method of analysis by internal-sample liquid scintillation employing 4 to 10 μ samples was developed as part of the investigation.

The mutual diffusion coefficients of 0.05 to 2.0 molar uranyl nitrate solutes diffusing into water solvents were obtained and the values reported. A numerical methods solution of Fick's Second Law, allowing the diffusion coefficient to be concentration dependent, was also applied to the experimental results. These calculated diffusion coefficients and the dependence of D on concentration were studied in the light of the Nernst-Hartley expression as corrected by Onsager and Fuoss.

A brief study was made of the effect of the nitrate ion on the diffusion of the uranyl ion. In these experiments, uranyl nitrate solutions as solutes were allowed to diffuse into nitric acid solutions as the solvents. The effect of the nitrate ion in the solvent was to reduce the diffusion rate of the uranyl ion as the nitrate ion concentration of the solvent was increased.

A study was made of two solutes consisting of a mixture of uranyl nitrate in 30% TBP-Amsco diffusing into a solvent of 30% TBP-Amsco solution with 2.0 M uranyl nitrate. The uranyl ion concentration of the resulting solute was found to be 0.454 M with respect to uranium. A second solute was prepared by dilution of the 0.454 M solute to obtain an uranium ion concentration of 0.10 M. Although a slight difference in the diffusion rates was noted, a statistical analysis of the data revealed that the measured difference was within the error of the experimental procedure and could not be considered significant.

CHAPTER II

THEORY

If a binary system of two miscible liquids contains local differences in concentration, a driving force is present which tends to eliminate these differences. Although the exact nature of the driving force is unknown, many theories have been developed to explain the phenomenon mathematically. This mass transport process which is called diffusion was compared to conductive heat transfer in 1855 by Fick who introduced the equation

$$J = -D(dC/dx) \quad (1)$$

for one dimensional diffusion. J , a vector quantity, is the flux or amount of one component crossing a plane of unit cross sectional area in unit time; dC/dx is the concentration gradient of the same component in the direction of the flux; and D is the proportionality constant called the diffusion coefficient. A negative sign is applied to indicate that the direction of diffusion is always opposite to an increasing (designated positive) concentration gradient.

Although, in practice, experimental conditions are often chosen so that D is nearly constant, it is not defined as a constant. The variation of D with concentration is frequently the effect of most interest. In fact the main importance of diffusion studies for electro-

lyte theory lies in the variation of the quantity D with concentration.

Equation 1 is of importance in the study of diffusion by steady-state methods in which the concentration-gradient dC/dx does not change with time. In most experimental methods currently in use, however, the variation of C with both time and distance is studied. For these cases, Equation 1 can be converted into a second-order partial differential equation connecting C , x , and the time, t , by the application of the equations of continuity to a differential volume-element normal to the x -axis (16). Consider the element of volume to be differentially small with sides Δx , Δy , and Δz units in length. According to Fick's First Law, Equation 1, the flux per unit area through the left face in the x direction can be expressed as

$$J_x = -D(\partial C/\partial x)$$

or for the area whose dimensions are Δy , Δz

$$J_x = -D(\partial C/\partial x)\Delta y\Delta z.$$

The value of the flux flowing out of the volume through the opposite face can be obtained by expanding J_x in a Taylor series and retaining only the first two terms as a reasonable approximation.

$$J_x + \Delta x = J_x + \frac{\partial}{\partial x} (J_x)\Delta x + \dots$$

The net flow by diffusion in the x direction is the difference of these two expressions

$$J_x - J_x + \Delta x = \frac{\partial}{\partial x} (D\partial C/\partial x) \Delta x\Delta y\Delta z \quad (2)$$

The net quantity flowing represents the concentration that must be stored in the elemental volume. This time rate of change in the concentration in the differential volume element can be expressed as

$$\Delta x \Delta y \Delta z \frac{\partial C}{\partial t}.$$

Equating the two quantities and dividing both sides by $\Delta x \Delta y \Delta z$ results in

$$\frac{\partial C}{\partial t} = \frac{\partial}{\partial x} \left(D \frac{\partial C}{\partial x} \right) \quad (3)$$

for one-dimensional diffusion, where D may be a function of x and C . Equation 3 is known as Fick's Second Law of diffusion.

In those instances where the diffusion coefficient, D , is a constant, Equation 3 becomes

$$\frac{\partial C}{\partial t} = D \frac{\partial^2 C}{\partial x^2} \quad (4)$$

Fick's relations are valid for a two-component system provided that there is no volume change on mixing (36, 47). In the derivation outlined above, the elemental volume was considered to be constant, and therefore, the dimensions of the volume could be referred to those of the apparatus. If a volume change occurs during the mixing of the solute and solvent, the elemental volume changes with respect to concentration and thus the dimensions of the volume are concentration dependent. In order to allow the dimension Δx , in the case of one dimensional diffusion, to remain constant, the reference frame for the dimensions must be changed. The choice of a reference frame is arbitrary and a matter of convenience in most cases. There are several possibilities discussed by Hartley and Crank (23). Bird, Stewart, and Lightfoot (7) show the derivations of the alternate reference frames for diffusion when there is a change in partial volumes

on mixing. Olander(36) presents an additional method to be applied in such cases. He concludes that for most binary liquids the effect of volume changes on mixing are too small to alter appreciably the diffusion coefficients measured in diaphragm cells or by the capillary cell technique. However, there are exceptions and each system should be examined for possible volume changes on mixing before the diffusion study is undertaken.

A standard method of obtaining a solution of the partial differential Equation 4 is to assume that the variables are separable (10, 48). We may assume that C can be expressed as a product of separate functions of x and t only,

$$C = X(x) T(t).$$

Substitution in Equation 4 yields

$$X \frac{dT}{dt} = DT \frac{d^2X}{dx^2}$$

which may be rewritten

$$\frac{1}{T} \frac{dT}{dt} = \frac{D}{X} \frac{d^2X}{dx^2}$$

We have on the left-hand side an expression depending on t only, while the right-hand side depends on x only. Both sides must therefore be equal to the same constant which, for convenience in the subsequent algebra, is taken as $-k^2D$. Two ordinary differential equations result:

$$\frac{1}{T} \frac{dT}{dt} = -k^2D$$

and

$$\frac{1}{X} \frac{d^2 X}{dx^2} = -k^2$$

of which solutions are

$$T = \exp(-k^2 Dt)$$

$$X = A \sin kx + B \cos kx,$$

leading to a solution of Equation 4 of the form

$$C = (A \sin kx + B \cos kx) \exp(-k^2 Dt) \quad (5)$$

where A and B are constants of integration. Since Equation 4 is a linear equation, the most general solution is obtained by summing solutions of type 5, so that

$$C = \sum_{m=1}^{\infty} (A_m \sin k_m x + B_m \cos k_m x) \exp. (-k_m^2 Dt)$$

where A_m , B_m , and k_m are determined by the initial and boundary conditions for any particular problem.

In the capillary method, the boundary conditions for a tube closed at $x = 0$ and open at $x = \ell$ are:

$$\text{At } t = 0, C = C_0 \text{ for } 0 < x < \ell, C = 0 \text{ for } x > \ell$$

$$\text{At } t > 0, C = 0 \text{ at } x = \ell \text{ and } \frac{\partial C}{\partial x} = 0 \text{ at } x = 0.$$

These conditions can be satisfied only if $k = \frac{2n+1}{2}\pi$, where $2n+1$ has been substituted for M for convenience so that n takes on values 0, 1, 2 - - - and $B_n = 0$. By Fourier analysis it is found that the

coefficients A_n are given by:

$$A_n = \frac{4C_0}{\pi(2n+1)}$$

So that

$$\frac{C}{C_0} = \sum_{n=0}^{\infty} \frac{4}{\pi(2n+1)} \exp. \left[-\pi^2(2n+1)^2 \frac{Dt}{4\mathcal{L}^2} \right] \sin \frac{\pi(2n+1)x}{2\mathcal{L}}$$

The average concentration in a uniform capillary at time t is:

$$C_{av.} = \frac{1}{\mathcal{L}} \int_0^{\mathcal{L}} C dx.$$

So that

$$\frac{C_{av.}}{C_0} = \sum_{n=0}^{\infty} \frac{8}{\pi^2(2n+1)^2} \exp. \left[-\pi^2(2n+1)^2 \frac{Dt}{4\mathcal{L}^2} \right] \quad (6)$$

Equation 6 does not include the volume of the capillary. Instead, its length \mathcal{L} may be used, provided the cross-section of the tube is uniform.

A graph or table of the right-hand side of Equation 6 can be prepared. Interpolation at the experimentally determined value

$\frac{C_{av.}}{C_0}$ gives Dt/\mathcal{L}^2 and hence D . In computing the function very few

terms need be taken as the series converges very rapidly for reasonably large times. The ratio of the first term ($n = 0$) to the second ($n = 1$) is $9 \exp(2\pi^2 Dt/\mathcal{L}^2)$. This ratio is greater than 1000 at the time the exponent Dt/\mathcal{L}^2 exceeds 0.24, and higher terms fall off even more rapidly. To illustrate the rate of change, when $Dt/\mathcal{L}^2 = 0.24$ the average concentration in the capillary has fallen to 45 per cent of

its initial value (47). In this study, a table of solutions to Equation 6 was composed employing a digital computer. Eight terms were included to insure a high accuracy for shorter diffusion periods. The computer program used is reproduced in Appendix C. The complete output table is so extensive that the space limitations prohibit its inclusion; however, a portion of the results, in the range generally employed in this study, is presented in Appendix C.

In the more important absolute methods of measuring diffusion coefficients, the experimental methods are such as to require solution of the partial differential Equation 3 for the appropriate boundary conditions. A discussion of the more significant solutions with a concentration dependent diffusion coefficient is presented by Crank (10).

In binary systems, the diffusion coefficient depends on the mobility of both molecules and is usually referred to as the mutual diffusion coefficient. Since the mobilities of two unlike molecules are likely to be different, one would expect the diffusivity of such a system to be concentration dependent.

Under these circumstances Equation 3 becomes

$$\frac{\partial C}{\partial t} = D \frac{\partial^2 C}{\partial x^2} - \frac{\partial D}{\partial x} \frac{\partial C}{\partial x} \quad (7)$$

The dependence of D may then be selected and the resulting equation subjected to solution by analytical or numerical methods. The use of a digital computer makes the latter method most useful, since the machines will do large numbers of iterative calculations in a reasonable short time. In this study the diffusion dependence was assumed

to be

$$D = D_0 + AC^P + BC^Q + EC^R + FC^S$$

where D_0 is the Nernst limiting value of the diffusion coefficient. A, B, E, and F are constants and C is the molar concentration of the diffusing substance. The quantities P, Q, R, and S are powers to which the concentration is raised. Substituting this model for D into Equation 7 and performing the indicated partial differentiations:

$$\frac{\partial C}{\partial t} = D \frac{\partial^2 C}{\partial x^2} + (PAC^{P-1} + QBC^{Q-1} + REC^{R-1} + FSC^{S-1}) \left(\frac{\partial C}{\partial x} \right)^2$$

This result may be solved by the application of standard numerical methods (52). The refinements and suggestions of Richtmyer (46) for numerical methods were responsible for much of the success of the machine calculations. The programs developed for the IBM 1620 and 7090 digital computers are presented in Appendix C.

In reality, the exact nature of the driving force in diffusion is not known. The use of the concentration gradient as the driving force is erroneous, since experimental evidence to date has failed to confirm a relationship (20). However, Fick's equation (generally called Fick's First Law) is used universally today to represent the diffusion process because of its simplicity and because of the experimental fact that a gradient is necessary to observe diffusion.

The early work of Fick suggested that the concentration gradient was the driving force for the diffusion process. This conclusion was reached by intuition and by analogy with heat transfer equations. It is now accepted that the concentration is not the true driving

force since this notion can not be verified experimentally or theoretically. The osmotic pressure gradient was often thought of as the driving force but this too was largely the result of intuitive argument, and it can be shown that this argument leads to the same result as the chemical potential gradient (30).

If two phases are in equilibrium, the chemical potential of any component in these phases must be the same throughout. It is reasonable to assume that the degree of deviation from equilibrium is determined by the difference in chemical potential between phases. This argument applies equally well to various regions of a single phase. At equilibrium, both concentration and chemical potential are constant throughout a single phase. When a concentration gradient exists, a chemical potential gradient also exists; however, the numerical values are not the same and they need not be proportional. It is generally accepted today that the chemical potential gradient is the driving force for the diffusion process.

The modern quantitative theory of electrolyte solutions is based on the concept of the interaction between the thermal motions of the ions and their electrical attractions and repulsions. The theory also involves, in its higher refinements, considerations of the physical dimensions of the ions and of their interactions with solvent molecules. By defining and considering an intrinsic diffusion coefficient for each component of a binary mixture of concentrated electrolytes, Hartley and Crank (23) have derived an expression capable of indicating the more important effects which have to be considered in diffusion. The Hartley and Crank expression for the mutual diffusion coefficient at any concentration is:

$$D = \left(\frac{d \ln N_A f_A}{d \ln N_A} \right) \frac{\eta_A^0}{\eta} \left[N_B D_{AB}^0 - N_A D_{AA}^0 \right] \quad (8)$$

where N_A and N_B are the mole fractions of component A and B, D_{AB}^0 is the diffusion coefficient of A at infinite dilution in B, D_{AA}^0 is the self-diffusion coefficient of A and pure A, η_A^0/η is the ratio of the viscosity of pure liquid A to the bulk viscosity of the solution, and the term $d \ln N_A f_A / d \ln N_A$ is the logarithmic differentiation of the activity. The details of the derivation as well as examples and a discussion of its application are given by Robinson and Stokes (47).

The Nernst-Hartley relation (47) considers the forces on single ions due to the gradient of chemical potential and the unequal mobilities of the ions. The simple Nernst-Hartley treatment leads to the formula,

$$D = D^0 \left(1 + C \frac{d \ln y}{dC} \right) \quad (9)$$

where D^0 is the limiting value of D at infinite dilution obtained by an expression due to Nernst and y is the molar activity coefficient at concentration C .

In the ordinary diffusion of a salt resulting from a concentration gradient, both ions must move in the same direction at the same speed to maintain electrical neutrality. In very dilute solutions the ions are far enough apart to be without influence on one another. As the density of the ions increases, there are two main effects of the interaction between the electric charges of the ions: these are the electrophoretic effect and the relaxation effect.

The electrophoretic effect arises in the following way. When an ion moves through a viscous medium, it tends to drag along with it the solution in its vicinity. Neighboring ions therefore have to move not in a stationary medium but with or against the stream depending on the relative direction of the two. The effect will clearly be concentration-dependent.

In general, the motion of ions under the influence of external forces will disturb the symmetrical distribution of the ions, and this disturbance would tend to decrease the velocity of the ions. In the solution in equilibrium, the "ionic atmosphere" (a convenient description of the ions outside the considered ion) is on a time-average, distributed with spherical symmetry, and exerts no resultant force on the central ion. The central ion may be pictured as moving to an off-center position and experiencing a restoring force, which rapidly dies away as the "atmosphere" is rearranged by the thermal motions of its constituent ions. The average restoring force experienced by the ion is called the relaxation effect.

In the case of diffusion of a simple electrolyte, Onsager and Fuoss (37, 38, 39, 40) evaluated the electrophoretic contribution to the motion of ions in terms of velocity of the ions and their absolute mobilities. The corrections are applied to the Nernst-Hartley expression and result in,

$$D = (D^0 + \Delta_1 + \Delta_2) \left(1 + c \frac{d \ln \gamma}{dc} \right) \quad (10)$$

The electrophoretic terms, Δ_1 and Δ_2 , are complex functions of the dielectric constant and viscosity of the solvent, the temperature and chemical potential gradient, and an electrical force due to the

"diffusion potential." The "diffusion potential" results from the electrical attraction of the faster moving for the slower moving ionic species. Although the authors, Onsager and Fuoss, proposed that Equation 10 be used in the study of both symmetrical and unsymmetrical electrolytes, Robinson and Stokes (47) pointed out that application has shown that unsymmetrical electrolytes generally should be studied by the expression:

$$D = (D^{\circ} + \Delta_1) \left(1 + c \frac{d \ln \gamma}{dc} \right). \quad (11)$$

The treatment of diffusion in concentrated 1:1 electrolyte solutions, while serving to indicate the more important effects which have to be considered, is in no sense final or completely satisfactory.

For concentrated electrolyte solutions a number of effects, negligible for the dilute solution, become of great importance.

These are:

1. That solvent molecules will in general move in the opposite direction to the solute.
2. That some of the ions may carry with them a permanently attached layer of solvent molecules, which acts as a part of the diffusing solute entity.
3. That the viscous forces may be considerably modified by the presence of large numbers of ions.

The theory of diffusion for higher valency types in concentrated solution is even more tentative. One reason for this is that the theory of electrophoretic corrections is less satisfactory, even for

dilute solutions. In addition, experimental data of sufficient accuracy to test the theories are very sparse (22).

Uranium ions in solution form one of the most intricate and interesting domains in the chemistry of this element. In common with all other ions in aqueous solution, the various uranium ions interact with the solvent water to a greater or less extent, depending to a considerable extent on the charge of the ion. Aqueous solutions of uranium salts always have an acid reaction indicative of hydrolysis. Although the uranyl ion only carries a charge of +2, it nevertheless behaves more like an ion of charge +4 than a simple doubly-charged cation. The hydrolytic reactions of UO_2^{++} have been exhaustively studied in recent years by a number of investigators. As a result, there is general agreement that polymeric ions are formed in the hydrolysis of uranyl ions (32). A study of the self-diffusion coefficients of uranyl ion in uranyl nitrate by Hahn (21) indicated that the formation of associated species as a result of increasing the acidity of uranyl nitrate affects the diffusion rates. The extent to which polynuclear formation occurs with uranium ions is still a subject for debate. The details of the current theories and results of experimental investigations with this group of extraordinary salts are presented by Katz and Seaborg (20).

CHAPTER III

EXPERIMENTAL APPARATUS

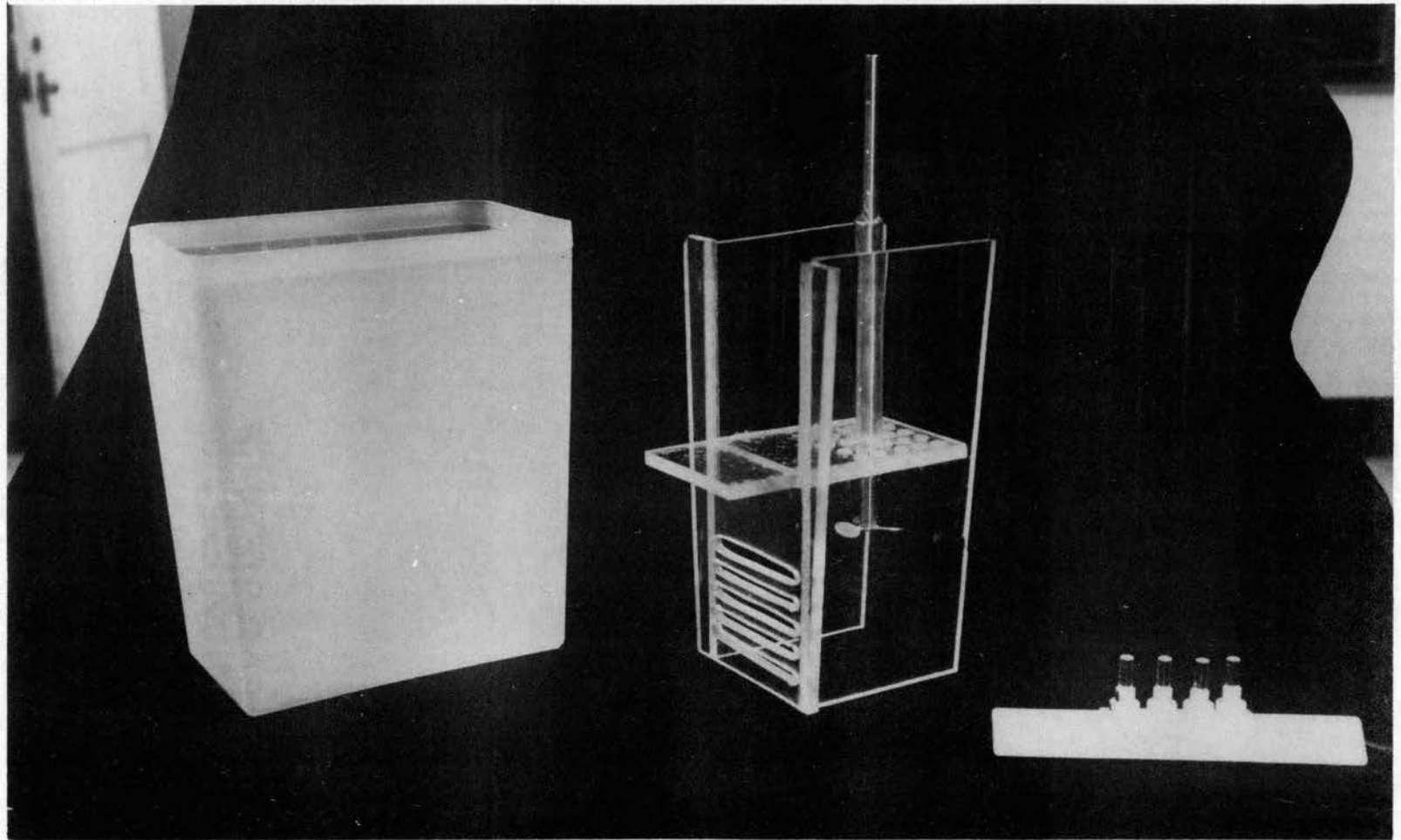
In principle, the capillary cell technique involves the free diffusion of ions from a column of solution confined in a small diameter capillary, usually less than 1 mm. in diameter, into an infinite reservoir of solution at a different concentration. The equipment employed for this study can be discussed under four major phases: the diffusion cell, the capillaries, the analytical necessities, and the constant temperature equipment.

The first and fourth phases resulted in an application or improvement of previously established techniques. The analytical problem resulted in the development of an internal liquid scintillation analysis. The method evolved was established on a routine basis and provided a sensitive and sufficiently reliable analysis for micro quantities of uranium ion.

Diffusion Cells

The diffusion cell, shown in Plate I, was patterned after the design of Mills and Godbole (35). The cell consisted of a rectangular polyethylene freezer carton approximately 5 inches by 7 inches by 9 inches deep. The reservoir volume was 3.4 liters with the baffles in place. The flow baffles were constructed of one-quarter

PLATE I

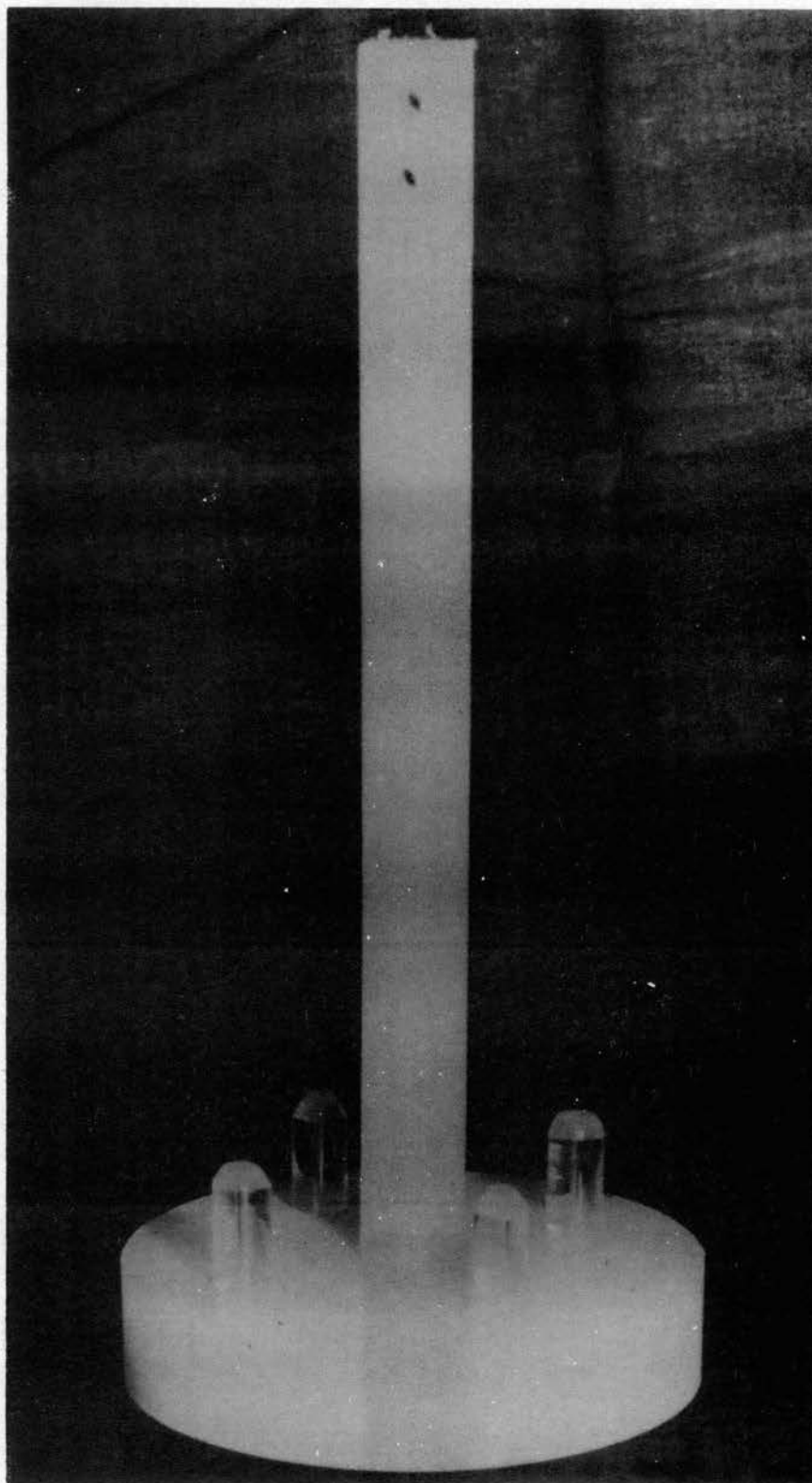


Capillary Diffusion Cell

inch thick Lucite. The baffles were assembled in a manner that divided the cell into four equal compartments. The upper two compartments were opened to each other by a rectangular section approximately 3 inches wide and 4 inches deep. The compartment containing the stirrer impeller was opened at the top by equally spaced $1/4$ inch holes. The impeller drew solvent down through these holes and forced it out of the compartment through a series of equally spaced $1/4$ inch slots in the vertical wall of the cell. A $1/2$ inch Lucite tube encased the impeller shaft in the top compartment to prevent the rotating shaft from setting up eddy currents that might disturb the laminar flow across the capillaries. Nylon screws in combination with epoxy resin glue were used to fasten the sections of the baffles together. The completed baffle assembly is shown in Plate I. The solvent volume was stirred by a variable speed, propeller type stirrer, Cole-Palmer Model 4650, Dual-Shaft Electronic Stirrer. The stirrer speed was calibrated to provide a liquid flow rate of 1 - 3 mm. per second across the capillary mouth as recommended by Mills (33).

The original capillary holders are visible in Plate I. They were made of Teflon and were designed to seal the bottoms of the capillaries. Experience showed that it was impossible for the holders to maintain a liquid-tight seal after being used several times. The design shown in Plate II was adopted and the capillaries were sealed by gluing a microscope cover glass to each capillary with epoxy resin cement. The excess glass and cement were then ground down to the outside dimension of the capillary. The holder was machined from polyethylene and weighted with stainless steel

PLATE II



Diffusion Capillaries in Holder

rods to reduce its bouyancy. The capillary cell holder containing the capillaries was attached to a fine-thread screw lowering and raising device just prior to the start of an experiment. The raising and lowering device can be seen in Plate III.

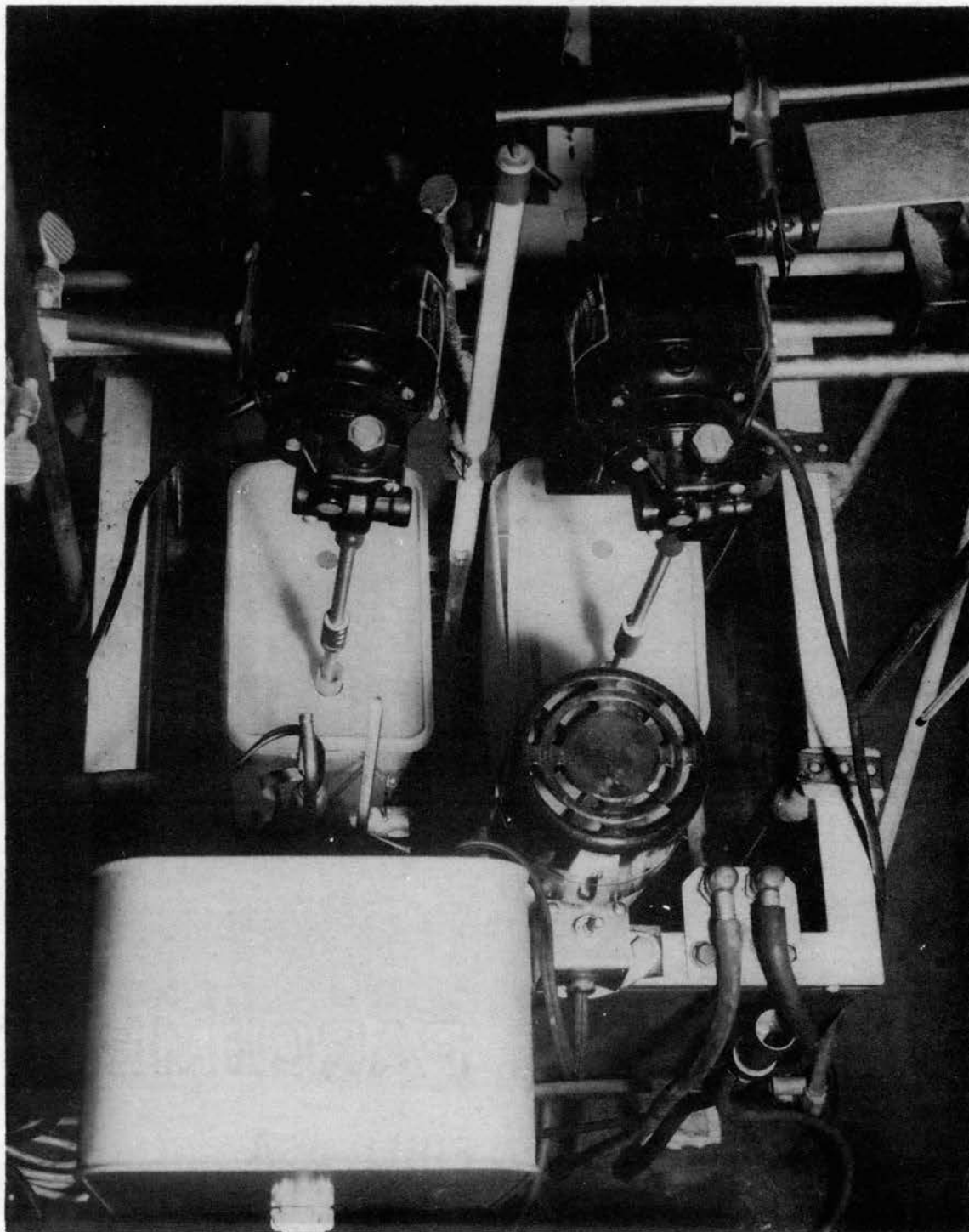
Capillaries

In this study the capillary cells were constructed from 0.0202 ± 0.003 inch O.D. (0.5 mm.) and 0.0303 ± 0.003 inch I.D. (0.75 mm.) precision bore capillary tubing obtained from Fischer and Porter Co. Each piece of tubing was checked for uniformity of its inside diameter. The tubing was placed in a Bausch and Lomb comparator under a X20 magnification and the length of a mercury thread was measured with the aid of a micrometer attachment. Sections that showed a 0.5 per cent or greater change in length of the mercury thread were discarded.

The capillaries were cut into sections two centimeters in length. The length of each section was measured several times with a micrometer and the average value reported. After sealing the bottoms, tapering and fire-polishing the tops, the volume of each capillary cell was measured by multiple weighings of mercury and the average value reported. All measurements were made in an air-conditioned laboratory maintained within 2 °F of 75 °F. The results of the length measurements and volume calibrations for both sizes of capillaries are reported in Tables XXX and XXXI, Appendix B.

Initially, the capillaries were used with a square cut across the open end. An investigation of the possible causes of inconsistent results revealed that as the capillaries were being immersed,

PLATE III



Diffusion Cells Installed in
Constant Temperature Bath

the solvent did not readily wet the tops of the capillaries. The capillaries could be immersed as much as 1/4 inch below the liquid surface without wetting. As the surface tension of the solvent was overcome, the liquid rushed across the capillary tops. Under this circumstance, one of two unfavorable reactions were possible. The sudden collapse of the wall of solvent around the top of the capillary could result in an air bubble being entrapped across the mouth of the capillary. The presence of the air bubble greatly reduced the diffusion rate of that particular sample. A portion of the initial solute could be pumped out and thus the final concentration in the capillary would be lower than that of a normal diffusion experiment.

In an effort to improve the wetting of the capillaries during the immersion, the open ends were ground to a taper of approximately 60 degrees. Although an improvement was noted, the wetting of the tapered portion was still not completely satisfactory. Next, the ground taper portion was carefully fire-polished, care being exercised not to warp the internal surface of the tubes. The combination of the taper followed by fire-polishing allowed the solvents to properly wet the capillaries during the insertion into the solvents and the problem of air entrapment and solute pumping previously encountered was greatly reduced.

Scintillation Equipment

Investigation of the use of liquid scintillation counting of alpha particles has been reported by a number of authors (3, 4, 5, 24, 28, 50). The method appeared to have the advantage of high sensitivity and to minimize the problem of error due to sample

handling during the preparation of planchets for alpha proportional counting.

The radioactive decay scheme for natural uranium is shown in Figure 1. Alpha radioactivity in natural uranium is due to the 4.21 Mev. and 4.76 Mev. alpha particles from uranium-238 and uranium-234, and from the 4.52 Mev. alpha from uranium-235 (45). Equilibrium activity from other members of the decay families is effectively removed by chemical processing during purification of the ore and preparation of the uranyl salt.

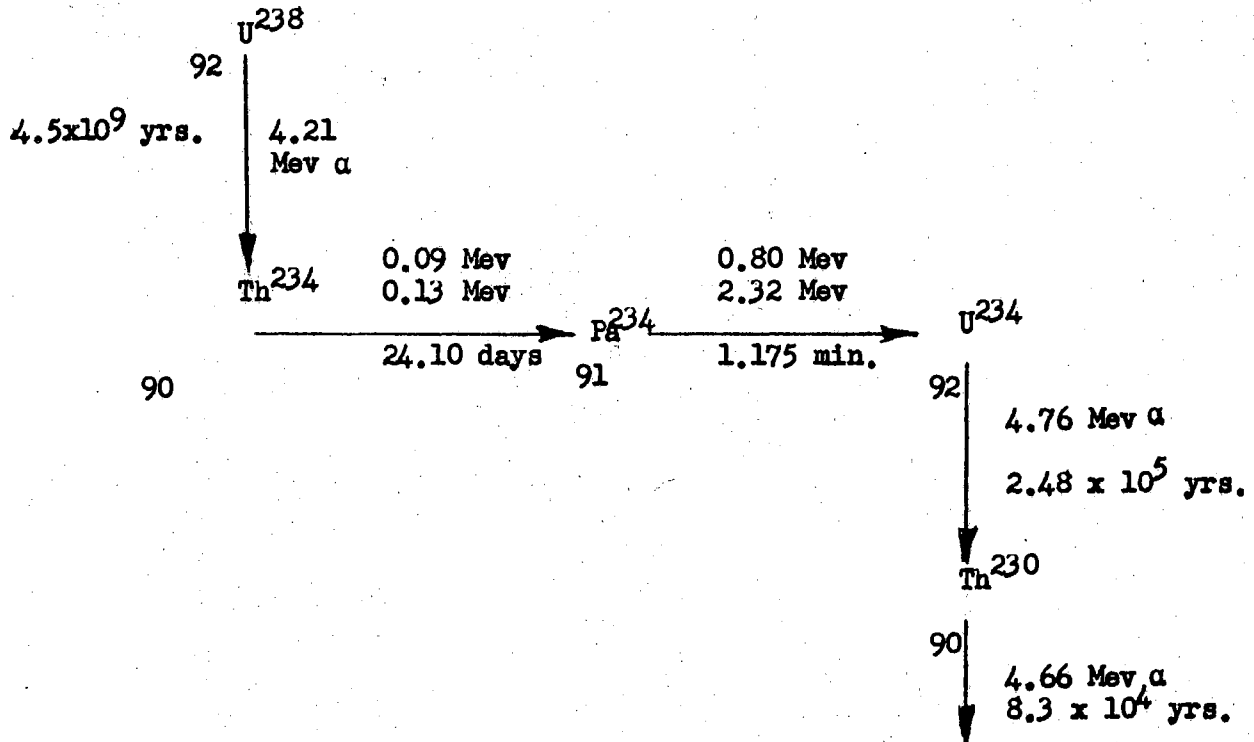
Reynolds (45) reports the disintegration ratio of U-235: U-234: U-238 in natural uranium as 0.046: 1:1, with a specific alpha activity of 1.503×10^6 dpm/g. Based on these ratios, integral counting rates of greater than 95% of the sample specific activity were obtained using a discriminator level of 9 volts.

The scintillation analyses were made using a single channel scintillation spectrometer manufactured by the Radiation Instrument Development Laboratories Co. The instrument consisted of their Model 30-1 amplifier and power supply, Model 33-2 single channel pulse height analyzer, and Model 49-10 one microsecond scaler. The spectrometer was coupled to a RIDL Model 10-2 scintillation head, housed in a RIDL Model 60-2 shield. The assembly is shown in Plate IV.

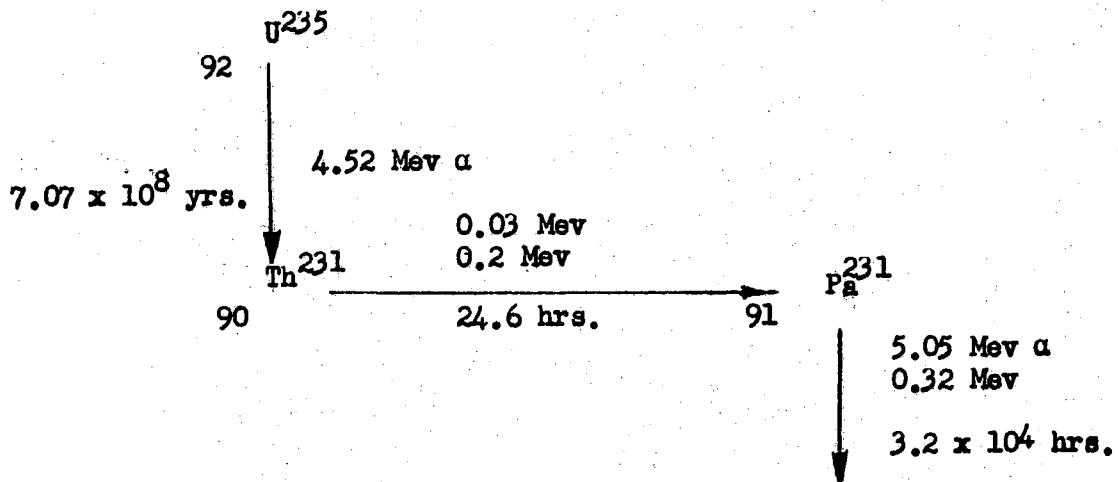
The original scintillation equipment was later modified in order to reduce the photomultiplier thermal-noise background count. This was accomplished by replacing the DuMont 6292 photomultiplier with a DuMont K1234 tube. The effect was equivalent to increasing the amplifier gain by a factor of about two. Separate D.C. filament

Figure 1
Uranium Decay Schemes

U^{238} Decay Scheme (15)



U^{235} Decay Scheme (15)



supply and B+ voltage supply for the cathode follower circuit in the detection head were installed to minimize spurious counts being introduced into the counting circuit.

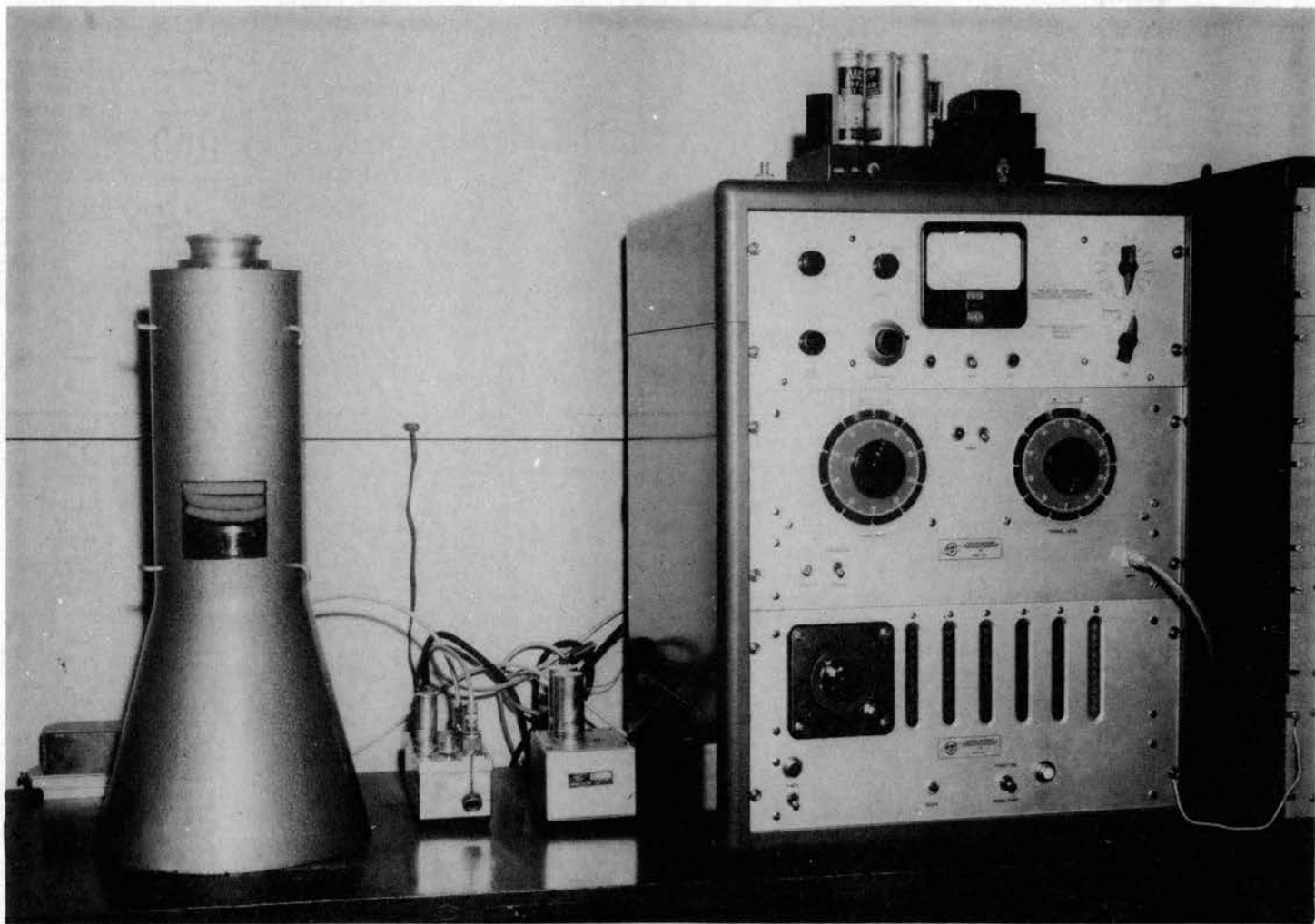
A RIDL Model 31-1 preamplifier and RIDL Model 31-6 preamplifier power supply were inserted immediately following the detection head. The Model 31-1 preamplifier was capable of increasing the photomultiplier signal by a factor of about 28, thus enabling the overall amplification gain of the unit to range as high as 44,800.

Satisfactory counting results were obtained with a phototube voltage of 860 volts and an overall amplifier gain of approximately 11,000. All sample counting was performed with an integral mode at a discriminator level of 13.5 volts. This energy level corresponded to the 9.0 volt level established with the equipment before the modifications were made.

Constant Temperature Bath

The diffusion runs were carried out at 25 °C, \pm 0.1 °C. The bath was a Freas, Model 161, equipped with a Precision Electronic Control relay. The relay was actuated by a mercury differential-type Precision micro-set thermoregulator and was capable of controlling the main bath temperature to within \pm .01 °C. The temperature of the diffusion cells was measured prior to each run by a Brooklyn Thermometer Co. precision thermometer, No. 22214, calibrated and certified by the manufacturer by comparison with a primary standard. After the diffusion run began, the bath temperature was constantly monitored with a Beckman differential thermometer provided with 0.01 °C scale divisions.

PLATE IV



Internal Sample Liquid Scintillation Counting Equipment

In order to minimize vibrations of the bath, stirrer, and relay being transmitted to the diffusion cells, these pieces of auxiliary equipment were remounted with sponge-rubber pads. In addition, the bath shelf was suspended from the bath rim with two-inch thick polyurethane foam pads at all metal-to-metal contact points.

Constant temperature baths operating at temperatures near room temperature require, for close control, a temperature sink approximately 15 °C below the control point. The temperature sink consisted of a cold water supply chilled by a Blue M, Model PCC-1A, portable refrigerator. The thermostat was capable of maintaining a preset temperature to within ± 1.0 °C. An auxiliary centrifugal pump continuously circulated the cool water through a copper coil located in the main bath.

CHAPTER IV

EXPERIMENTAL PROCEDURE

In preparation for a diffusion run, the constant temperature bath was operated at the control point (25 °C) for at least four hours. The temperature of the diffusion cells was observed with the calibrated Brooklyn Thermometer previously described. During the four hour period, if the temperature of the cell did not change more than ± 0.01 °C, the bath was considered stable and the run was initiated.

The capillaries were prepared for use by careful cleaning with chromic acid solution, followed by thorough rinsing with demineralized water. The capillaries were finally cleaned inside and out with C. P. grade acetone and thoroughly dried. Care was exercised to insure that no oil film remained on the outer fire-polished tapered surface of the capillaries. Any oil film present on these surfaces adversely affected the wetting of the glass capillary during immersion in the diffusion cell.

The solute to be studied was charged into each capillary using a Hamilton 10 lambda microsyringe. The microsyringe was inserted in a simple holding device to assist in the operation. Each capillary was flushed three times with fresh solute. The fourth filling was considered the diffusion sample. In order to compensate for possible evaporation of the solute prior to its immersion in the solvent and

to minimize bubble formation at the mouth of the capillary during the immersion, each capillary contained an excess of solute (approximately 0.01λ). The capillaries and solutes were stored and charged in an air-conditioned laboratory maintained at $75 \text{ }^\circ\text{F} \pm 2.0 \text{ }^\circ\text{F}$. Immediately after the capillaries were filled, they were placed in the lowering device of the diffusion cells and immersed to initiate the diffusion run.

The capillary holders were lowered slowly and with as uniform a rate as possible. The retention time above the bath was short to prevent excessive evaporation of the solutions in the capillaries. During the immersion the capillaries were observed with the aid of a three power reading glass. This was done to observe that each capillary was properly wetted and to detect any occlusion of air over the mouth of the capillary. If an air bubble was observed, the particular capillary was noted and the results generally were found to reflect the condition by yielding a diffusion coefficient considerable lower than the average value. The total diffusion time was estimated by imposing the conditions $Dt/L^2 = 0.24$ as suggested by Crank (10). During the diffusion runs, the capillary holder was suspended in the solvent and was not allowed to touch any portion of the diffusion cell. This precaution was taken as an additional measure to insure that the capillaries were not vibrated while the diffusion was in progress. At the end of the diffusing period the run was terminated by carefully raising the capillary cell holder. The total diffusing time was controlled to within \pm ten seconds of a 40 to 48 hour diffusion time.

The samples were immediately removed to the counting laboratory

and prepared for scintillation counting. The contents of the capillaries were removed by using a jeweler's loupe and a Hamilton 10 lambda microsyringe. Care was exercised during the removal to prevent spillage or overflowing of the capillary contents by displacement with the syringe needle. Each capillary was rinsed with three volumes of demineralized water to assure a reasonably complete transfer of the sample. The solute sample and the rinse volumes were transferred to a 5 dram low-potassium scintillation vial procured from the Wheaton Glass Co., Millstown, Virginia. Next, one milliliter of absolute ethyl alcohol was added to insure miscibility of the sample with the scintillation solvent as suggested by Seliger (50). Five milliliters of the scintillation solution was then added to each sample completing its preparation for counting.

At the time the diffusion samples were transferred and prepared for counting, a four lambda sample of each initial solute was prepared in an identical manner. The sample was measured with a calibrated Hamilton 10 lambda microsyringe as recorded in Table XXXII, Appendix B. Both the standard samples and the diffusion samples were then stored in a light tight container for 24 hours before being placed in the scintillation counter. This was done to allow the decay of any light that may have been absorbed by the solution during sample preparation.

The viscosities of the various solutes and solvents used in this study are reported in Table XXXIII and Figure 19, Appendix B. The viscosities were obtained using standard five milliliter Ostwald viscosimeters at $25\text{ }^{\circ}\text{C} \pm 0.05\text{ }^{\circ}\text{C}$. The densities were determined by multiple weighings of the contents of a calibrated 10 ml. pipette.

CHAPTER V

RESULT AND DISCUSSION

Internal Liquid Scintillation:

A report by Hayes (24) revealed that the most promising wave-length shifter to incorporate in a liquid scintillator was 0.1 g/L of POPOP 1, 4 - Di - 2 - (5 - phenyloxazolyl) - benzene . He suggested for water-soluble samples that 4 g/L of PPO (2, 4 - diphenyloxazole) and 50 g/L of Naphthalene in 1, 4 dioxane be used as the primary scintillator and solvent. Farmer and Berstein (18) reported high counting efficiencies in samples up to 20% water by making use of p - dioxane solution containing 0.5 per cent p - terphenyl. Seliger (50) reported excellent energy resolution and high counting efficiency for alpha particles when using a scintillator containing PBD (phenyl-biphenyl-oxadiazolol - 1, 3, 4) and POPOP in toluene. Samples containing water were dissolved in the scintillator by the addition of absolute ethyl alcohol. The volume ratio of water to ethyl alcohol to toluene was 1:50:1000.

Preliminary experiments with 2.0 molar uranyl nitrate samples showed that the best counting efficiency would be obtained using xylene or toluene as the scintillation solvent with 0.1 g/L of POPOP as a wave-length shifter and 0.5 weight per cent p - terphenyl as the primary scintillator. The differential spectra for this phase of the study were obtained by employing a 5 volt discriminator window.

Figure 2 shows the differential scintillation count rate as a function of uranium concentration with the toluene as the solvent. A shift in the peak-counts as the concentration was decreased is evidenced. Figure 3 shows the differential count rate of the same concentrations with xylene as the solvent. Although there is a slight shift in the peak with decreasing concentration, the shift is not as severe as was the case with toluene. Xylene did not yield as high a counting efficiency as toluene. This was evidenced by a lower peak count for each concentration reported.

In order to achieve as high a counting efficiency as possible and at the same time minimize the shift in peak heights, a 50:50 mixture of toluene and xylene was used as the scintillation solvent. Figure 4 shows a typical differential count rate as a function of uranium concentration when employing the toluene-xylene mixture as a solvent. The counting efficiency was somewhat less than pure toluene and greater than xylene. The shift in the peak counts as the concentration or uranyl ions was changed was not as severe as with toluene. For these reasons, the decision was made to use the 50:50 mixture as the scintillation solvent in the analyses for this study. The ratio of sample volume to ethyl alcohol to scintillator was maintained at 1:100:500 throughout the study. The increase in ethyl alcohol was necessitated by the water rinses used in transferring from the capillaries to the scintillation vials. Count rates made on samples with various scintillator volumes indicated that satisfactory efficiencies could be obtained with the lower sample-to-scintillator volume ratio.

The effect of the thorium 234 beta was checked by separating

Figure 2

Differential Scintillation Spectrum
for Uranyl Nitrate
(Primary Solvent-Toluene)

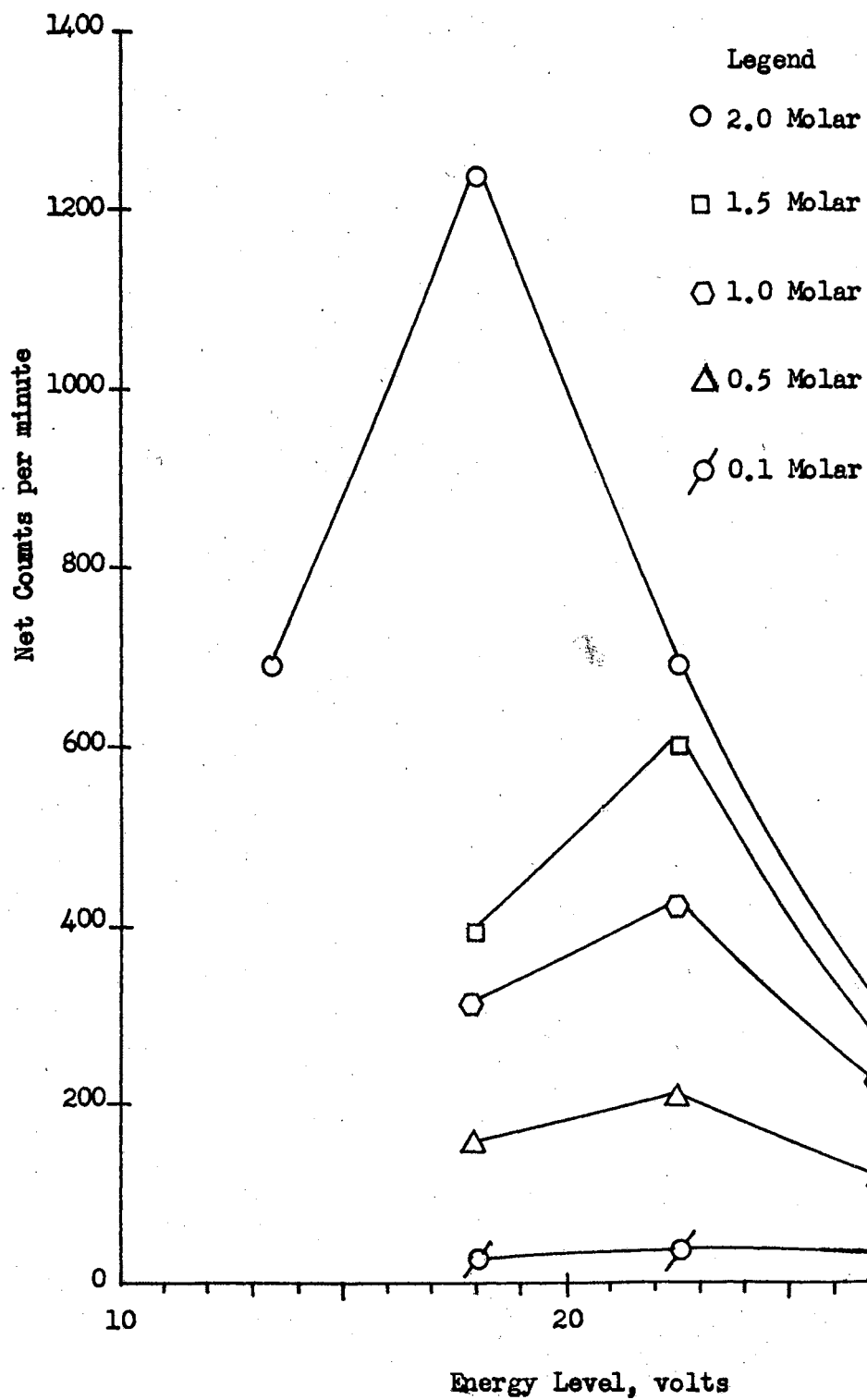


Figure 3

Differential Scintillation Spectrum
For Uranyl Nitrate
(Primary Solvent-Xylene)

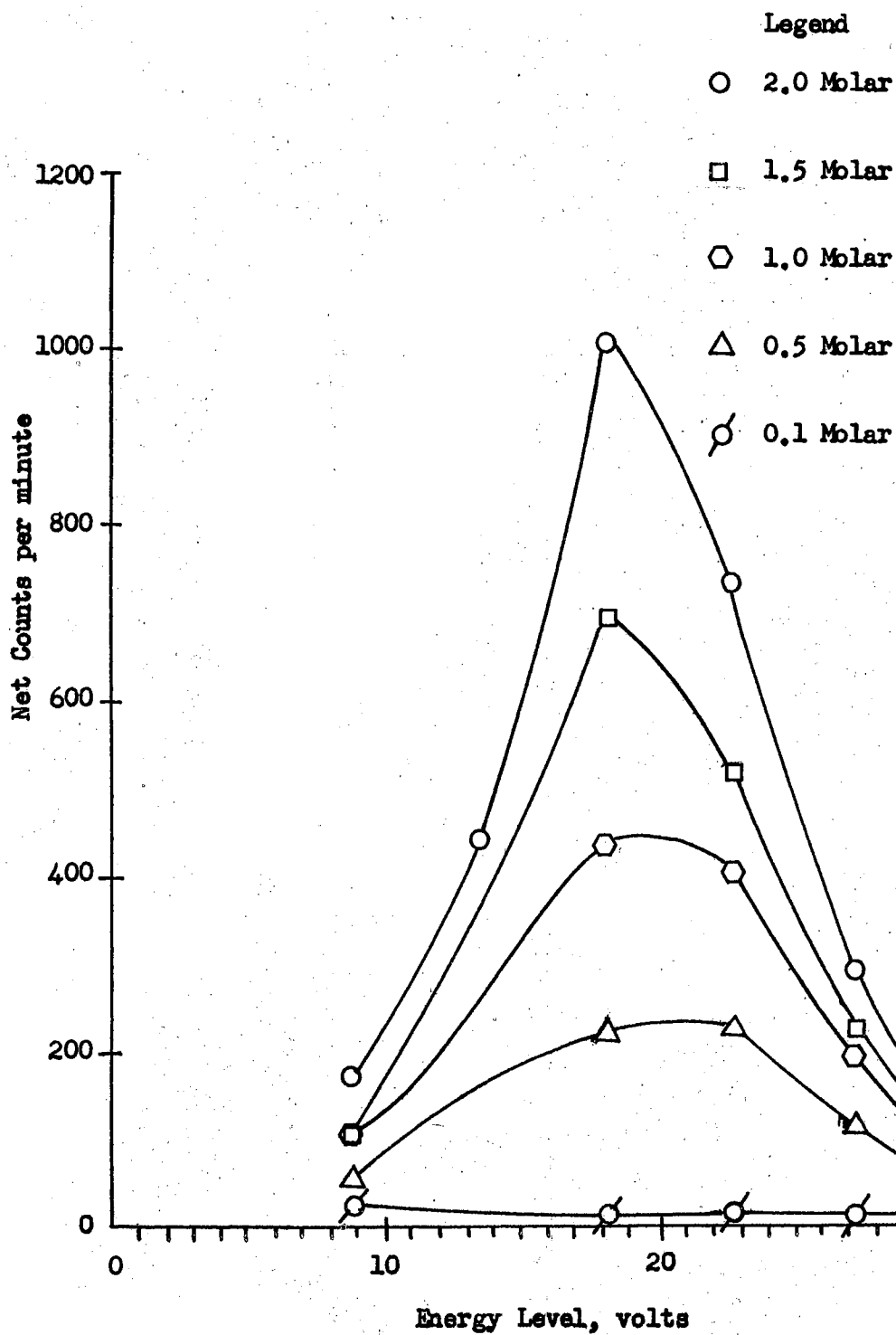
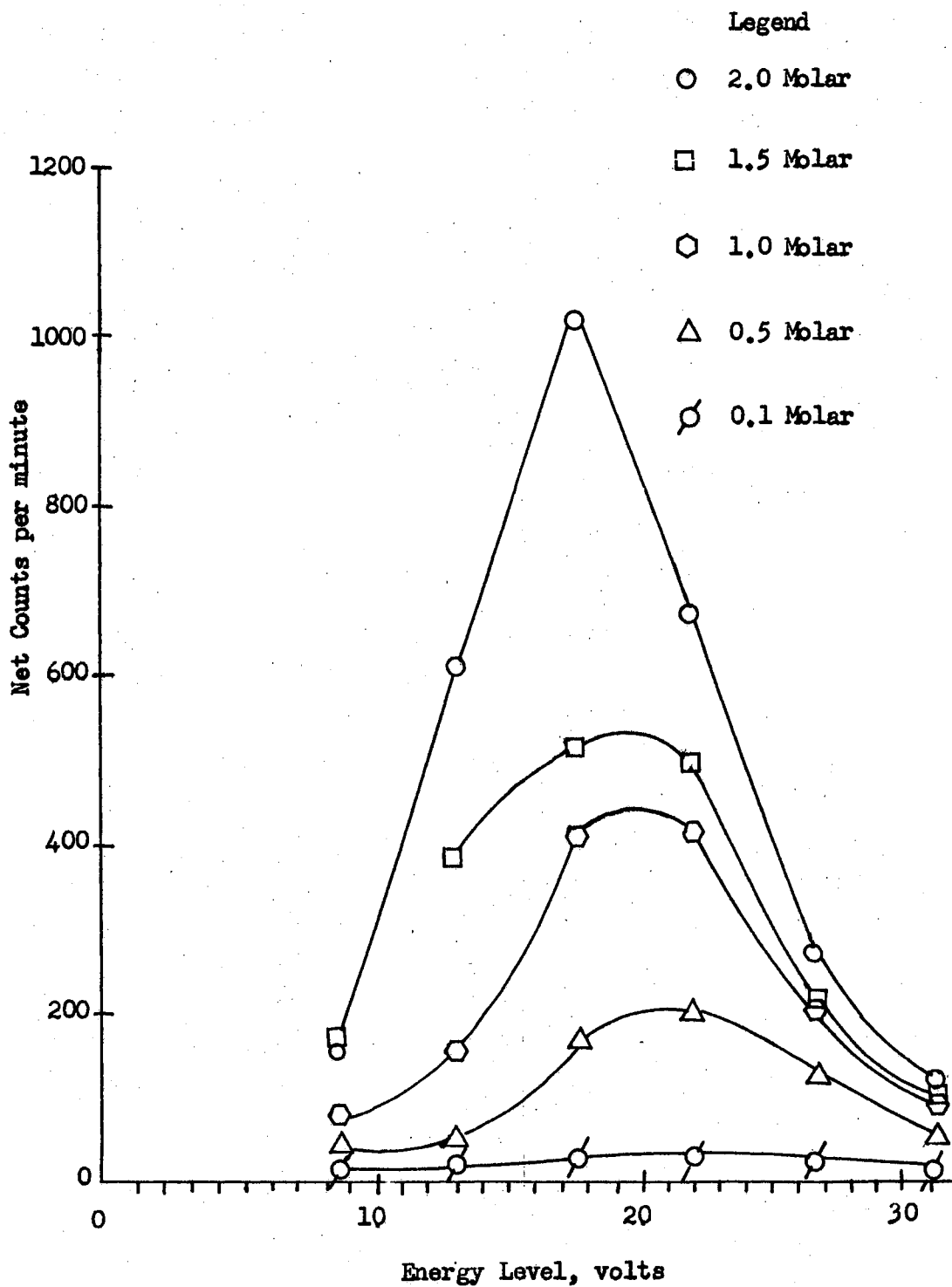


Figure 4

Differential Scintillation Spectrum
for Uranyl Nitrate
(Primary Solvent 50-50 Xylene-Toluene)



the thorium isotope using Dowex 50-W cation exchange resin. Spectrum of the separated solution showed no change with time as the thorium grew back. This effect was anticipated since the energy levels of the alpha particles allowed the spectrometer to be operated at energy levels generally much too high to detect beta or gamma scintillation.

In order to ascertain that the diffusion of a natural uranium salt was not a selective molecular phenomenon, a differential scintillation spectrum was obtained on capillary samples after 50 hours of diffusion. The differential spectrum of the solutes before and after diffusion were found to be identical in respect to energy levels. As a result, there was no selective molecular diffusion occurring that could be detected by the analytical methods of this study.

The resolution of the instrument was tested by running a mixture of uranyl nitrate (4.18 Mev. alpha) and Ra D-E-F (5.3 Mev. alpha). This was done to establish the possibility of a simultaneous quantitative analysis of two or more alpha emitting salts in a mixture. Figure 5 presents the differential spectrum of 2.0 molar uranyl nitrate and 2.0 molar Ra D-E-F. Figure 6 gives the differential spectrum of a 50:50 mixture of the two salts. In determining the spectrum of the mixture the window voltage was reduced from 5.0 to 1.0 volt. The results indicated that the instrument was incapable of a quantitative discrimination between these two alpha activities in a mixture.

A typical differential and integral spectrum of 2.0 molar uranyl nitrate is presented in Figure 7. In this study all of the counting rates were obtained by an integral count at an energy level located at the minimum point on the differential spectrum. This energy level was at 9.0 volts in the case illustrated.

Figure 5
Differential Scintillation Spectrum
for
Uranium - 238 and Radium D-E-F

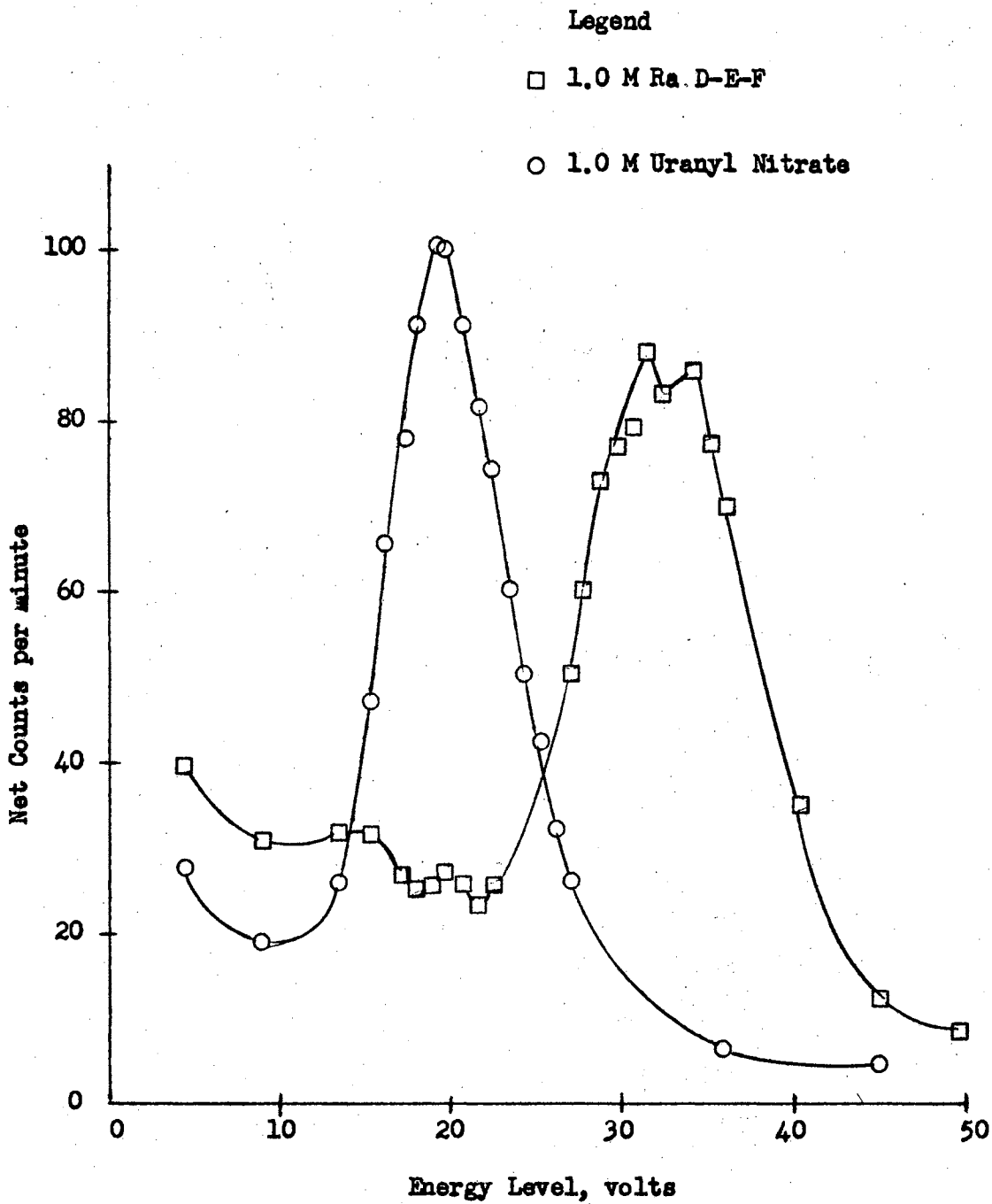


Figure 6
Differential Scintillation Spectrum
for Uranium and Ra-D-E-F
Mixture

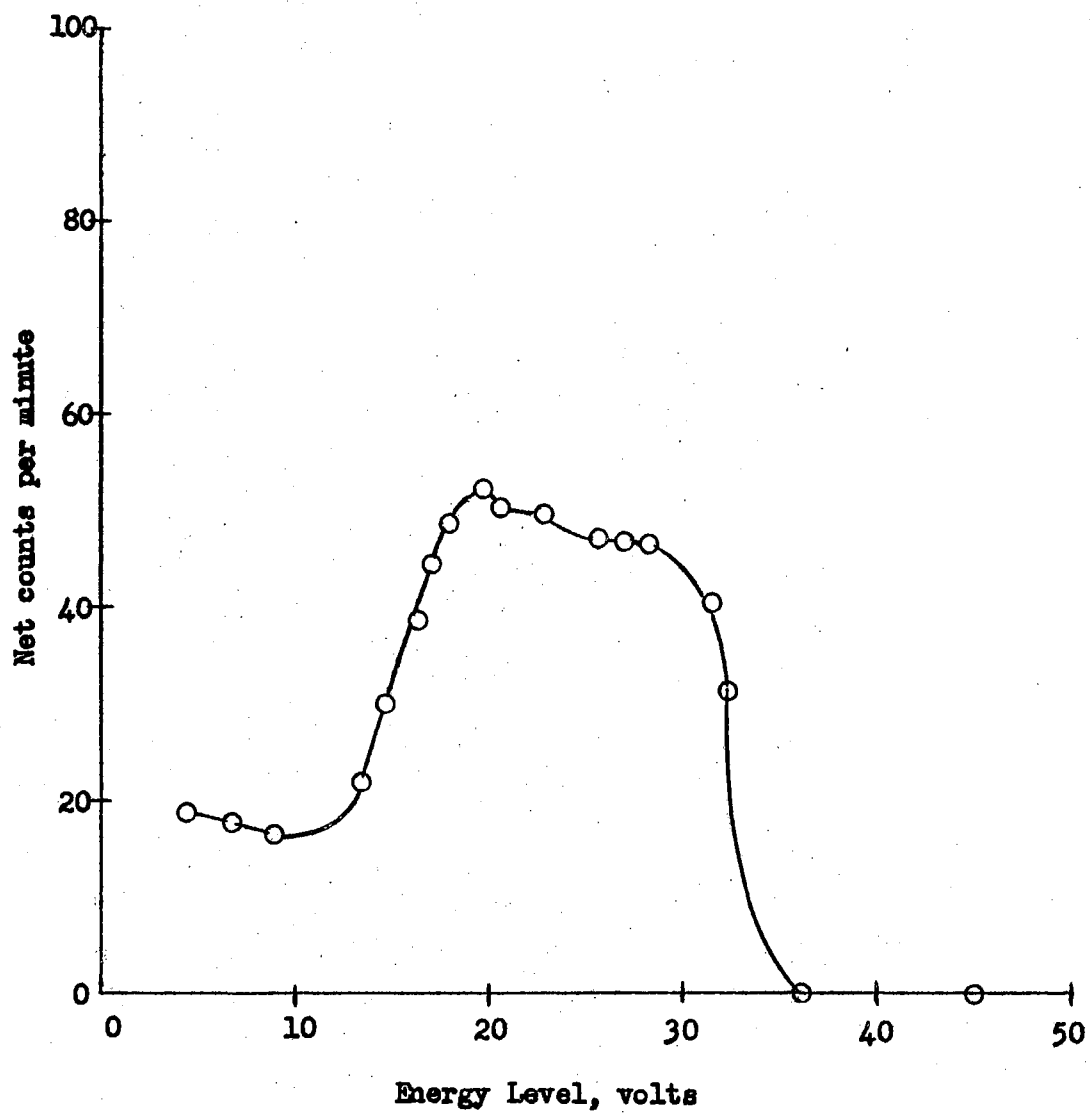


TABLE I

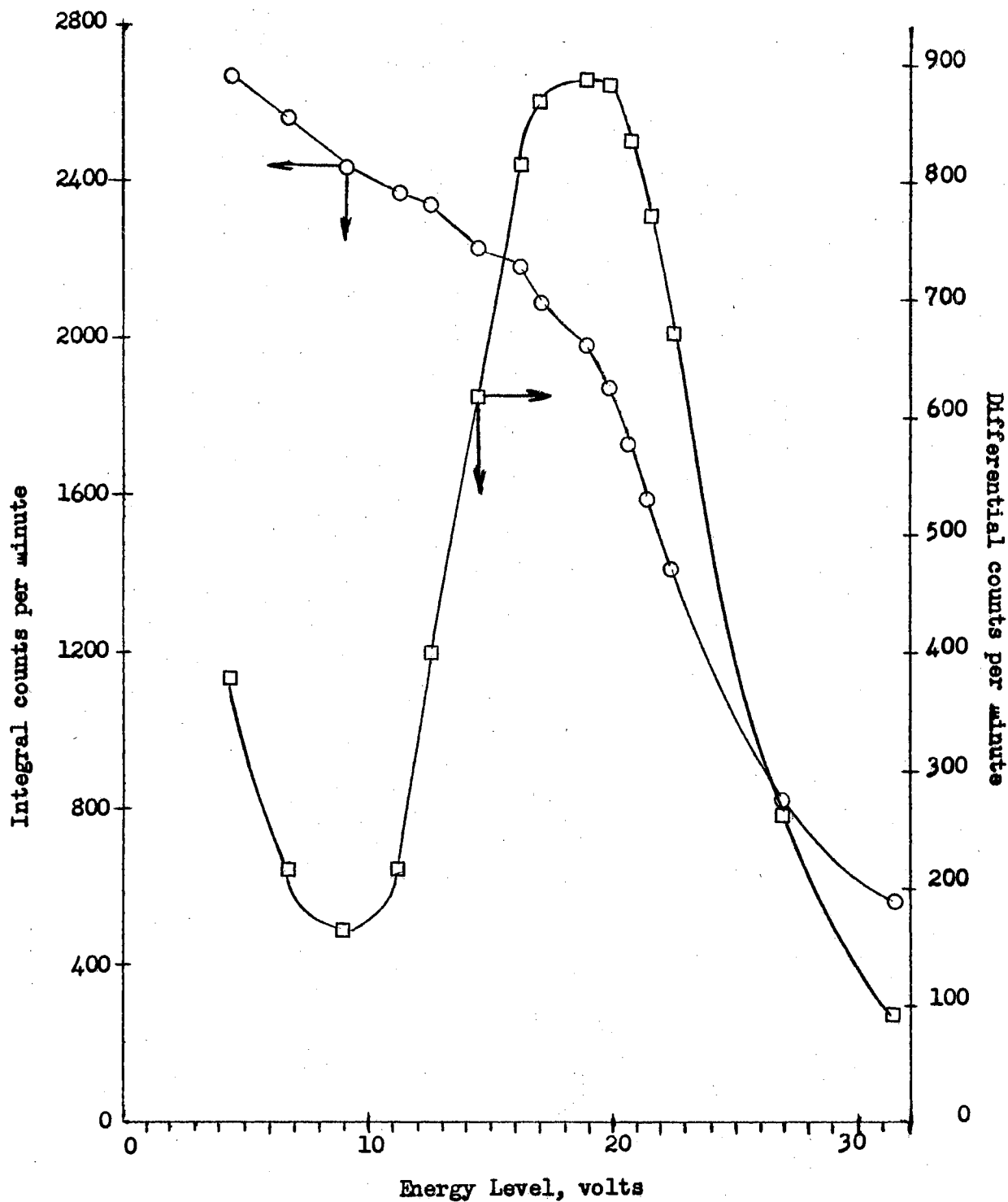
Integral and Differential Scintillation Spectrum Data
for 2 Molar Uranyl Nitrate
(Primary Solvent = 50:50 Xylene-Toluene)

Photomultiplier voltage = 1220
Window width voltage = 5.0
Amplifier gain:
Coarse = 1.0
Fine = 100

Energy Level, Volts	Differential Count			Integral Count		
	Total, 10 minutes	Background, 10 minutes	Net per Minute	Total 10 minutes	Background, 10 minutes	Net per minute
31.5	997	86	91.0	5716	10	570.6
27.0	2834	178	266.0	8302	19	828.3
22.5	7216	321	670.0	14184	48	1413.7
21.6	7890	333	756.0	16042	92	1595.0
20.7	8700	372	833.0	17408	125	1728.3
19.8	9160	351	881.0	18932	215	1871.7
18.9	9177	327	885.0	20266	376	1989.0
17.0	9136	326	881.0	21436	519	2091.7
16.1	8483	301	818.0	22513	669	2184.4
14.3	6398	219	618.0	23150	889	2226.1
12.5	4193	201	399.0	24480	1064	2341.6
11.25	2290	145	216.0	25026	1245	2378.1
9.0	1878	224	165.0	25745	1389	2435.6
6.75	2564	398	217.0	27237	1615	2562.2
4.5	4053	1261	379.0	29209	2541	2666.8

Figure 7

Integral and Differential Scintillation
Spectrum of 2.0 M Uranyl Nitrate
as a Function of Energy Level
(Primary Solvent = 50:50 Xylene-toluene)



The uranyl nitrate solutions employed in the study were prepared from A.C.S. reagent grade uranyl nitrate purchased from the General Chemical Division of Allied Chemical. The uranyl nitrate was a crystalline hexahydrate salt of natural uranium. One liter of 2 molar uranyl nitrate solution was prepared by weighing the salt on a large pan balance and diluting to the proper volume with demineralized water. All other standard solute concentrations were prepared by careful dilution of the 2 molar stock solution. The balance was sensitive to a 0.1 gram change in weight. Thus, the accuracy of the weighing was 1 part in 10,000 and the resulting uranyl nitrate solution was considered to be 2.0 M within the error of the experimental measurements used.

A spectrophotometric determination for uranium presented by Dizdar and Obrenovic (12) was used to establish the uranium concentration of the solutes used in calibrating the liquid scintillation counting technique. The authors have stated that the results were reproducible within ± 1.0 per cent. Experience in our laboratory with the method, using a Beckman Model DU Spectrophotometer, showed that the results were reproducible to within ± 0.5 per cent. In view of the precision of the method, it was accepted as the standard for calibrations.

A tabulation of random samples of the standard solutes used in the course of the study is in Table XXIX. The concentrations used as the abscissa are the average values obtained from the spectrophotometric analyses of the solutes. Figures 8 and 9 show the resulting plot of these data. For ease of study, the concentration range was divided into two parts. The two curves represent the

Figure 8

Integral Liquid Scintillation Count Rate
as a Linear Function of Uranium Concentration
(Lower range)

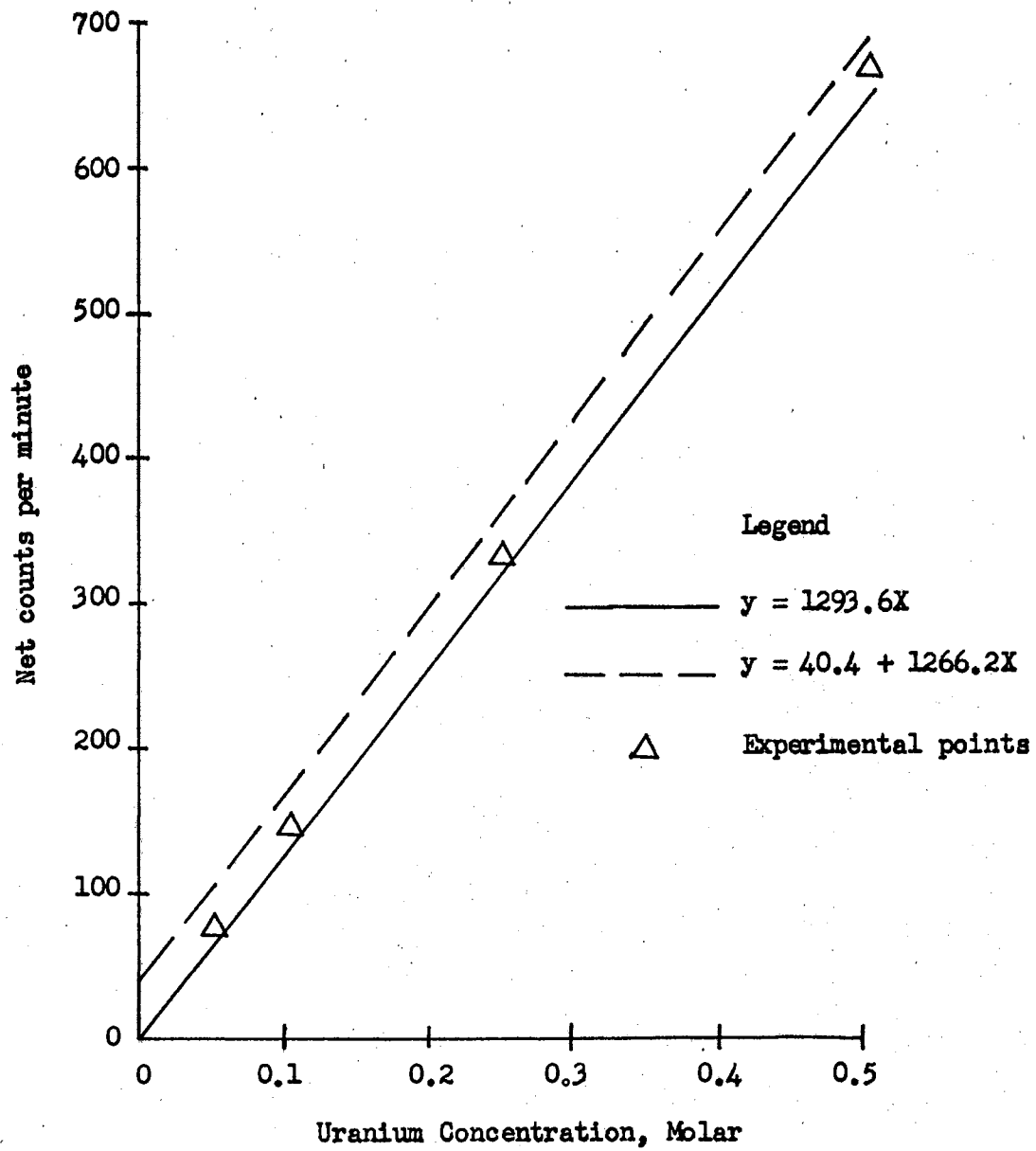
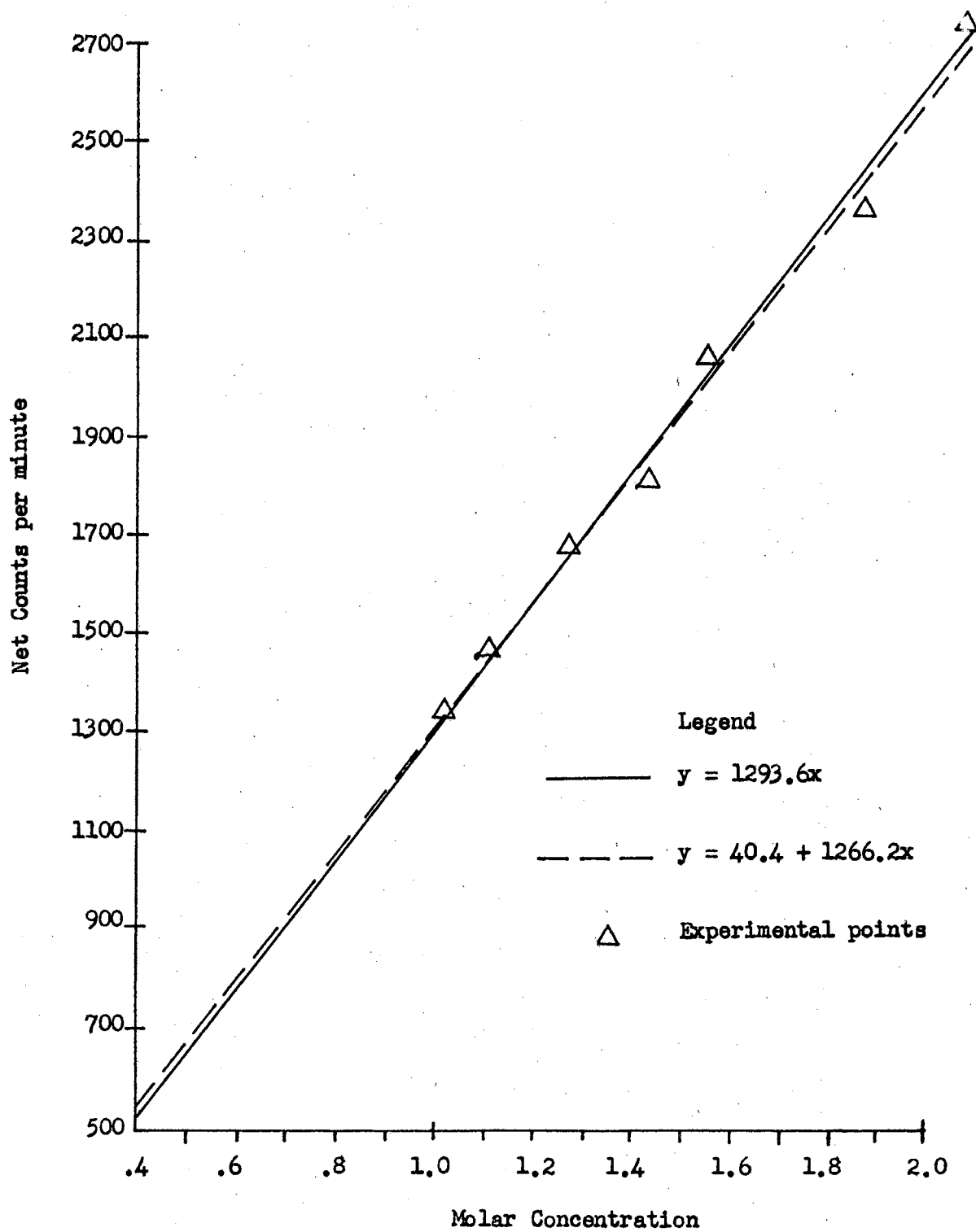


Figure 9

Integral Liquid Scintillation Count Rate as a
Linear Function of Uranium Concentration
(Upper range)



results of a least-mean-square fit over the data presented. The equation of the dashed line is

$$y = 40.4 + 1266.2X \quad (23)$$

while the equation of the solid line is

$$y = 1293.6X \quad (24)$$

The points represent the average values of the liquid scintillation counting rate at the solute concentration shown.

Figure 8 contains the results of the counting with lower concentrations and shows that the linear relationship with zero intercept more nearly fits the experimental points. The second curve extrapolates through a zero point of 40.4 counts per minute.

The data used in the regression calculations for this curve included the count rates obtained for samples of liquid scintillator without uranyl salts. Although the scintillator consistently showed a background count of approximately 44 cpm, the actual count rates for samples containing uranyl nitrate in concentrations of less than 0.5 molar apparently behaved in a fashion most accurately described by a linear relationship with a zero intercept. In the concentrations ranging above 0.5 molar, that portion of the background count attributed to the liquid scintillator represented a negligible part of the total count rate. This effect can be seen in Figure 9 which indicates that both types of the regression curves tend to merge into a single straight-line relationship as the concentration increases.

Table XXIX is a tabulation of the average values of the count rate for the several standard solute solutions. The averages were

obtained by considering a minimum of ten determinations made at various times during the course of the study. The standard sample deviation of the average values ranged from ± 0.90 to ± 2.98 per cent. The magnitude of the deviation was random, indicating that the deviation was probably due to a random sample-volume error coupled with the statistical error of radioactive counting. In all scintillation counting analyses the sample total-count was above 25,000. Based on the established statistics of radioactive counting, the total count coupled with the background count of the equipment permitted the reproducibility of the sample count rates to be $\pm 1.0\%$ or less (44).

A brief study of scintillation characteristics of the uranyl nitrate solutions revealed that the integral rates decreased with time. A decrease in the counting rate of 5 per cent was noted after a sample had been stored in a light-tight container for 24 hours after preparation. The rate of decrease was then noted to be about 1.0 per cent after each additional 24 hours of storage in the dark. Generally, the sample counting rate would stabilize after six days of storage in the light-tight container. Samples that had been allowed to become stable were exposed for one hour to the fluorescent lights of the laboratory. An increase in the count rates occurred, but the original higher rates were never attained. Thus, approximately 50 per cent of the measured drift was attributed to scintillation of the samples due to light absorption during sample preparation. The unaccounted drift was assumed to be due to the combined quenching effects of the water, ethyl alcohol, and dissolved air in the samples. The reproducibility of the counting rates after the samples had been stored for 24 hours was found to be within the experimental error of

the diffusion runs. The procedure of analyzing the uranyl nitrate samples after 24 hours of storage in a light-tight container was adopted since it provided an optimum combination of the elapsed time for analyses and the accuracy of the analyses.

The linear relationship expressed by Equation 24 was considered to express the relationship between the scintillation counting rate and the uranyl ion concentration within the error of the experimental procedure. On the basis of the linear expression, the ratio of the final concentration in the capillary to the initial concentration was taken to be the ratio of the respective liquid scintillation counting rates. In order to assure that the ratio obtained was as equitable as possible, a standard sample of the initial concentration was prepared and analyzed simultaneously with each diffusion run sample. In addition, thermal-noise background counts were made before and after each sample. This procedure was a precaution against the possibility of spurious counts being unknowingly included in the various counting rates.

Diffusion of Uranyl ion into Water

The study of the diffusion of uranyl nitrate into water was made employing a randomized complete-block experimental design. An illustration of the calculations involved in the capillary method is included in Appendix C. The design and analysis of the data was in accord with generally accepted statistical methods and may be found in any standard text on statistics [i.e., Steel and Torrie (52)]. The F tests to determine that the treatment differences were or were not significant were made at a 0.05 probability level. The analysis of variance data are presented in Tables XX through XXV, Appendix A. Two analyses

TABLE II

Summary of Uranyl Nitrate Diffusing into Water

Initial Solute Conc., Molar	Average Final Conc., Molar	Final Conc. Standard Error, Per Cent	Average \sqrt{C} Molar	Average \sqrt{C} Standard Error	Average $D \times 10^6$ $\text{cm}^2 \text{sec}^{-1}$	Average $D \times 10^6$ Standard Error, Per Cent
0.05	0.022		0.190		7.10	
0.25	0.114	4.38	0.426	.001	6.84	6.5
0.50	0.228	0.96	0.603	.004	6.90	4.5
0.60	0.260	1.02	0.656	.001	7.37	1.6
0.71	0.292	0.97	0.708	.001	7.90	1.5
0.75	0.307	0.65	0.727	.002	8.04	1.1
0.86	0.346	1.12	0.777	.001	8.05	1.6
1.00	0.409	3.75	0.825	.004	8.19	5.4
1.50	0.620	2.67	1.030	.004	8.03	4.0
2.00	0.813	2.36	1.186	.004	8.21	3.0

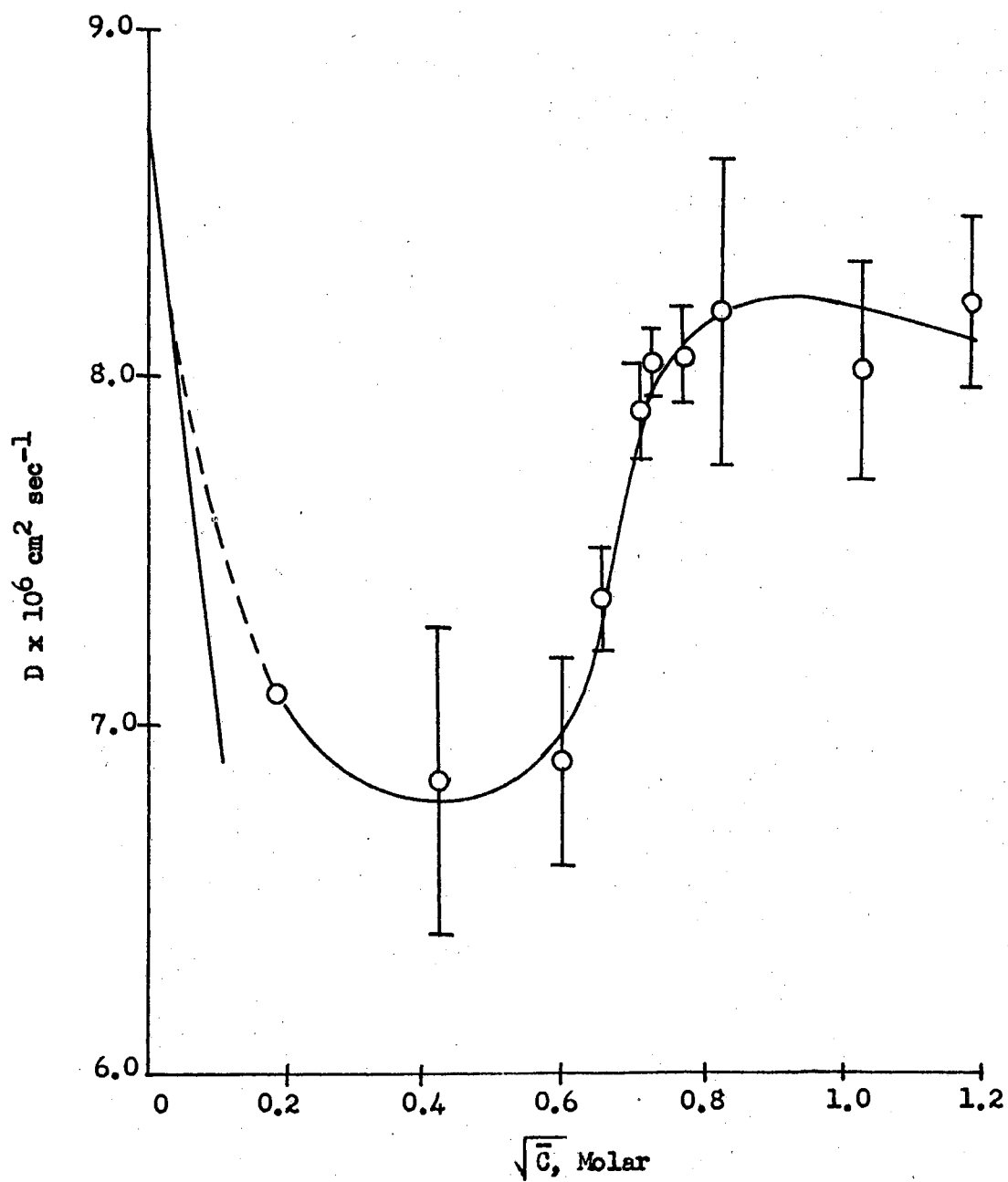
are presented. One presents a series of runs employing uranyl ion concentrations between 0.05 and 0.75 molar, while the second table gives the results of all of the diffusion runs involving water as the solvent. This was done to study the lower concentration runs separately. The sample standard deviations of the lower concentrations were lower than those experienced in the analyses of the total diffusion runs. This was due, probably, to the limited number of runs at the lower concentrations and some good fortune during these few runs.

Figure 10 presents the integral diffusion coefficient as a function of the square root of the average concentration. The results were obtained by assuming that D was constant and employing Equation 6. The sample standard deviations of the calculated D are indicated for each point. The concentrations and respective diffusion coefficients are tabulated in Table XIX, Appendix A. The sample standard deviations were obtained from the analysis of variance for the random complete-block experimental design.

The experimental work for the diffusion of uranyl nitrate into water was performed in three distinct sets of runs. The largest number of runs was with the initial uranium concentrations of 0.5, 1.0, 1.5 and 2.0 molar. This group comprised the initial experiments. Later in the study, the decision was made to extend the concentration to lower values. The counting periods for the sample from two lower concentrations [0.05 and 0.25 molar $UO_2(NO_3)_2$] were found to be much too long for reliable counting rates. The counting rates required 8 to 10 hours of counting time in order to obtain total counts that would insure the desirable ± 1.0 per cent reproducibility. Experience with the scintillation equipment had shown that despite the

Figure 10

Integral Diffusion Coefficient of Uranyl
Nitrate into Water as a Function
of Concentration
(Constant D)



elaborate precautions taken to stabilize the various electronic components, random transients occurred during long counting periods. For this reason only two runs were made at these lower concentrations.

The last group to be studied was in the concentration range of 0.5 to 0.96 molar uranium. This group was included in an effort to establish the diffusion coefficient between 0.5 and 1.0 molar uranium. A total of five determinations was made. The precision of the results reflects the experience gained during the many diffusion experiments performed prior to this particular set.

The standard errors of the experimental points, as reflected in Figure 10, are sufficiently broad enough to allow a rather arbitrary curve to be drawn through the data. The narrow deviation experienced in the cases of the mid-range concentrations, however, suggest that the type of curve shown will best satisfy the reported results. The dotted portion of the curve in Figure 10 represents an extrapolation to the Nernst limiting value of D . The solid, short line to the left represents the limiting slope value of dilute solutions. The limiting value expression is discussed by Harned and Owen (22) and the values and calculations used for this study are presented in Appendix C.

The resulting curve, representing the integral diffusion coefficient of uranyl nitrate diffusion into water, although peculiar in shape, is not an uncommon occurrence in the study of the diffusion behavior of electrolytes. The sharp decline in D as the concentration is initially increased is predicted by the accepted theory of dilute electrolytes. The abrupt increase above an initial solute concentration of 0.5 M, followed by a leveling off or slight decline in D , has been reported for other electrolytes. Evidence of this behavior was reported

and discussed by Harned and Owen (22) and Robinson and Stokes (47) for other electrolytes.

Intuitively one would not expect the diffusion coefficient to be constant over all ranges of concentration. Many forms for the dependency of D have been proposed [see Crank (10)] Equation 7,

$$\frac{\partial C}{\partial T} = D \frac{\partial^2 C}{\partial X^2} + \frac{\partial D}{\partial X} \frac{\partial C}{\partial X}$$

which accounts for a changing D , was used to study the uranyl nitrate-water data. A polynomial approximation to D was written for use on a digital computer. The input and output format, as well as the source program for the solution, are presented in Appendix C. In practice, a polynomial model was assumed to describe the dependence of D on concentration. The model was regressed with assumed values of D to obtain the regression coefficients. The regression was made by digital computer employing a least-mean-square curve fit.

The coefficients obtained as a result of the regression were used as input data in the numerical solution. A one-dimensional unsteady state solution was obtained using the capillary length as one independent variable and the diffusion time as the other. The solution was obtained using central difference methods in the case of distance and forward difference in the case of time. Two different parameter grids were employed in the study. The coarse grid solution consisted of 10 increments in the capillary length and 100 increments in the diffusion time. The fine grid solution was 25 increments in distance with 625 increments in time. Machine time dictated the use of the two solutions. The coarse grid, being relatively fast, was used on

an IBM 1620 to obtain approximate results. For the final computation, the finer grid solution was used on an IBM 7090 to assure a more precise numerical solution. The solution was made assuming reflection and superposition at the closed end of the capillary. The procedure of reflection and superposition is mathematically sound as pointed out by Crank (10). For a detailed outline of the transformations and digital computer program developed for the solution, the reader is referred to Appendix C.

The final result was a concentration profile over the length of the capillary at the end of the diffusion time. The average value of this profile was obtained by numerical integration and represented the concentration that would have been obtained by chemical analysis. This average concentration was compared with the experimentally measured value. Any necessary adjustments were then made in the model for D to correct the calculated results and the procedure repeated. By trial and error the following model was obtained which best fitted the experimental data from this study for uranyl nitrate diffusing into water:

$$D = 8.7379 \times 10^{-6} - 24.463 \times 10^{-6} C^{0.5} + 39.566 \times 10^{-6} C^{1.0} \\ - 17.857 \times 10^{-6} C^{2.0} + 3.355 \times 10^{-6} C^{3.0} \quad (25)$$

In all cases, the constant term was taken to be the limiting value for D as expressed by Nernst. The exponent of the first concentration term was set as 0.5. The choice of these two particular values was made on the basis of the limiting value equation for diffusion. The equation is the result of an application of the Onsager-Fuoss theory for dilute solutions (22). Figure 11 presents Equation 25.

TABLE III

Final Least Means Square Regression Fit
of
Diffusion Coefficient as a Function of Concentration

$$(D = A + BC^{.5} + EC^{1.0} + UC^{2.0} + VC^{3.0})$$

Uranyl Nitrate Molar Concentration	Calculated Diffusion Coefficient $\times 10^6 \text{ cm}^2 \text{ sec}^{-1}$
0.000	8.7379
0.050	5.2016
0.100	4.7828
0.200	5.0222
0.250	5.3327
0.300	5.6903
0.400	6.4475
0.500	7.1748
0.600	7.8208
0.700	8.3631
0.800	8.7943
0.900	9.1153
1.000	9.3322
1.100	9.4546
1.200	9.4944
1.300	9.4653
1.400	9.3821
1.500	9.2605
1.600	9.1171
1.700	8.9688
1.800	8.8333
1.900	8.7283
2.000	8.6720

Standard Estimate of Error = 0.1494

Coefficients

$$A = 8.738 \times 10^6$$

$$B = -24.463 \times 10^{-6}$$

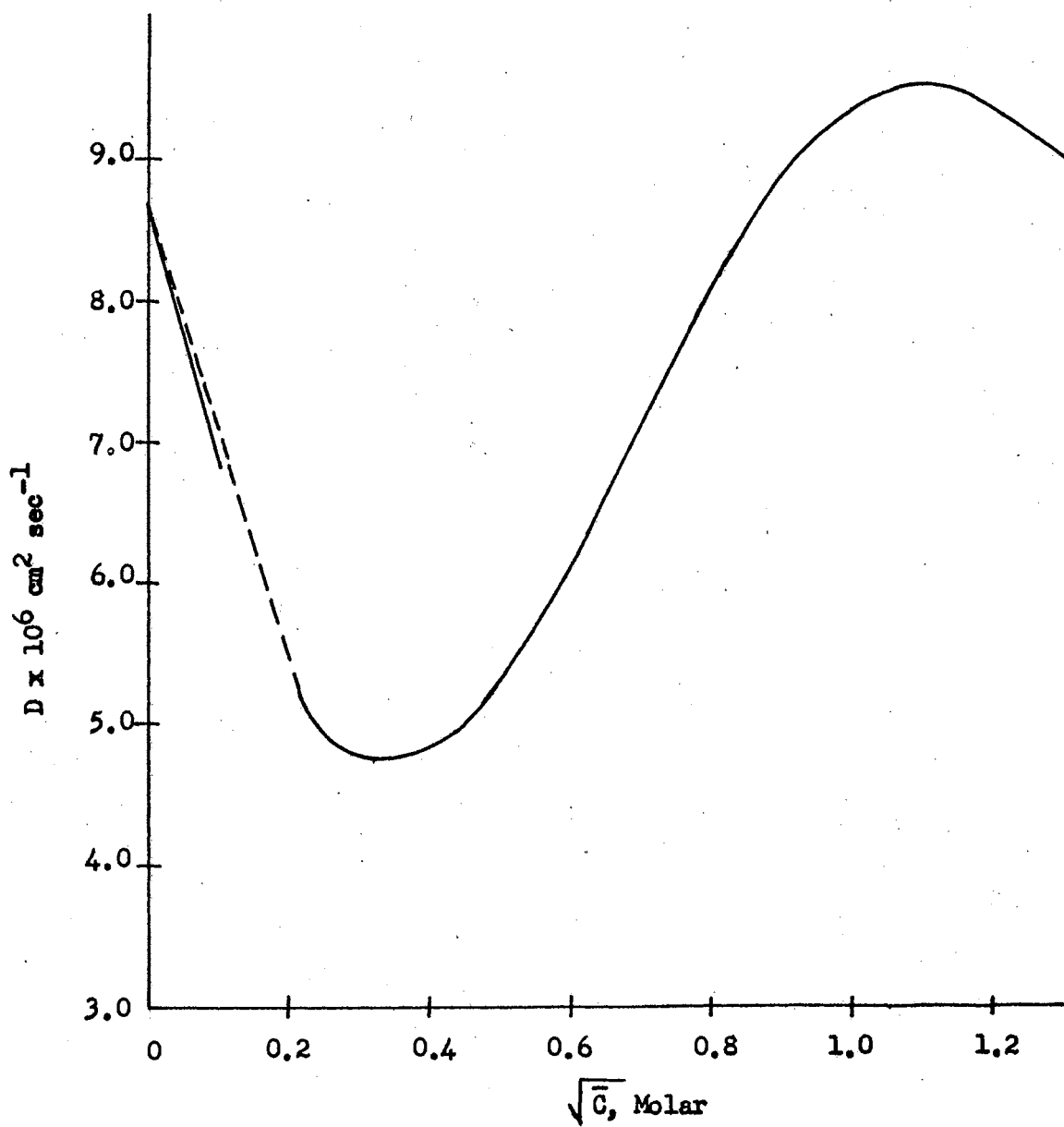
$$E = 39.566 \times 10^{-6}$$

$$U = 17.857 \times 10^{-6}$$

$$V = 3.55 \times 10^{-6}$$

Figure 11

Differential Diffusion
Coefficient of Uranyl Nitrate into Water
as a
Function of Concentration



The Onsager and Fuoss relationship, Equation 11, is generally used to study unsymmetrical electrolytes. The relationship is

$$D = (D^0 + \Delta_1) \left(1 + C \frac{d \ln \gamma}{dc} \right)$$

where Δ_1 is a complex function of the dielectric constant and viscosity of the solvent, the temperature and chemical potential gradient and the "diffusion potential." The Onsager-Fuoss expression may be modified to express Δ_1 as a function of concentration.

$$D = (D^0 + f(c)) \left(1 + C \frac{d \ln \gamma}{dc} \right) \quad (26)$$

The expression of D as a function of concentration for uranyl nitrate diffusing into water was presented in Equation 25. Thus this study shows that

$$f(c) = -24.463 \times 10^6 c^{0.5} + 39.566 \times 10^{-6} c^{1.0} \\ -17.85 \times 10^{-6} c^{2.0} + 3.355 \times 10^{-6} c^{3.0}$$

The error in the formal solution and the numerical solution includes the error of analysis. The formal solution depends on the ratio of the final average concentration to the initial concentration. This ratio includes an analysis error of the same magnitude in both elements and the combined error must be greater than either portion. The numerical solution relies on the final concentration only and thus would embrace a smaller error due to analytical procedures. The formal solution is an exponential series. An error analysis of the formal solution in the C/C_0 ratio of 0.40 revealed that a change of 1.0 per cent in the C/C_0 ratio was reflected by a 2.5 per cent change in the calculated value of D. This may be confirmed by examining Table XXXVIII.

The numerical method solution involves two errors: the error in the forward difference method for concentration as a function of time and the error in the central difference method for the concentration as a function of distance. The forward difference calculations contain an error of the order of ΔT (which is 0.01 for the coarse grid and 0.0016 for the fine grid solution). The central difference calculations contain an error of the order of $(\Delta X)^2$ (which is 0.01 in the case of the coarse grid and 0.0016 in the case of the fine grid). In either case, the sum of these two errors is of the order of twice the time increment. Thus, it is possible to obtain accuracies as high as needed by increasing the time and distance increments (49). In general, then, the numerical solution allows a smaller calculational error than does the formal solution. For diffusion times short enough to allow from 15 to 25 per cent of the initial contents to diffuse out of the capillary, the numerical solution has an even greater accuracy. At these ranges, the analyses are less accurate for both methods of solution, but the transcendental solution error would be considerably larger in this range because of the exponential form of the solution equation.

The 0.05 M and 0.25 M points are probably the least accurate of the data. These experiments were not performed a sufficient number of times to allow claims of accuracy. Experience with the curve-fitting and numerical solution showed that the lower concentrations affected all of the concentrations above them to a considerable extent. Since the replicated experimental data were not evenly distributed among the various concentrations, a more equitable regression would be obtained by weighing the experimental data according to the number

of replicates used at each concentration. The weighing procedure was adopted for the regression calculations. The curve, as presented, represents the best fit to the weighted experimental data. The shape of the higher concentration portion could have been changed somewhat, upward about 2.0%, by ignoring the two lowest concentration average values in assaying the calculated results. Certainly more precise data at the lower concentrations are needed.

The similarity between the curves presented in Figure 10 and Figure 11 should be noted. The deviations between the integral and differential diffusion coefficients for various uranyl nitrate concentrations are summarized in Table IV. Table IV also tabulates the deviations of the experimentally determined final concentrations from the final concentrations calculated by the numerical method solution. With one exception the deviations between the two values are within ± 5.0 per cent. This could have been improved by additional small changes in the model for D, but little advantage would have accrued over the results as reported. The results of the formal solution and the numerical solution are presented in Figure 10 and Figure 11. The dotted portion of the curves represent an extrapolation to Nernst's limiting value for D, while the solid lines drawn from D downward are the limiting slope values for dilute solutions of uranyl nitrate as shown in the calculations in Appendix C. In both cases, the lower concentration point shows that the curve is approaching the limiting slope value from above, which would indicate that the slope of the curve at very low concentration does agree with the theory for dilute solutions.

The activity factor, $(1 + C \frac{d \ln Y}{dc})$, of the Nernst-Hartley expres-

TABLE IV

Comparison of Experimental and Calculated Results
Uranyl Nitrate Diffusing into Water

Initial Conc., Molar	Average		Percent Deviation of Calculated Value	Diffusion Coefficient $\times 10^6 \text{ cm sec}^{-1}$		Percent Deviation of Differential Value
	<u>Final Molar Concentration</u> Experimental	Calculated		Integral	Differential	
0.05	0.022	0.021	-4.55	7.10	5.20	-26.76
0.25	0.114	0.116	+1.75	6.84	5.33	-22.08
0.50	0.228	0.231	+1.32	6.90	7.17	+ 3.91
0.60	0.260	--	--	7.37	7.82	+ 6.11
0.71	0.292	--	--	7.90	8.37	+ 5.95
0.75	0.307	--	--	8.04	8.60	+ 6.97
0.86	0.346	--	--	8.05	9.05	+12.42
1.00	0.409	0.431	+5.38	8.19	9.33	+13.92
1.50	0.620	0.609	-1.77	8.03	9.26	+15.32
2.00	0.813	0.782	-3.81	8.21	8.67	+ 5.60

sion for D ,

$$D = D^0 \left(1 + C \frac{d \ln \gamma}{dC} \right)$$

is a separately available experimental quantity. Robinson and Stokes (47) show that the variation in the diffusion coefficient, D , with concentration is in most cases many times greater than that of the quantity $D / \left(1 + C \frac{d \ln \gamma}{dC} \right)$. As a result, the greater part of the change in D may be attributed to the non-ideality in thermodynamic behavior which is allowed for by the factor $\left(1 + C \frac{d \ln \gamma}{dC} \right)$. Thus a thermodynamic corrected diffusion coefficient is defined as being

$$\mathcal{D} = \frac{D}{\left(1 + C \frac{d \ln \gamma}{dC} \right)}$$

Figure 12 and Figure 13 present the differential and integral diffusion coefficients of this study corrected by the thermodynamic factor as a function of uranyl nitrate concentration. The thermodynamic correction factors were obtained by making use of the data from Robinson and Stokes (47). Figure 20, Appendix C, presents the activity and activity coefficient data for uranyl nitrate as derived from the tables in Robinson and Stokes (47). Figure 21, Appendix C, presents the computer results of the calculation for $\left(1 + C \frac{d \ln \gamma}{dC} \right)$. Two increment sizes were used and the final results were obtained from the smoothed curve drawn through the two machine calculations. This was done to minimize the oscillations in the solution that resulted when the concentration increment was reduced.

The shape of the two curves is a reflection of the reported values of the measured integral coefficients and the calculated differential coefficients. The variation of the quantity \mathcal{D} is indeed

much less than that of D , as reported by Robinson and Stokes (47).

The rather abrupt change in the behavior of \mathcal{D} with increasing uranyl ion concentration indicates that a species other than the simple uranyl ion must be present in the solutions. The formation of ion pairs, the hydration or polymerization of the uranyl nitrate might explain the observed phenomenon. The extrapolation of the two curves to the Nernst limiting diffusion coefficient value at zero concentration showed, in the case of the integral coefficient calculations, an unexpected deviation. In the case of the differential diffusion coefficients, the extrapolation to the limiting value was a smooth continuation of the curve at the lowest concentration point considered. The fact that the slope of the extrapolated portion of the curve did not change suggested that the solution of Fick's Second Law, assuming a concentration-dependent D , provided a diffusion coefficient that was more amenable to the observed diffusion behavior of dilute electrolytes.

Figure 14 and Figure 15 are two of the results of the coarse grid numerical solution and present the concentration profile in the capillary as a function of time. Figure 16 presents the final concentration profile in a capillary calculated by the numerical solution employing the fine grid. A comparison of Figure 15 with Figure 16 shows that the final distribution is, for practical purposes, identical in both cases. Thus the coarse grid solution was as accurate as the fine grid solution for establishing the concentration distribution in the capillaries. The integrated average values from both cases, as reported in Tables XVIII, IX, and X, differ by approximately 1.6 per cent. The finer grid would result in a more accurate integrated average value, since the increment size was much smaller. The finer

TABLE V

Thermodynamic Correction Factor
as a
Function of Uranyl Nitrate Concentration
(Smoothed values)

Molar Concentration	Corrected Factor	Molar Concentration	Corrected Factor
0.0	1.000	1.20	1.958
0.05	0.800	1.25	2.015
0.10	0.860	1.30	2.065
0.15	0.925	1.35	2.110
0.20	0.970	1.40	2.160
0.25	1.024	1.45	2.215
0.30	1.062	1.50	2.265
0.35	1.095	1.55	2.315
0.40	1.145	1.60	2.370
0.45	1.188	1.65	2.420
0.50	1.245	1.70	2.480
0.55	1.297	1.75	2.530
0.60	1.345	1.80	2.555
0.65	1.395	1.85	2.580
0.70	1.445	1.90	2.595
0.75	1.500	1.95	2.610
0.80	1.550	2.00	2.620
0.85	1.605	2.05	2.628
0.90	1.660	2.10	2.630
0.95	1.705	2.15	2.635
1.00	1.760	2.20	2.635
1.05	1.810	2.25	2.632
1.10	1.850	2.30	2.630
1.15	1.910	2.35	2.625

TABLE VI

Thermodynamic-Corrected Integral Diffusion
Coefficient as a Function of
Uranyl Nitrate Concentration

Uranyl Nitrate, Molar Conc.	Thermodynamic Correction Factor	$D \times 10^6$	$\mathcal{D} \times 10^6$
	$(1 + C \frac{d \ln \gamma}{dC})$	$\text{cm}^2 \text{ sec}^{-1}$	$\text{cm}^2 \text{ sec}^{-1}$
0.000	1.000	8.72	8.72
0.036	0.800	7.10	8.86
0.182	0.960	6.84	7.13
0.364	1.110	6.90	6.22
0.430	1.175	7.37	6.27
0.501	1.245	7.90	6.35
0.528	1.277	8.04	6.30
0.603	1.350	8.05	5.96
0.704	1.450	8.19	5.65
1.060	1.825	8.03	4.40
1.406	2.175	8.21	3.77

Figure 12

Thermodynamic-Corrected Integral
Diffusion Coefficient of Uranyl Nitrate
into Water as a Function of Concentration

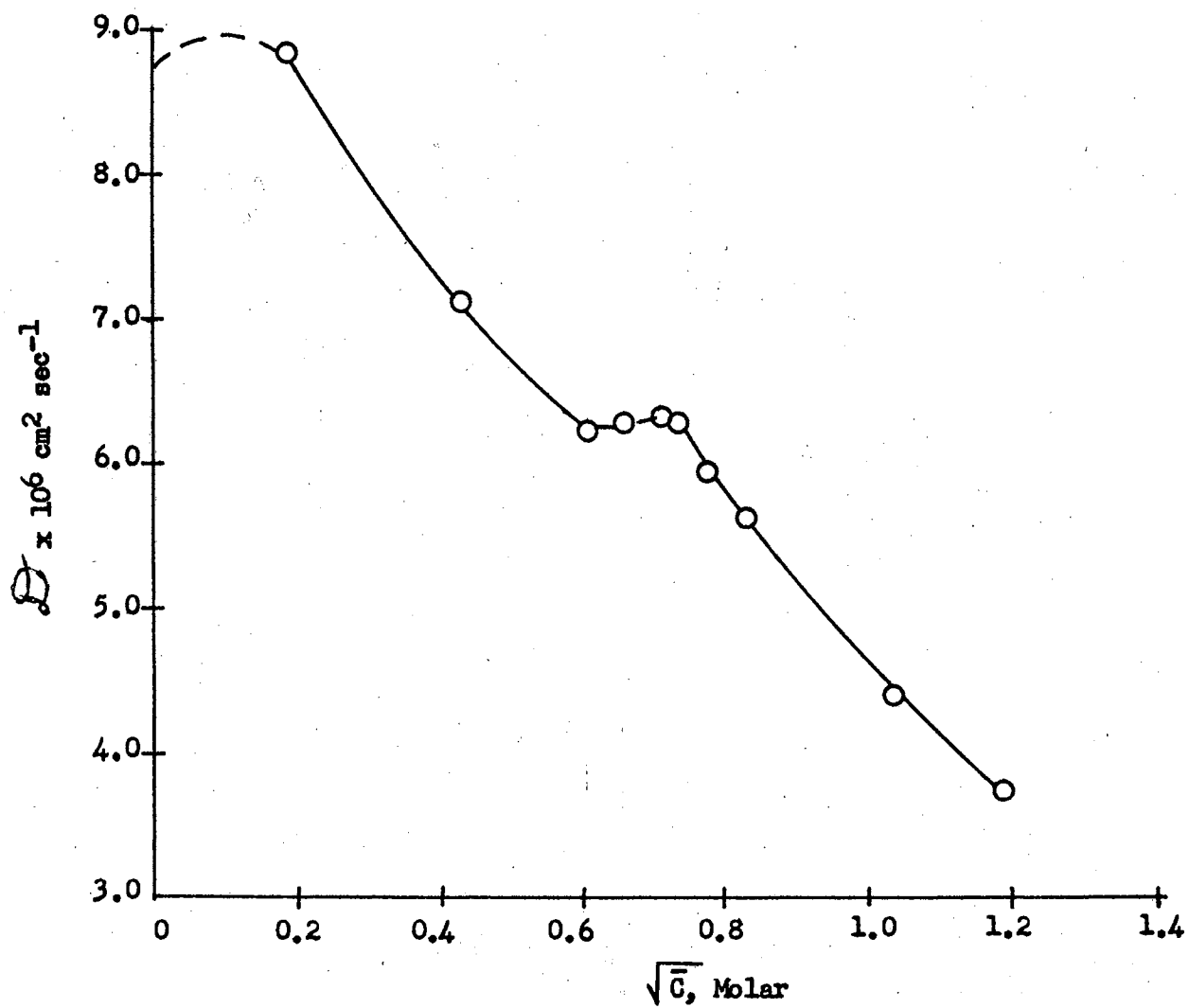


TABLE VII

Thermodynamic-Corrected Differential Diffusion
Coefficient as a Function of
Uranyl Nitrate Concentration

Uranyl Nitrate, Molar Conc.	Thermodynamic Correction Factor $(1 + C \frac{d \ln \gamma}{dC})$	$D \times 10^6$ $\text{cm}^2 \text{sec}^{-1}$	$\mathcal{D} \times 10^6$ $\text{cm}^2 \text{sec}^{-1}$
0.00	1.00	8.73	8.73
0.05	.791	5.20	6.57
0.10	.850	4.78	5.62
0.20	.970	5.02	5.18
0.30	1.060	5.69	5.37
0.40	1.145	6.45	5.63
0.50	1.245	7.17	5.76
0.60	1.345	7.82	5.81
0.70	1.445	8.36	5.79
0.80	1.550	8.79	5.67
0.90	1.660	9.12	5.49
1.00	1.757	9.33	5.31
1.10	1.860	9.45	5.08
1.20	1.960	9.49	4.84
1.30	2.065	9.47	4.59
1.40	2.165	9.38	4.33
1.50	2.270	9.26	4.08
1.60	2.370	9.12	3.85
1.70	2.485	8.97	3.61
1.80	2.555	8.83	3.46
1.90	2.595	8.73	3.36
2.00	2.620	8.67	3.31

Figure 13

Thermodynamic-Corrected Differential Diffusion Coefficient of
Uranyl Nitrate as a Function of Concentration

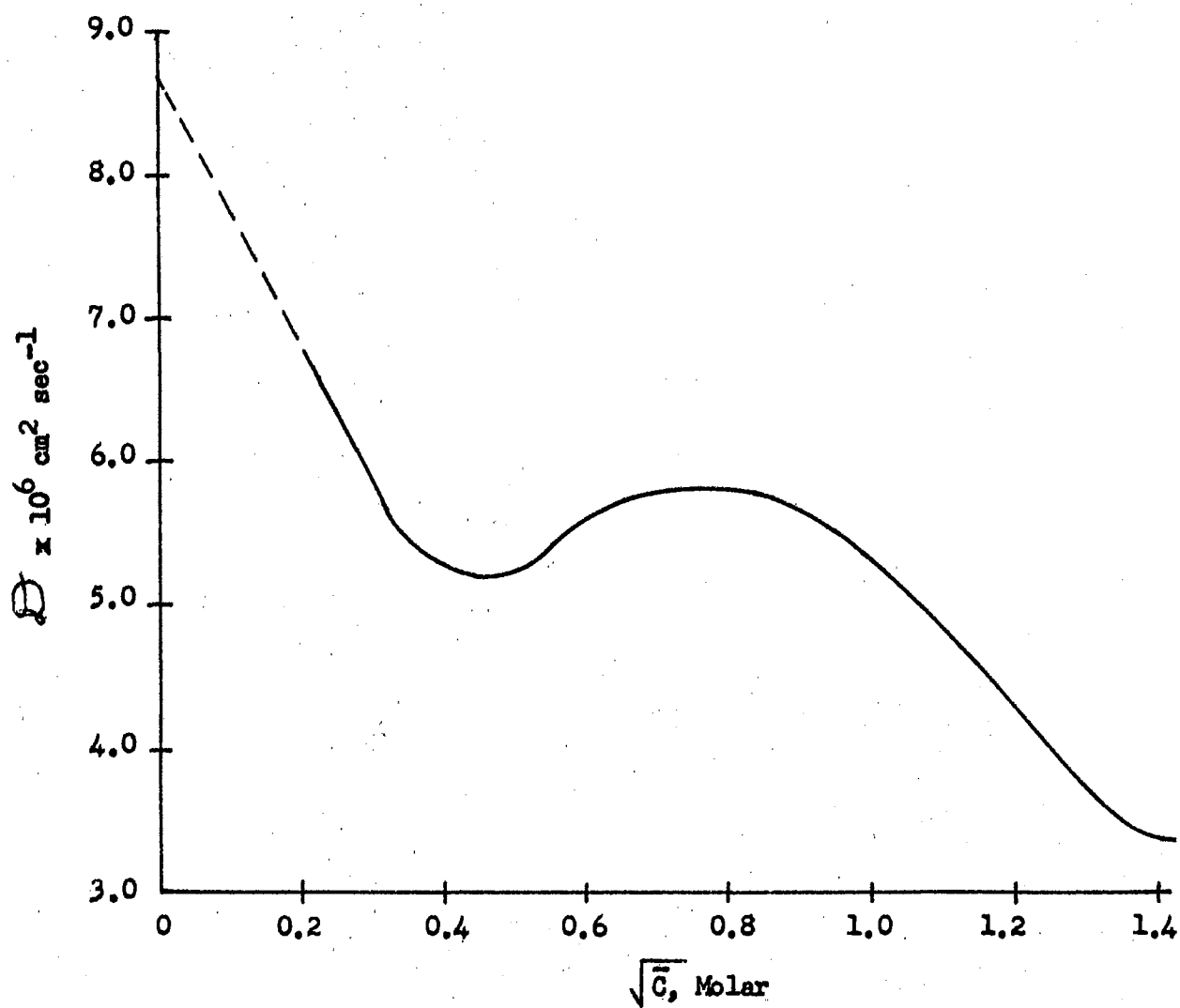


TABLE VIII

Uranyl Nitrate Concentration Distribution in Capillary
as a
Function of Time
(Coarse Grid Numerical Solution)
 $C_0 = 2.0 \text{ M}$

Capillary Length Increment	Time Increment						
	0.01	0.1	0.2	0.4	0.6	0.8	1.0
0.1	1.366	0.707	0.575	0.461	0.398	0.351	0.309
0.2	2.000	1.158	0.940	0.757	0.658	0.584	0.520
0.3	2.000	1.509	1.236	0.007	0.868	0.771	0.687
0.4	2.000	1.756	1.480	1.206	1.049	0.929	0.827
0.5	2.000	1.899	1.672	1.386	1.206	1.065	0.946
0.6	2.000	1.965	1.809	1.538	1.341	1.180	1.045
0.7	2.000	1.991	1.898	1.660	1.451	1.274	1.125
0.8	2.000	1.998	1.949	1.748	1.534	1.345	1.184
0.9	2.000	1.999	1.975	1.803	1.587	1.390	1.222
1.0	2.000	2.000	1.984	1.825	1.609	1.408	1.236

Final average concentration = 0.7936 M

Figure 14

Concentration in Capillary as a Function of Time
(Initial Concentration = 2.0 M)

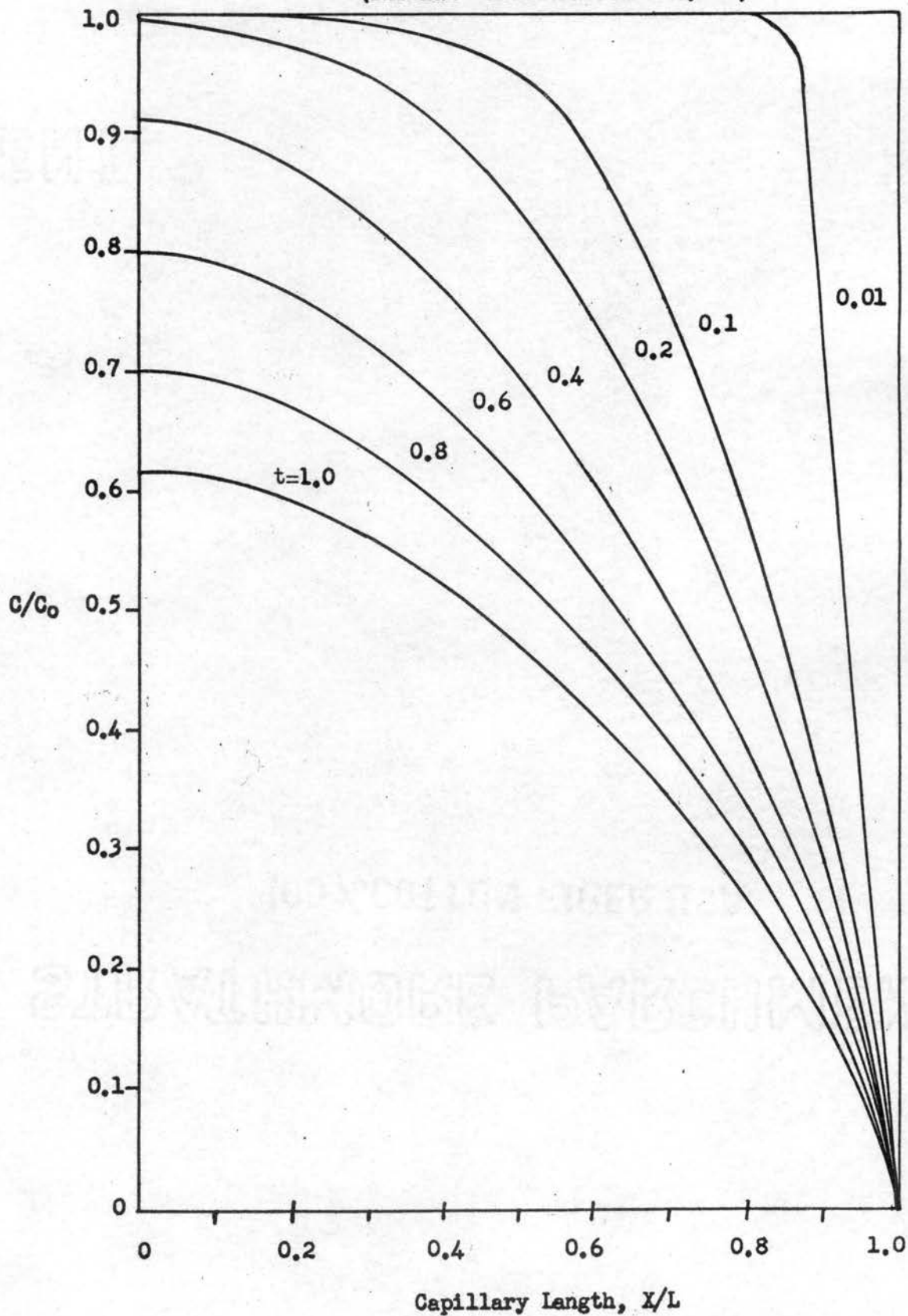


TABLE IX

Uranyl Nitrate Concentration in Capillary
as a
Function of Time
(Coarse Grid Numerical Solution)
 $C_0 = 0.05 \text{ M}$

Capillary Length Increment	Time Increment						
	0.01	0.1	0.2	0.4	0.6	0.8	1.0
0.1	0.040	0.017	0.012	0.008	0.006	0.005	0.005
0.2	0.050	0.032	0.024	0.017	0.013	0.012	0.010
0.3	0.050	0.043	0.034	0.025	0.020	0.018	0.015
0.4	0.050	0.048	0.041	0.032	0.027	0.023	0.021
0.5	0.050	0.049	0.046	0.038	0.033	0.029	0.025
0.6	0.050	0.049	0.048	0.043	0.038	0.033	0.030
0.7	0.050	0.049	0.049	0.046	0.041	0.037	0.033
0.8	0.050	0.050	0.049	0.048	0.044	0.039	0.036
0.9	0.050	0.050	0.050	0.049	0.045	0.041	0.037
1.0	0.050	0.050	0.050	0.050	0.046	0.042	0.038

Final average concentration = 0.02166 M

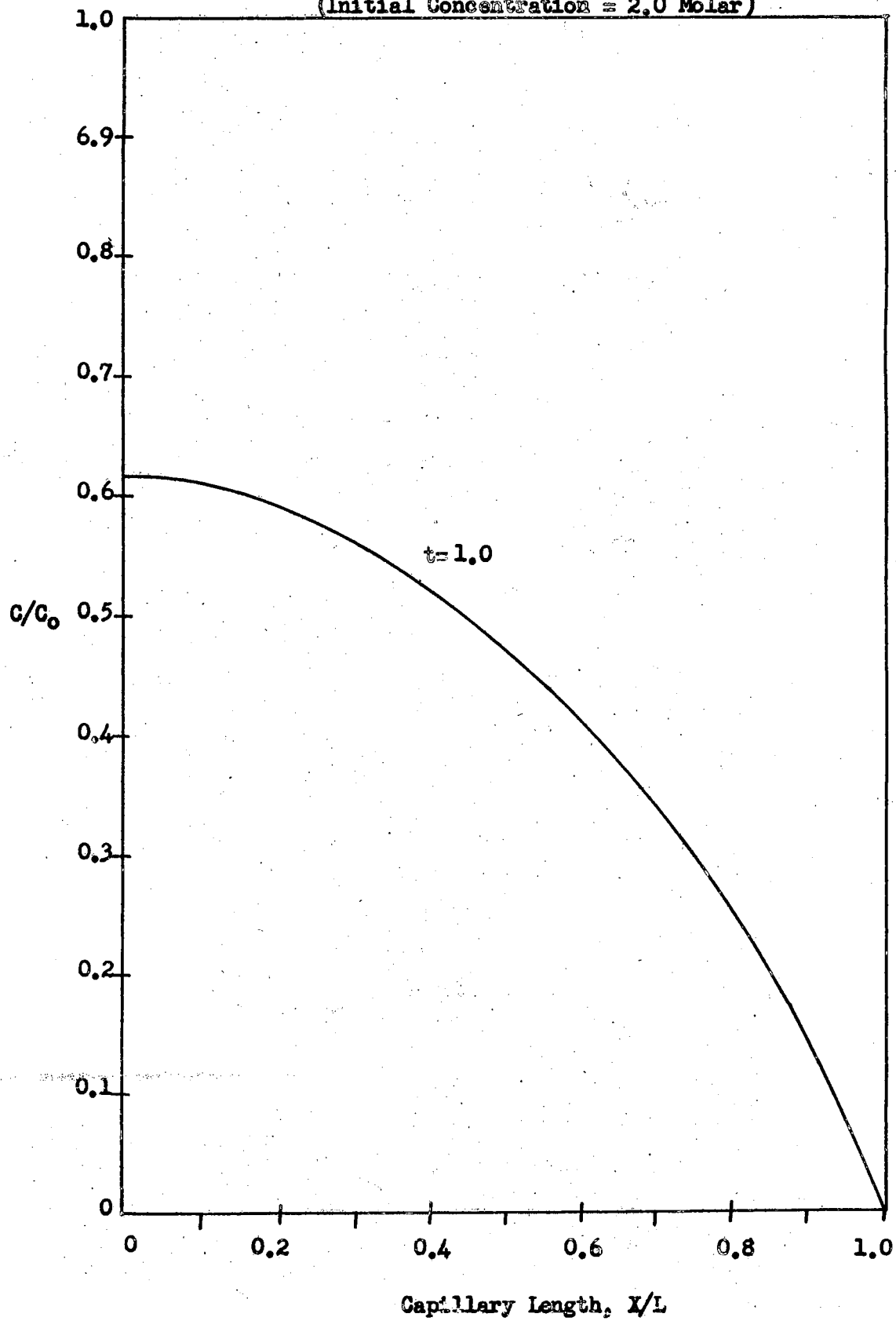
TABLE X

Final Uranyl Nitrate Concentration Distribution in Capillary
(Numerical Solution)

Capillary Length Increment	Molar Concentration					
Initial Conc.	0.050000	0.25000	0.50000	1.00000	1.50000	2.00000
25	0.00186	0.00945	0.02062	0.04882	0.08359	0.12306
24	0.00382	0.02018	0.04504	0.10687	0.17545	0.24363
23	0.00585	0.03178	0.07160	0.16522	0.25907	0.34680
22	0.00794	0.04400	0.09900	0.21990	0.33310	0.43649
21	0.01006	0.05656	0.12621	0.26999	0.39917	0.51640
20	0.01219	0.06926	0.15254	0.31567	0.45884	0.58895
19	0.01432	0.08187	0.17757	0.35737	0.51325	0.65565
18	0.01643	0.09423	0.20109	0.39554	0.56323	0.71748
17	0.01851	0.10617	0.22302	0.43055	0.60933	0.77510
16	0.02054	0.11760	0.24335	0.46269	0.65196	0.82892
15	0.02252	0.12842	0.26209	0.49220	0.69140	0.87923
14	0.02441	0.13856	0.27930	0.51926	0.72786	0.92620
13	0.2662	0.14798	0.29503	0.54401	0.76148	0.97995
12	0.02793	0.15666	0.30932	0.56656	0.79235	1.01050
11	0.02952	0.16458	0.32222	0.58700	0.82053	1.04787
10	0.03100	0.18173	0.33378	0.60538	0.84608	1.08203
9	0.03234	0.17812	0.34404	0.62177	0.86900	1.11292
8	0.03355	0.18374	0.35303	0.63619	0.88930	1.14050
7	0.03461	0.18859	0.36078	0.64868	0.90699	1.16468
6	0.03552	0.19270	0.36731	0.65926	0.92205	1.18539
5	0.03628	0.19605	0.37266	0.66795	0.93448	1.20256
4	0.03687	0.19867	0.37683	0.67476	0.94426	1.21614
3	0.03730	0.20056	0.37983	0.67970	0.95138	1.22606
2	0.03757	0.20171	0.38169	0.68277	0.95583	1.23228
1	0.03767	0.20214	0.38239	0.68398	0.95762	1.23478
Average Conc.	0.021001	0.116301	0.230871	0.430801	0.609221	0.782101

Figure 16

Concentration in Capillary as a Function of Time
Fine Grid Numerical Solution
(Initial Concentration = 2.0 Molar)



grid problem required extremely long solution times when using an IBM 1620. The machine size and time available for calculations might dictate the selection of a coarse grid; if so, the results of this study indicate that the increased accuracy of the finer grid is within the experimental error of the methods employed. In addition, the coarse grid solution was reprogrammed to allow the use of 12 decimal places in all calculations instead of the customary 8 places. The final results were unchanged, indicating that truncation error in the numerical methods was not an appreciable factor.

An attempt was made to measure the diffusion coefficients with smaller concentration differences. A 1.0 M uranyl nitrate solvent was carefully prepared and analyzed for uranium content. Solutes were prepared with uranium concentrations of 1.05, 1.10, 1.15, 1.20, 1.30, 1.50, and 1.75 M. The measurement of the final capillary concentration involved the difference between the sample count and the count of the solvent. The error of the experimental procedure involved in the difference introduced as much as a 50 per cent fluctuation in the calculated diffusion coefficients. Considerable time and effort was expended to improve the results, but with little success. The most promising technique would appear to be the use of either U-235 or U-233 isotopes to enhance the counting statistics of low concentration solutes.

An effort was made to determine a relationship between the measured and calculated diffusion coefficients and the viscosities of the solutes and water solvent. The brief study was unable to establish any consistent relationship between the diffusion coefficients of uranyl nitrate and the measured viscosities of the solutes

and water solvent.

Uranyl Nitrate Diffusing into Nitric Acid

A series of diffusion experiments was undertaken to study qualitatively the diffusion of uranyl nitrate into nitric acid. The pertinent data collected are listed in Table XXVI, of Appendix A. Figures 17 and 18 present the results of the study. The diffusion coefficients were the averaged results of four replicates in each case. In most instances the standard error in the diffusion coefficient was ± 5.0 per cent or less. The scale chosen for the presentation was too small to accurately reflect the standard errors of this magnitude. The circles around each data point are an approximation of this magnitude. In those cases where the diffusion standard error exceeds ± 5.0 per cent, the deviation about the mean value was shown as a vertical line at the point in question.

An increase in nitric acid concentration in the solvent lowered the measured diffusion rate of the uranyl ion. A study of the family of curves reveals an "undulation" of the diffusion curve which progresses from the higher concentrations toward the lower concentrations as the acid content of the solvent is increased. One possible explanation is that the diffusion rates are affected by the hydrolysis of the uranyl nitrate and the hydrolysis is affected by the counter-diffusion of the nitrate ion. The diffusion rate of the nitrate ion is dependent on the nitrate ion concentration. At some concentration of nitric acid concurrent diffusion of the nitrate ion may occur, while counter-current diffusion may take place at a different concentration, and a

condition of no net difference in nitrate ion diffusion may occur at still another nitric acid concentration. In addition, polymer formation by the uranyl nitrate may cause such behavior. This polymerization is also affected by the pH of the solute. The observed phenomenon necessitates much more careful and detailed study, in an effort to fully explain and quantitatively assay the behavior.

Uranium Diffusion into 30% TBP-Amsco

A brief study was made of the diffusion rates of uranyl nitrate into a mixture of 30% tributyl phosphate and Amsco. The solute was obtained by saturating a 30% TBP-Amsco solution with uranyl nitrate. The analyses by spectrophotometer of the resulting solute showed that the uranyl ion concentration was 0.454 molar. A second solute was prepared by volumetric dilution with 30% TBP-Amsco of the saturated solute. Analyses of the more dilute solute showed the uranyl ion concentration to be 0.100 molar. The experimental data was presented in Table XXVII, Appendix A, while Table XII, page 80, is a summary of the results.

The summary of the TBP-Amsco data points out the effect of shorter diffusion times on the error in the diffusion coefficient. In general the magnitude of the error in D was much larger for an equivalent \bar{C} when the C/C_0 ratio was above 0.45. The condition is borne out by the standard errors shown in the summary Table XII. An average value of the diffusion coefficients obtained in runs T-2 and T-3 was $1.88 \times 10^{-6} \text{ cm}^2 \text{ sec}^{-1}$ and for runs T-6 and T-7 the average D was $1.78 \times 10^{-6} \text{ cm}^2 \text{ sec}^{-1}$. While this was a difference of approximately 5.3 per cent, the number of runs made was not sufficiently

TABLE XI

Summary of Diffusion Data
on Uranyl Nitrate Diffusing into Nitric Acid

Solvent Nitric Acid, Conc., Molar	Initial Solute Conc., Molar	Average \bar{C}	Average	Average	Average
			\bar{C}	Standard Error Per Cent	$D \times 10^6$ $\text{cm}^2 \text{sec}^{-1}$
4.0	0.5	0.615	0.98	3.90	3.62
	1.0	0.884	1.02	3.39	10.04
	1.5	1.048	0.30	4.73	4.84
	2.0	1.219	0.67	5.33	6.02
2.0	0.5	0.637	0.31	3.29	6.08
	1.0	0.891	0.53	3.95	7.39
	1.5	1.069	0.20	5.23	2.85
	2.0	1.223	0.32	5.78	4.29
1.5	0.5	0.631	1.13	3.87	18.24
	1.0	0.883	0.12	4.38	5.71
	1.5	1.070	0.43	5.47	3.25
	2.0	1.229	0.68	5.54	2.38
1.0	0.5	0.622	0.56	4.72	7.96
	1.0	0.866	2.94	5.71	11.54
	1.5	1.067	0.33	5.19	4.14
	2.0	1.204	0.96	7.01	3.40
0.5	0.5	0.622	0.56	4.62	8.70
	1.0	0.855	0.36	6.60	2.02
	1.5	1.047	0.68	6.62	7.10
	2.0	1.165	2.85	7.42	3.18
0.1	0.5	0.600	0.48	7.10	5.30
	1.0	0.839	0.41	8.01	4.34
	1.5	1.028	1.41	8.04	4.37
	2.0	1.157	2.07	8.71	4.28

Figure 17

Integral Diffusion Coefficient of Uranyl Nitrate
into Nitric Acid as a Function of Concentration

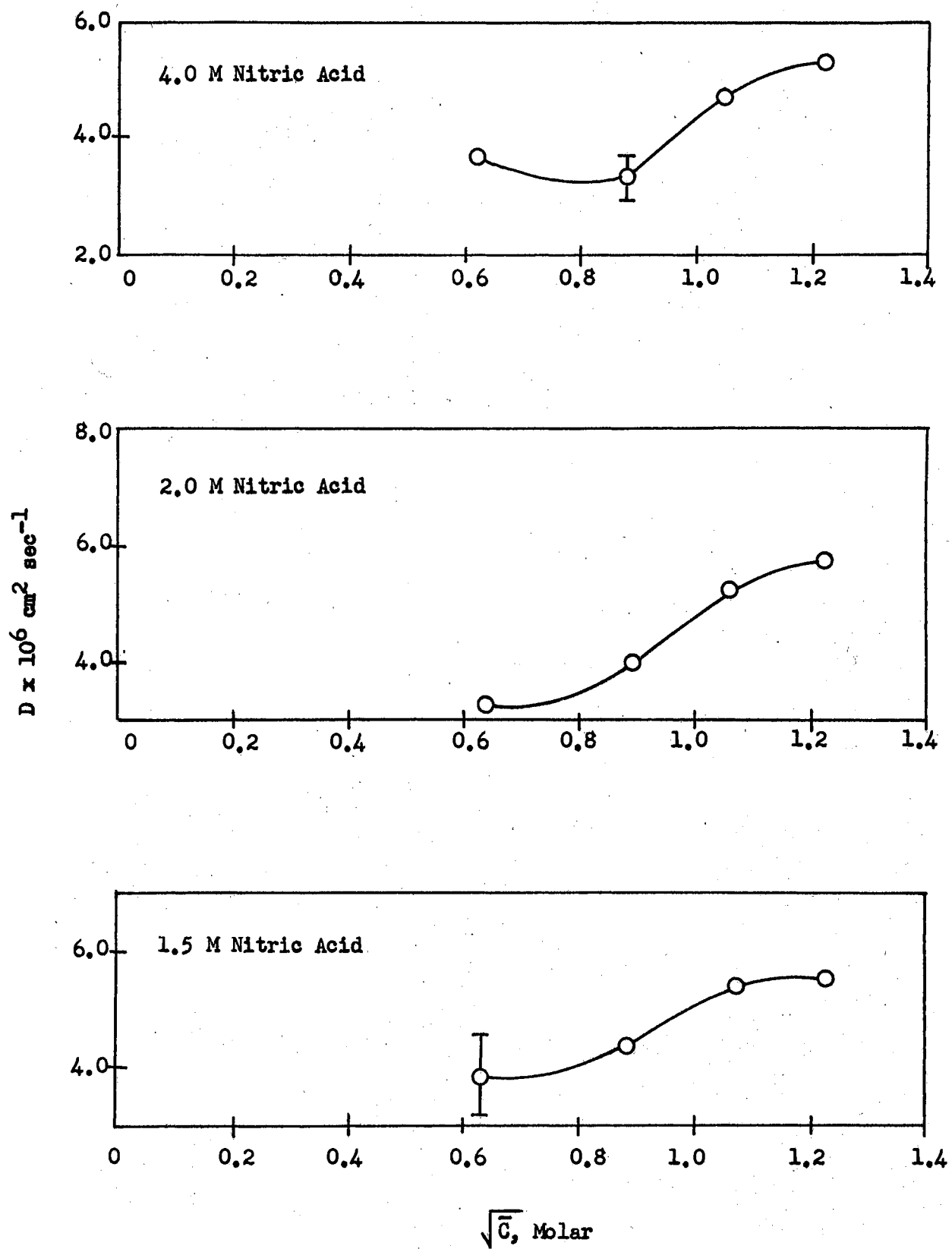
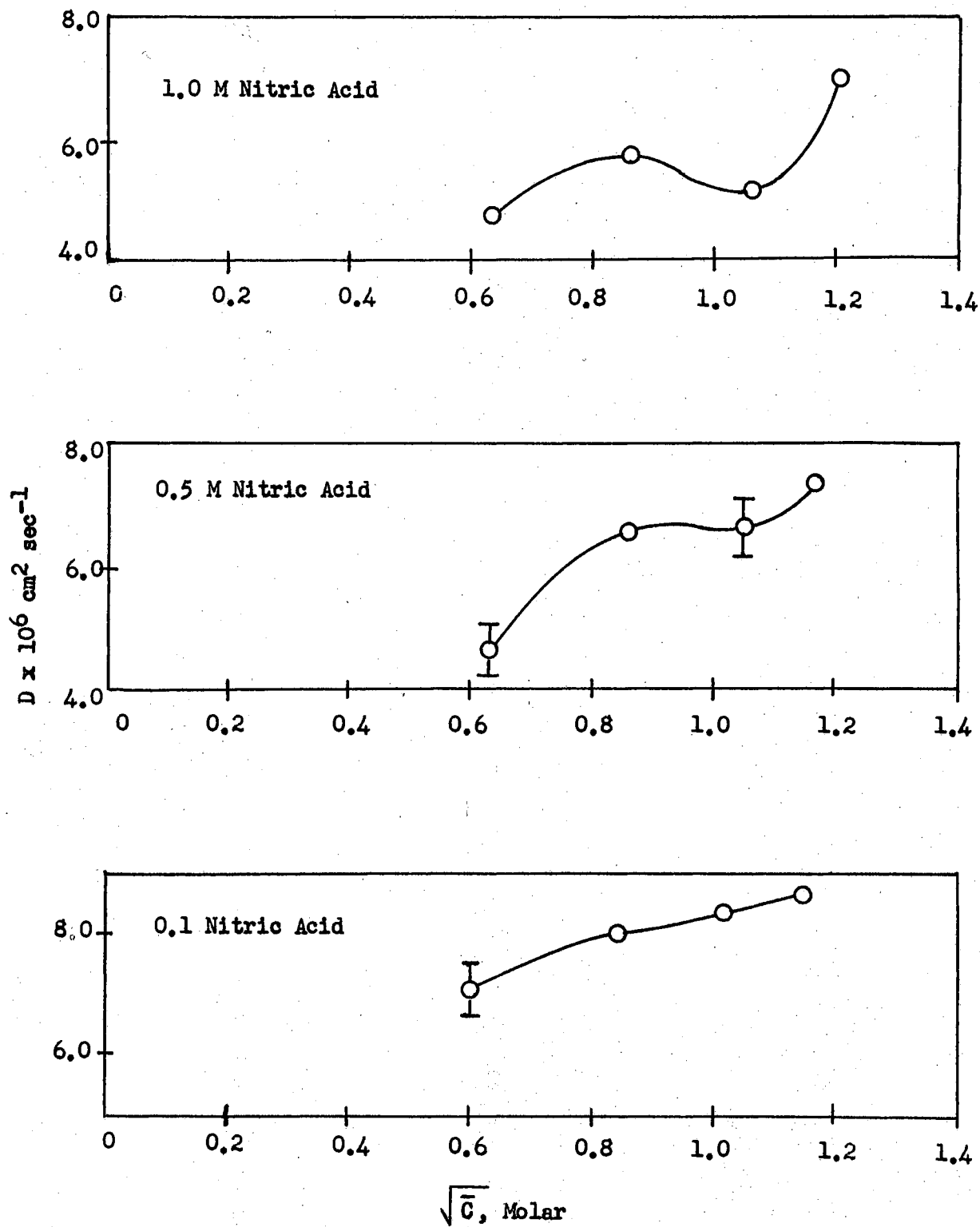


Figure 18

Integral Diffusion Coefficient of Uranyl Nitrate
into Nitric Acid as a Function of Concentration
(Continued)



large to assure that this difference was significant.

TABLE XII

Summary of Experimental Data
 Uranyl Nitrate Diffusing into Tributyl Phosphate-Amsco

Run No.	Time, Hours	Solute Initial Conc., Molar	Average \bar{C}	Average	Average	Average
				\bar{C}	Standard Error Per cent	$D \times 10^6$ $\text{cm}^2 \text{sec}^{-1}$
T-1	60	0.454	.610	0.82	2.00	14.25
T-2	120	0.454	.585	0.31	1.85	4.56
T-3	144	0.454	.575	0.25	1.91	2.93
T-6	144	0.100	.272	0.30	1.77	4.12
T-7	144	0.100	.272	0.85	1.79	8.88

CHAPTER VI

CONCLUSIONS AND RECOMMENDATIONS

The diffusion of uranyl nitrate has been studied employing the capillary cell method.

The integral diffusion coefficients of the system uranyl nitrate diffusing into water have been calculated. A formal solution of Fick's Second Law was employed with the assumption that the diffusion coefficient was not concentration dependent.

The differential diffusion coefficient of uranyl nitrate diffusing into water has been determined by assuming a polynomial relationship between the diffusion coefficient and the concentration. The relationship between the diffusion coefficient and the uranyl nitrate concentrations studied was determined as

$$D = 8.7379 \times 10^{-6} + 24.463 \times 10^{-6} C^{0.5} \\ + 39.566 \times 10^{-6} C^{1.0} - 17.857 \times 10^{-6} C^{2.0} \\ + 3.355 \times 10^{-6} C^{3.0}$$

The numerical method solution of Fick's Second Law was capable of calculating final average concentrations in the capillaries within 5.0 per cent of the experimentally determined values.

The diffusion coefficient as a function of concentration for the system uranyl nitrate diffusing into water exhibited two deflection points. A minimum occurred between the concentrations of 0.10

and 0.20 M uranyl ion. A maximum deflection point occurred at a uranyl concentration between 0.70 and 1.0 M. Between the concentrations of 1.0 and 2.0 M uranyl ion, the diffusion coefficient again decreased with increasing concentration of the uranium.

The concentration profiles calculated by the numerical method indicate that the concentration of the solute near the closed end of the capillaries changes with time.

The experimental determination of the effect of nitric acid concentration in the solvent on the diffusion coefficient of uranyl nitrate showed that as the nitrate concentration increased the diffusion coefficient of the uranyl nitrate decreased. The decrease in the diffusion coefficient with increasing nitric acid was greater for the higher concentrations of uranyl nitrate.

The experimental determination of the diffusion coefficient of a uranyl nitrate-tributyl phosphate complex diffusing into a 30% TBP-Amsco solvent was reported. The experimental methods used in this study were unable to determine a significant difference in the diffusion coefficients reported for a solute containing 0.454 M uranyl ion and for a 0.10 M uranyl ion solute.

An internal sample liquid scintillation technique was developed for the determination of the alpha activity of small-volume samples. The method requires rather ordinary radioactive counting equipment and has the advantage of a minimum of sample handling preparatory to analysis. The accuracy of the determinations was within 2.0 per cent of the values reported by spectrophotometric methods and well within the experimental error of the capillary technique employed in the study.

Recommendations

The uranyl nitrate solutes be enriched with U-235 or U-233 salts to enhance the accuracy of the radioactive counting and a similar study be undertaken to obtain more accurate diffusion coefficients.

The capillary technique be employed in a study of the diffusion of uranyl nitrate diluted with an aqueous solution traced with tritium. This study should be made in an effort to determine the effect of hydrolysis on the diffusion coefficients.

The effect of ion size on diffusion should be studied by employing the nitrate salts of other radioactive heavy metals on the solute in the capillary method.

The numerical solution method should be applied to other experimental systems in which there is reason to believe that the diffusion coefficient is concentration dependent.

The effect of the anion gradient on the uranyl ion diffusion be studied by employing the diaphragm cell technique.

SELECTED BIBLIOGRAPHY

1. Anderson, Donald Keith.
PhD Thesis. "Mutual Diffusion in Associated Binary Liquid Mixtures." University of Washington (1960).
2. Anderson, J. S. and K. J. Saddington.
J. Chem. Soc., Suppl. No. 2; S381 (1946).
3. Axtmann, R. C. and Lecont Cathy.
Int. J. Appl. Rad. and Iso., 4; 261 (1954).
4. Basson, J. K. and J. Steyn
J. of Phys. Soc. Proceedings, Sec. A, 67; 297 (1954).
5. Basson, J. K.
Anal. Chem., 28; 1472 (1956).
6. Bell, C. G., Jr. and F. W. Hayes.
Liquid Scintillation Counting.
Pergamon Press, New York, 1958.
7. Bird, R. B., W. E. Stewart, and E. N. Lightfoot.
Transport Phenomena.
John Wiley and Sons, New York, 1960.
8. Brown, R. D., W. B. Bunger, W. L. Marshall, and C. H. Secoy.
J. Amer. Chem. Soc., 76; 1532 (1954).
9. Caldwell, C. S. and A. L. Babb.
J. Phys. Chem., 60; 51 (1956).
10. Crank, J.
The Mathematics of Diffusion.
Oxford University Press, London, 1955.
11. Davidson, J. D. and P. Feigelson.
Int. J. of Appl. Rad. and Isotopes, 2; 1 (1957).
12. Dizdar, Z. I., and I. D. Obrenovic.
Proc. Int. Conf. on the Peaceful Uses of Atomic Energy, 28;
543, New York, United Nations, 1958.
13. Eckert, E. R. G. and R. M. Drake, Jr.
Heat and Mass Transfer, 2nd ed.
McGraw-Hill Book Co., Inc., New York, 1959.

14. English, A. C., T. E. Granshaw, P. Demers, J. A. Harney, E. P. Hincks, J. A. Verden, and A. N. May.
Phys. Rev., 72; 253 (1947).
15. Ewell, R. H., and H. Eyring.
J. Chem. Phys. 5; 726 (1936).
16. Eyring, H. J.
Chem. Phys. 4; 283 (1936).
17. Eyring, H. and J. Hirschfelder.
J. Phys. Chem., 41; 249 (1937).
18. Farmer, C. and I. A. Berstein.
Science, 115; 460 (1952).
19. Goldenberg, N. and E. S. Amis.
Z. Physik Chem. 22; 63 (1959).
20. Gosting, L. J.
Advances in Protein Chemistry, Vol. XI
Anson, Bailey and Edsall, Ed.
Academic Press, Inc., New York, 1956.
21. Hahn, H. T.
U. S. Atomic Energy Commission Document. HW 31803 Rev. (1954).
22. Harned, H. S. and B. B. Owen.
The Physical Chemistry of Electrolyte Solutions.
Reinhold Publishing Corp., 3rd ed., New York, 1958.
23. Hartley, G. S. and J. Crank.
Trans. Faraday Soc. 45; 801 (1949).
24. Hayes, F. N., D. G. Ott, and V. N. Kerr.
Nucleonics, 14, No. 1; 42 (1956).
25. Hayes, F. N.
Int. J. of Appl. Rad. and Isotopes, 1; 46 (1956).
26. Hirschfelder, J., D. Stevenson, and H. Eyring.
J. Chem. Phys., 5; 896 (1937).
27. Hwang, Jenn Linn.
J. Chem. Phys. 20; 1320 (1952).
28. Kallmann, H. P., M. Furst, and F. H. Brown.
Nucleonics, 14; No. 4; 48 (1956).
29. Katz, Joseph J. and Glenn T. Seaborg.
The Chemistry of the Actinide Elements.
John Wiley and Sons., Inc., New York, 1957,

30. Lewis, G. N., M. Randall, K. S. Pitzer, and L. Brewer.
Thermodynamics, 2nd ed.
McGraw-Hill Book Co., Inc., New York, 1961.
31. Longworth, L. G.
J. Am. Chem. Soc., 69; 2510 (1947).
32. McKay, H. A. C.
Chem. and Ind., 51; 1549 (1954).
33. Mills, R.
J. Am. Chem. Soc., 77; 3454 (1955).
34. Mills, R. and J. W. Kennedy.
J. Amer. Chem. Soc. 75; 5696 (1953).
35. Mills, R. and E. W. Godbole.
Australian J. Chem., 11; 1 (1958).
36. Olander, Donald R.
J. Phys. Chem. 67; 1011 (1963).
37. Onsager, L. and R. M. Fuoss.
Phys. Rev., 37; 405 (1931).
38. Onsager, L. and R. M. Fuoss.
Phys. Rev., 38; 2265 (1931).
39. Onsager, L. and R. M. Fuoss.
J. Phys. Chem., 36; 2689 (1932).
40. Onsager, L. and R. M. Fuoss.
Ann. N. Y. Acad. Sci., 46; 241 (1945).
41. Othmer, D. F. and M. S. Thaker.
Ind. and Eng. Chem., 45; 589 (1953).
42. Overman, R. T. and H. M. Clark.
Radioisotope Techniques.
McGraw-Hill Book Co., Inc., New York, 1960.
43. Powell, R. E., W. E. Roseveare, and H. Eyring.
Ind and Eng. Chem., 33; 430 (1941).
44. Price, William J.
Nuclear Radiation Detection.
McGraw-Hill Book Co., Inc., New York, 1958.
45. Reynolds, S. A. and Bruce, R. F, et al Ed.
Progress in Nuclear Energy, Series III, Vol. 2, p 562.
Pergamon Press, New York, 1958.

46. Richtmyer, R. D.
Difference Methods for Initial-value Problems.
Interscience Publishers, New York, 1957.
47. Robinson, R. A. and Stokes, R. H.
Electrolyte Solutions, 2nd Ed.
Butterworths Scientific Publications, London, 1954.
48. Roseveare, W. E., R. E. Powell, and H. Eyring.
J. Appl. Phys., 12; 669 (1941).
49. Salvadori, M. G. and M. L. Baron.
Numerical Methods in Engineering, 2nd ed.
Prentice-Hall, Inc., Englewood Cliffs., N. J., 1961.
50. Seliger, H. H.
Int. J. Appl. Rad. and Isotopes, 8, No. 1; 29 (1960)
51. Stearn, A. E., E. M. Irish, and H. Eyring.
J. Phys. Chem., 44; 981 (1940).
52. Steel, Robert G. D. and James H. Torrie.
Principles and Procedures of Statistics.
McGraw-Hill Book Co., Inc., New York, 1960.
53. Sutherland, W.
Phil. Mag. 2; 784 (1905).
54. Wang, J. H.
J. Amer. Chem. Soc., 73; 510 (1951).
55. Wang, J. H.
J. Amer. Chem. Soc., 73; 4181 (1952).
56. Wang, J. H.
J. Amer. Chem. Soc., 74; 1182 (1952).
57. Wang, J. H. and J. W. Kennedy.
J. Amer. Chem. Soc., 72; 2080 (1950).
58. Wilke, C. R. and Pin Chang.
A.I.Ch.E. J., 1; 264 (1955).
59. Williams J. W. and L. C. Cady.
Chem. Rev., 14; 171 (1934).

APPENDIX A

TABLE XIII

Differential Scintillation Spectrum Data
for Uranyl Nitrate
(Primary Solvent-Toluene)

Photomultiplier voltage = 1185

Window width, voltage = 5.0

Amplifier gain:

Coarse = 1.0

Fine = 100

Conc. Uranyl Nitrate	Energy Level, Volts	Total Count, 10 Min.	Background Count per minute	Net Count per minute
2.0	31.5	1248	0.0	124.8
	27.0	3039	0.6	303.3
	22.5	6947	1.8	692.9
	18.0	12441	4.8	1239.3
	13.5	7293	35.8	693.5
1.5	31.5	1134	0.0	113.4
	27.0	2700	0.6	269.4
	22.5	6022	1.8	600.4
	18.0	4020	4.8	397.2
1.0	31.5	991	0.0	99.1
	27.0	2300	0.6	229.4
	22.5	4252	1.8	423.4
	18.0	3201	4.8	315.3
0.5	31.5	484	0.0	48.4
	27.0	1189	0.6	118.3
	22.5	2034	1.8	201.6
	18.0	1643	4.8	159.5
0.1	31.5	143	0.0	14.3
	27.0	304	0.6	29.8
	22.5	409	1.8	39.1
	18.0	334	4.8	28.6

TABLE XIV

Differential Scintillation Spectrum Data
for Uranyl Nitrate
(Primary Solvent-Xylene)

Photomultiplier voltage = 1185

Window width voltage = 5.0

Amplifier gain:

Coarse = 1.0

Fine = 100

Conc. Uranyl Nitrate	Energy Level, Volts	Total Count, 10 min.	Background Count per minute	Net Count per minute
2.0	31.5	960	0.0	96.0
	27.0	3010	7.9	293.1
	22.5	7604	25.5	734.9
	18.0	10616	52.8	1008.8
	13.5	5250	81.7	443.3
	9.0	2990	124.0	175.0
1.5	31.5	535	0.0	53.5
	27.0	2368	7.9	228.9
	22.5	5404	25.5	514.9
	18.0	7496	52.8	696.8
	9.0	2260	124.0	102.0
	1.0	31.5	434	0.0
27.0		2013	7.9	193.4
22.5		4314	25.5	405.9
18.0		4872	52.8	434.4
9.0		2258	124.0	101.8
0.5		31.5	237	0.0
	27.0	1194	7.9	111.5
	22.5	2542	25.5	228.7
	18.0	2734	52.8	220.6
	9.0	1811	124.0	57.1
	0.1	31.5	62	0.0
27.0		219	7.9	14.0
22.5		403	25.5	14.8
18.0		678	52.8	15.0
9.0		1487	124.0	24.7

TABLE XV

Differential Scintillation Spectrum Data
for Uranyl Nitrate
(Primary Solvent 50:50-Xylene-Toluene)

Photomultiplier voltage = 1185
 Window width voltage = 5.0
 Amplifier gain
 Coarse = 1.0
 Fine = 100

Conc. Uranyl Nitrate	Energy Level, Volts	Total Count, 10 min.	Background Count per minute	Net Count per minute
2.0	31.5	1198	6.8	113.0
	27.0	2844	19.0	265.4
	22.5	7078	38.3	669.5
	18.0	10910	76.8	1014.2
	13.5	7274	118.6	608.8
	9.0	3630	205.4	157.6
1.5	31.5	843	0.9	83.4
	27.0	2178	7.9	209.9
	22.5	5168	25.5	491.3
	18.0	7628	52.8	710.0
	13.5	4687	81.7	387.0
	9.0	2935	118.1	175.4
1.0	31.5	860	2.9	83.1
	27.0	2019	5.9	196.0
	22.5	4211	14.0	407.1
	18.0	4405	38.5	402.0
	13.5	2148	63.6	151.2
	9.0	1762	97.1	79.1
0.5	31.5	488	0.3	48.5
	27.0	1172	4.5	112.7
	22.5	2089	15.2	193.7
	18.0	2018	38.5	163.3
	13.5	1165	67.0	49.5
	9.0	1361	94.0	42.1
01	31.5	97	2.0	7.7
	27.0	239	5.9	18.0
	22.5	405	14.0	26.5
	18.0	636	38.5	25.1
	13.5	820	83.6	18.4
	9.0	1097	97.1	12.6

TABLE XVI

Differential Scintillation Spectrum Data
for Ra D-E-F (Po-210)

Photomultiplier tube voltage = 1170
 Window width voltage = 1.0
 Amplifier gain
 Coarse = 1.0
 Fine = 75

Energy Level, Volts,	Total Count, 10 min.	Background Count per minute	Net Count per minute
90.0	0	0.0	0.0
85.5	3	0.0	0.3
81.0	4	0.0	0.4
76.5	7	0.0	0.7
72.0	13	0.0	1.3
67.5	18	0.0	1.8
63.0	29	0.0	2.9
58.5	46	0.0	4.6
54.0	61	0.0	6.1
49.5	86	0.0	8.6
45.0	123	0.0	12.3
40.5	353	0.0	35.3
36.0	702	0.0	70.2
35.1	772	0.0	77.2
34.2	860	0.0	86.0
33.3	836	0.0	83.6
32.4	882	0.0	88.2
31.5	881	0.0	88.1
30.6	794	0.0	79.4
29.7	776	0.0	77.6
28.8	730	0.0	73.0
27.9	606	0.0	60.6
27.0	508	0.4	50.4
22.5	268	0.8	26.0
21.6	243	0.9	23.4
20.7	272	1.0	26.2
19.8	282	1.0	27.2
18.9	270	1.0	26.0
18.0	264	1.1	25.3
17.1	281	1.1	27.0
15.3	325	1.2	31.3
13.5	332	1.2	32.0
9.0	350	4.0	31.0
4.5	718	32.0	39.8

TABLE XVII

Differential Scintillation Spectrum Data
for Po-210 - U-238 Mixture

Photomultiplier tube voltage = 1170

Window width voltage = 0.5

Amplifier gain

Coarse = 1.0

Fine = 75

Energy Level Volts,	Total Count, 10 min.	Background Count per minute	Net Count per minute
90.00	0	0.0	0.0
81.00	0	0.0	0.0
72.00	0	0.0	0.0
63.0	0	0.0	0.0
54.00	0	0.0	0.0
45.00	0	0.0	0.0
36.00	0	0.0	0.0
32.40	317	0.5	31.2
31.95	326	0.8	31.8
31.50	343	1.0	33.3
31.05	364	1.0	35.4
30.15	413	0.6	40.7
29.70	414	0.6	40.8
29.25	437	0.6	43.1
2880	473	0.5	46.8
28.35	473	0.5	46.8
27.90	479	0.5	47.4
27.45	482	0.5	47.7
27.00	474	0.5	46.9
26.55	478	0.7	46.1
26.10	468	0.5	46.3
25.65	480	0.8	47.2
25.20	477	0.6	46.3
25.75	474	1.0	46.4
25.30	482	0.9	47.3
24.85	476	1.0	46.9
24.40	473	1.0	46.4
22.95	508	1.0	49.8
22.50	502	0.8	49.4
22.05	512	0.8	50.4
21.60	514	0.9	50.5
21.15	533	1.0	52.4
20.70	532	1.0	52.2
20.25	534	1.2	52.2
19.80	533	1.2	52.1
19.35	529	1.0	51.9

TABLE XVII (Continued)

Energy Level, volt,	Total Count, 10 min.	Background count per minute	Net Count per minute
18.90	531	1.0	52.1
18.45	532	1.0	52.2
18.00	496	1.0	48.6
17.55	483	1.0	47.3
17.10	460	2.0	44.9
16.65	438	1.1	42.7
16.20	399	1.1	38.8
15.75	373	1.1	36.2
15.30	347	1.2	33.5
14.85	312	1.1	30.1
14.40	277	1.2	26.5
13.95	248	1.2	23.6
13.50	234	1.2	22.2
11.25	194	1.4	17.8
9.00	209	4.0	16.9
6.75	268	9.0	17.8
4.50	360	17.0	19.0

TABLE XVIII

Differential Scintillation Spectrum Data
for 1.0 Molar Uranyl Nitrate

Photomultiplier voltage = 1170
 Window width voltage = 1.0
 Amplifier gain
 Coarse = 1.0
 Fine = 75

Energy Level, volts,	Total Count per minute	Background Count per minute	Net Count per minute
90	16	0.0	1.6
81	19	0.0	1.9
72	25	0.0	2.5
63	34	0.0	3.4
54	41	0.0	4.1
45	44	0.0	4.4
36	73	0.0	7.3
27	270	0.4	26.6
26.1	332	0.5	32.7
25.2	433	0.5	42.8
24.3	514	0.6	50.8
23.4	612	0.7	60.5
22.5	757	0.8	74.9
21.6	824	0.9	81.5
20.7	932	1.0	91.2
19.8	1024	2.0	100.4
18.9	1024	2.0	100.4
18.0	924	1.2	91.2
17.1	793	1.2	78.1
16.2	670	1.2	65.8
15.3	483	1.2	47.1
13.5	274	1.2	26.2
9.0	230	4.0	19.0
4.5	601	31.9	28.2

TABLE XIX

EXPERIMENTAL DATA

Uranyl Nitrate Diffusing into Water

Temp. = 25 °C ± .01 °C

Diffusion Time = 40 hours

Run No.	Capillary No.	Solute Initial Conc., Molar	C/C ₀	Solute Final Conc., Molar	\bar{C} , Molar	$\sqrt{\bar{C}}$	D x 10 ⁶ cm ² sec ⁻¹
27	1	0.05	0.445	0.022	0.36	0.190	7.10
	4	0.25	0.439	0.110	0.180	0.424	7.28
	5	0.50	0.428	0.214	0.307	0.597	7.53
	7	0.75	0.412	0.309	0.530	0.641	7.95
28	1	0.25	0.474	0.119	0.179	0.544	6.39
	4	0.50	0.425	0.213	0.356	0.597	7.60
	7	0.75	0.406	0.305	0.527	0.596	8.12
202	1	0.50	0.445	0.223	0.362	0.602	7.16
	5	0.60	0.425	0.255	0.428	0.654	7.59
	3	0.71	0.424	0.301	0.506	0.711	7.60
	9	0.86	0.386	0.332	0.596	0.772	8.42
203	10	0.50	0.429	0.215	0.358	0.598	7.26
	7	0.60	0.443	0.266	0.433	0.658	7.11
	11	0.71	0.415	0.295	0.503	0.709	7.65
	8	0.86	0.400	0.344	0.602	0.776	8.29

TABLE XIX (Continued)

Run No.	Capillary No.	Solute Initial Conc., Molar	C/C_0	Solute Final Conc., Molar	\bar{C} , Molar	$\sqrt{\bar{C}}$	$D \times 10^6$ cm ² sec ⁻¹
204	1	0.50	0.467	0.234	0.367	0.606	6.58
	5	0.60	0.422	0.253	0.427	0.653	7.69
	3	0.71	0.403	0.286	0.498	0.706	8.19
	9	0.86	0.408	0.351	0.606	0.778	7.78
205	1	0.50	0.469	0.235	0.368	0.607	6.53
	5	0.60	0.443	0.266	0.433	0.658	7.11
	3	0.71	0.404	0.287	0.499	0.706	8.17
	9	0.86	0.408	0.351	0.606	0.778	7.78
206	10	0.50	0.447	0.224	0.362	0.602	6.80
	7	0.60	0.434	0.260	0.430	0.656	7.35
	11	0.71	0.407	0.289	0.500	0.707	7.89
	8	0.86	0.410	0.352	0.607	0.779	8.00
16	III-1	0.50	0.578	0.289	0.395	0.628	4.01
	III-2	1.00	0.374	0.374	0.687	0.829	9.21
	III-3	1.50	0.438	0.657	1.079	1.039	7.39
	III-4	2.00	0.402	0.804	1.402	1.184	8.36
17	I-1	0.50	0.427	0.213	0.357	0.597	7.56
	I-2	1.00	0.420	0.428	0.714	0.845	7.60
	I-4	2.00	0.475	0.950	1.475	1.214	6.45
18	I-1	0.50	0.439	0.219	0.360	0.599	7.22
	I-2	1.00	0.445	0.445	0.723	0.850	7.13
	I-4	2.00	0.393	0.786	1.393	1.180	8.66

TABLE XIX (Continued)

Run No.	Capillary No.	Solute Initial Conc., Molar	C/C ₀	Solute Final Conc., Molar	\bar{C} , Molar	$\sqrt{\bar{C}}$	D x 10 ⁶ cm ² sec ⁻¹
20	III-1	0.50	0.578	0.289	0.394	0.628	4.47
	III-2	1.00	0.376	0.376	0.688	0.829	9.23
	III-3	1.50	0.373	0.559	1.029	1.015	9.24
	III-4	2.00	0.393	0.786	1.393	1.180	8.42
21	7	0.50	0.319	0.209	0.355	0.596	7.75
	5	1.00	0.476	0.476	0.738	0.759	6.29
	4	1.50	0.439	0.659	1.079	1.039	7.28
	1	2.00	0.391	0.782	1.391	1.179	8.68
22	4	1.50	0.424	0.637	1.068	1.034	7.69
	1	2.00	0.436	0.855	1.426	1.195	7.62
23	1	0.50	0.390	0.195	0.347	0.589	8.73
	4	1.00	0.381	0.381	0.690	0.831	8.98
	5	1.50	0.416	0.625	1.062	1.031	7.84
	7	2.00	0.379	0.759	1.379	1.175	8.93
24	1	0.50	0.428	0.214	0.357	0.598	7.67
	7	2.00	0.401	0.802	1.401	1.184	8.35
25	1	0.50	0.460	0.230	0.365	0.604	6.67
	4	1.00	0.384	0.384	0.692	0.832	8.87
	5	1.50	0.389	0.585	1.045	1.021	8.71
	7	2.00	0.396	0.793	1.396	1.182	8.42

TABLE XX

Analysis of Variance
Randomized Complete - Block Design
Uranyl Nitrate into Water

Source	df	SS	MS	F
Blocks	9	10.18	1.13	
Treatments	3	15.03	5.01	3.620##
Error	21	28.93	1.38	
Total	33	54.14	1.64	

F is significant

Average Values

Initial Conc., Molar	$D \times 10^6$ $\text{cm}^2 \text{ sec}^{-1}$	Sample Standard Error, Per cent
0.50	6.81	8.0
1.00	8.20	1.5
1.50	8.18	3.3
2.00	8.29	2.65

TABLE XXI

Analysis of Variance
Randomized Complete - Block Design
Uranyl Nitrate into Water
(Low concentrations)

Source	df	SS	MS	F
Blocks	1	0.09	0.09	
Treatments	3	1.82	0.606	3.46
Error	2	0.35	0.175	
Total	6	2.26	0.377	

Average Values

Initial Conc., Molar	$D \times 10^6$ $\text{cm}^2 \text{sec}^{-1}$	Sample Standard Error, Per cent
0.05	7.10	---
0.25	6.84	2.0
0.50	7.61	0.5
0.75	8.03	1.25

TABLE XXII

Analysis of Variance
Randomized Complete - Block Design
Uranyl Nitrate Diffusing into 2.0 M Nitric Acid

Source	df	SS	MS	F
Blocks	3	2.72	0.906	
Treatments	3	7.39	2.463	5.262##
Error	8	3.75	0.468	
Total	14	13.86	0.985	

F is significant

Average Values

Initial Conc., Molar	$D \times 10^6$ $\text{cm}^2 \text{sec}^{-1}$	Sample Standard Error, Per cent
0.50	3.25	4.36
1.00	3.95	7.40
1.50	5.23	2.80
2.00	5.78	4.20

TABLE XXIII

Analysis of Variance
Randomized Complete - Block Design
Uranyl Nitrate Diffusing into 1.0 M Nitric Acid

Source	df	SS	MS	F
Blocks	2	1.30	0.650	
Treatments	3	10.00	3.333	15.72##
Error	4	0.85	0.212	
Total	9	12.15	1.350	

F is significant

Average Values

Initial Conc., Molar	$D \times 10^6$ $\text{cm}^2 \text{sec}^{-1}$	Sample Standard Error, Per cent
0.50	4.51	8.1
1.00	5.50	11.2
1.50	5.19	17.9
2.00	7.01	3.1

TABLE XXIV

Analysis of Variance
Randomized Complete - Block Design
Uranyl Nitrate Diffusing into 0.5 M Nitric Acid

Source	df	SS	MS	F
Blocks	2	0.50	0.25	
Treatments	3	13.08	4.36	11.27###
Error	6	2.32	0.387	
Total	11	15.90	1.45	

F is significant

Average Values

Initial Conc., Molar	$D \times 10^6$ $\text{cm}^2 \text{sec}^{-1}$	Sample Standard Error, Per cent
0.50	4.62	2.75
1.00	6.60	3.50
1.50	6.28	7.40
2.00	7.42	3.80

TABLE XXV

Analysis of Variance
Randomized Complete - Block Design
Uranyl Nitrate Diffusing into 0.1 M Nitric Acid

Source	df	SS	MS	F
Blocks	3	1.90	0.633	
Treatments	3	4.90	1.633	3.099
Error	9	4.74	0.527	
Total	15	11.54	0.769	

Average Values

Initial Conc., Molar	$D \times 10^6$ $\text{cm}^2 \text{sec}^{-1}$	Sample Standard Error, Per cent
0.50	7.10	5.25
1.00	8.00	4.40
1.50	8.04	4.40
2.00	8.71	4.25

TABLE XXVI

Experimental Data

Uranyl Nitrate Diffusing into Nitric Acid

Temp. = 25 °C, \pm .01 °C

Diffusion Time = 48 hours

Concentration of Acid Solvent = 4.0 M HNO₃

Run No.	Capillary No.	Solute Initial Conc., Molar	C/C ₀	Solute Final Conc., Molar	\bar{C} , Molar	\sqrt{C}	D x 10 ⁶ cm ² sec ⁻¹
47	7	1.00	0.571	0.571	0.785	0.884	3.50
	11	1.50	0.493	0.729	1.120	1.058	4.76
	8	2.00	0.445	0.891	1.445	1.202	5.87
48	10	0.50	0.549	0.275	0.387	0.622	3.74
	7	1.00	0.645	0.645	0.822	0.907	2.40
	11	1.50	0.423	0.785	1.012	1.006	4.21
	8	2.00	0.519	1.037	1.519	1.232	4.40
49	10	0.50	0.530	0.268	0.384	0.620	3.91
	7	1.00	0.540	0.540	0.770	0.887	3.94
	11	1.50	0.459	0.689	1.094	1.046	5.32
	8	2.00	0.456	0.912	1.456	1.207	5.53
50	10	0.50	0.461	0.231	0.365	0.604	3.45
	7	1.00	0.499	0.499	0.750	0.866	3.70
	11	1.50	0.559	0.838	1.169	1.081	4.64
	8	2.00	0.520	1.040	1.520	1.233	5.53

TABLE XXVI (Continued)

Concentration of Acid Solvent - 2.0 M HNO₃

Run No.	Capillary No.	Solute Initial Conc., Molar	C/C ₀	Solute Final Conc., Molar	\bar{C} , Molar	$\sqrt{\bar{C}}$	D x 10 ⁶ cm ² sec ⁻¹
19	III-3	1.00	0.619	0.619	0.810	0.900	3.37
	III-2	1.50	0.514	0.771	1.136	1.066	5.46
	III-1	2.00	0.516	1.032	1.516	1.231	5.29
29	1	0.50	0.611	0.306	0.403	0.635	3.49
	4	1.00	0.574	0.574	0.787	0.887	4.18
	5	1.50	0.534	0.801	1.151	1.073	4.95
	7	2.00	0.484	0.968	1.484	1.218	6.09
30	7	0.50	0.632	0.316	0.408	0.369	3.09
	5	1.00	0.566	0.566	0.783	0.885	4.30
	4	1.50	0.521	0.782	1.141	1.068	5.28
	1	2.00	0.492	0.984	1.492	1.221	5.96

Concentration of Acid Solvent = 1.5 M HNO₃

31	5	1.00	0.533	0.533	0.767	0.876	4.97
	4	1.50	0.521	0.782	1.141	1.068	5.28
	1	2.00	0.490	0.981	1.490	1.221	6.00
32	1	0.50	0.617	0.309	0.404	0.636	3.38
	2	1.00	0.562	0.562	0.781	0.884	4.31
	3	1.50	0.493	0.839	1.170	1.081	5.86
	5	2.00	0.482	0.969	1.482	1.219	6.07

TABLE XXVI (Continued)

Run No.	Capillary No.	Solute Initial Conc., Molar	C/C ₀	Solute Final Conc., Molar	\bar{C} , Molar	$\sqrt{\bar{C}}$	D x 10 ⁶ cm ² sec ⁻¹
33	1	0.50	0.522	0.261	0.381	0.617	5.27
	2	1.00	0.591	0.591	0.796	0.892	3.76
	3	1.50	0.532	0.798	1.149	1.072	4.98
	5	2.00	0.566	1.131	1.566	1.251	4.30
34	1	0.50	0.641	0.320	0.410	0.640	2.98
	2	1.00	0.554	0.554	0.777	0.881	4.48
	3	1.50	0.496	0.745	1.122	1.059	5.77
	5	2.00	0.497	0.995	1.497	1.224	5.77
Concentration of Acid Solvent = 1.0 M HNO ₃							
35	5	0.50	0.528	0.264	0.382	0.618	5.09
	3	1.00	0.473	0.473	0.737	0.858	6.32
	2	1.50	0.517	0.776	1.138	1.067	5.14
	1	2.00	0.441	0.883	1.442	1.200	7.24
36	5	0.50	0.564	0.282	0.391	0.625	4.34
	3	1.00	0.527	0.527	0.764	0.874	5.09
	2	1.50	0.502	0.753	1.126	1.061	5.59
	1	2.00	0.441	0.882	1.441	1.200	7.25
37	6	1.50	0.536	0.804	1.152	1.073	4.85
	8	2.00	0.465	0.931	1.465	1.211	6.53

TABLE XXVI (Continued)

Concentration of Acid Solvent = 0.50 M HNO₃

Run No.	Capillary No.	Solute Initial Conc., Molar	C/C ₀	Solute Final Conc., Molar	\bar{C} , Molar	$\sqrt{\bar{C}}$	D x 10 ⁶ cm ² sec ⁻¹
38	2	0.50	0.570	0.285	0.392	0.626	4.16
	3	1.00	0.447	0.447	0.724	0.851	6.99
	6	1.50	0.447	0.670	1.085	1.042	6.94
	8	2.00	0.428	0.857	1.428	1.195	7.49
39 III	2	0.50	0.563	0.282	0.391	0.625	4.28
	3	1.00	0.456	0.456	0.728	0.853	6.77
	6	1.50	0.436	0.655	1.077	1.038	6.22
	8	2.00	0.418	0.835	1.418	1.099	7.79
40	8	0.50	0.512	0.256	0.378	0.615	5.42
	6	1.00	0.483	0.482	0.742	0.861	6.04
	3	1.50	0.50	0.750	1.125	1.061	5.69
	2	2.00	0.445	0.889	1.445	1.202	6.98
Concentration of Acid Solvent = 0.10 M HNO ₃							
41	8	0.50	0.425	0.212	0.356	0.597	7.60
	6	1.00	0.435	0.435	0.718	0.847	7.25
	3	1.50	0.442	0.663	1.081	1.040	7.12
	2	2.00	0.416	0.832	1.416	1.190	7.74
42	2	0.50	0.484	0.242	0.371	0.609	5.99
	3	1.00	0.384	0.384	0.692	0.832	8.76
	6	1.50	0.401	0.601	1.051	1.025	8.20
	8	2.00	0.388	0.776	1.388	1.178	8.66

TABLE XXVI (Continued)

Run No.	Capillary No.	Solute Initial Conc., Molar	C/C_0	Solute Final Conc., Molar	\bar{C} , Molar	$\sqrt{\bar{C}}$	$D \times 10^6$ cm ² sec ⁻¹
43	2	0.50	0.432	0.216	0.358	0.598	7.27
	3	1.00	0.396	0.396	0.698	0.835	8.40
	6	1.50	0.407	0.611	1.056	1.027	8.01
	8	2.00	0.360	0.720	1.360	1.086	9.54
44	8	0.50	0.427	0.214	0.357	0.597	7.53
	6	1.00	0.422	0.422	0.711	0.843	7.61
	3	1.50	0.382	0.573	1.037	1.018	8.82
	2	2.00	0.376	0.753	1.376	1.173	8.90

TABLE XXVII

Experimental Data

Data from Diffusion of Uranyl Nitrate Complex
into 30% Tributyl Phosphate-Amsco Mixture

Temp. = 25 °C, ± .01 °C

Run No.	Capillary No.	Time, Hours	Solute Initial Conc., Molar	C/C ₀	Solute Final Conc., Molar	\bar{C} , Molar	\sqrt{C}	D x 10 ⁶ cm ² sec ⁻¹
T-1	1	60	0.454	0.599	0.272	0.363	0.602	2.46
	3		0.454	0.631	0.286	0.370	0.608	2.06
	4		0.454	0.689	0.313	0.384	0.619	1.48
T-2	1	120	0.454	0.496	0.225	0.340	0.583	1.96
	2		0.454	0.519	0.236	0.345	0.587	1.74
	3		0.454	0.529	0.240	0.347	0.589	1.68
	4		0.454	0.486	0.221	0.338	0.581	2.03
T-3	1	144	0.454	0.464	0.211	0.333	0.577	1.85
	2		0.454	0.464	0.211	0.333	0.577	1.80
	3		0.454	0.452	0.205	0.330	0.574	1.91
	4		0.454	0.434	0.197	0.326	0.571	2.06
T-6	1	144	0.100	0.476	0.048	0.074	0.272	1.76
	2		0.100	0.499	0.050	0.075	0.274	1.57
	3		0.100	0.451	0.045	0.073	0.270	1.91
	4		0.100	0.465	0.047	0.074	0.272	1.84

TABLE XXVII (Continued)

Run No.	Capillary No.	Time, Hours	Solute Initial Conc., Molar	C/C_0	Solute Final Conc., Molar	\bar{C} , Molar	\sqrt{C}	$D \times 10^6$ cm ² sec ⁻¹
T-7	6	144	0.100	0.428	0.043	0.072	0.268	2.07
	7		0.100	0.472	0.047	0.074	0.272	1.77
	8		0.100	0.510	0.051	0.076	0.276	1.52

TABLE XXVIII

Experimental Data

Effect of Strontium on Diffusion of Uranium

Temp. = 25 °C, \pm 0.01 °C

Solute = 1.5 M Uranyl, 0.2 g/L Strontium Nitrate, 1.0 M Nitric Acid

Run No.	Capillary No.	Time, Hours	Solute Initial Conc., Molar	C/C ₀	Solute Final Conc., Molar	\bar{C} , Molar	\sqrt{C}	D x 10 ⁶ cm ² sec ⁻¹
Sr 1	5	40	1.5	0.415	0.623	1.062	1.031	7.88
	6		1.5	0.468	0.702	1.101	1.049	6.41
	7		1.5	0.387	0.581	1.041	1.021	8.70
	8		1.5	0.380	0.570	1.035	1.017	8.90
Sr 4	5	40	1.5	0.410	0.615	1.058	1.029	8.01
	6		1.5	0.482	0.723	1.112	1.055	6.07
	7		1.5	0.420	0.630	1.065	1.032	7.73
	8		1.5	0.399	0.599	1.050	1.025	8.31

Solute = 1.5 M Uranyl Nitrate, 0.2 g/L Strontium Nitrate, 1.0 M Nitric Acid
Solvent = 1.0 Nitric Acid

Sr 3	1	48	1.5	0.388	0.582	1.041	1.020	7.32
	2		1.5	0.507	7.61	1.131	1.063	4.57
	3		1.5	0.423	0.635	1.068	1.033	6.35
	4		1.5	0.405	0.608	1.054	1.027	6.86

TABLE XXVIII (Continued)

Solute = 1.5 M Uranyl Nitrate, 0.2 g/L Strontium Nitrate, 1.0 M Nitric Acid
 Solvent = 1.0 M HNO₃, 0.2 g/L Strontium Nitrate

Run No.	Capillary No.	Time, Hours	Solute Initial Conc., Molar	C/C ₀	Solute Final Conc., Molar	\bar{C} , Molar	\bar{C}	D x 10 ⁶ cm ² sec ⁻¹
Sr 2	1	48	1.5	0.392	0.588	1.044	1.022	7.12
	2		1.5	0.471	0.707	1.104	1.051	5.25
	3		1.5	0.388	0.582	1.041	1.020	7.20
	4		1.5	0.400	0.600	1.050	1.025	6.91

TABLE XXIX

Average Liquid Scintillation Counting
Rate as a Function of Uranium
Concentration

Spectrophotometric Concentration, Molar	Average Scintillation Count Rate CPM	Estimate of Sample Standard Deviation, Per cent
0.05	77.6	2.83
0.104	148.3	0.90
0.505	670.0	0.80
1.006	1345.5	1.11
1.042	1367.3	2.61
1.091	1432.1	2.98
1.133	1514.1	0.72
1.243	1640.9	0.87
1.415	1808.6	0.99
1.553	2076.8	1.74
1.883	2329.4	0.60
2.087	2732.2	1.02

APPENDIX B

Table XXX
 Calibration of 0.5 mm Bore Capillary
 Measurements made at 25 °C

Tubing Section Number	Mercury Thread Length, inches	Standard Deviation
1	0.20509	± 0.00001
2	0.20519	± 0.00002
3	0.20518	± 0.00001
4	0.20513	± 0.00001
5	0.20518	± 0.00002
6	0.20504	± 0.00001
7	0.20531	± 0.00002
8	0.20513	± 0.00002
9	0.20513	± 0.00002
Average	0.20516	± 0.00013

Ratio maximum diameter to average diameter = 1.0011

Ratio minimum diameter to average diameter = 1.0002

Diameter of capillary sections varied ± 0.056%

Capillary Number	Length, cm.	Standard Deviation, %	Volume, lambda	Standard Deviation, %
I - 1	2.0450	0.020	4.2600	0.50
I - 2	2.0540	0.050	4.1170	0.40
I - 3	2.0590	0.020	4.4270	0.60
I - 4	2.0610	0.050	4.4640	0.30
II - 1	2.0450	0.030	4.1910	0.50
II - 2	2.0310	0.040	3.9330	0.40
II - 3	2.0550	0.020	4.4120	0.33
III - 1	2.2160	0.020	4.3510	0.90
III - 2	2.0570	0.025	4.4270	0.50
III - 3	2.1740	0.030	4.2690	1.80
III 0 4	2.1890	0.050	4.2990	1.00

Specific volume Hg at 25 °C = 0.0738888 ml/g.

TABLE XXXI

Calibration of 0.75 mm Bore Capillary
Measurements made at 25 °C

Tubing Section Number	Mercury Thread Length, inches	Standard Deviation
1	0.76095	± 0.00003
2	0.76400	± 0.00002
3	0.76030	± 0.00001
4	0.76290	± 0.00002
5	0.76100	± 0.00002
6	0.75903	± 0.00001
7	0.76240	± 0.00002
Average	0.76151	± 0.00204

Ratio maximum diameter to average diameter = 1.00133

Ratio minimum diameter to average diameter = 0.99866

Diameter of capillary sections varied ± 0.133%

Capillary Number	Length, cm.	Standard Deviation, %	Volume, lambda	Standard Deviation
1	2.0559	0.037	9.0514	0.00
2	2.0297	0.050	9.2546	0.50
3	2.0411	0.024	8.6413	0.50
4	2.0538	0.049	9.0809	0.20
5	2.0444	0.024	9.2065	0.00
6	2.0335	0.024	0.0883	0.60
7	2.0439	0.024	9.2065	0.10
8	2.0427	0.024	8.6332	0.05
9	2.0066	0.010	8.8954	0.10
10	2.0137	0.010	8.8673	0.05
11	2.0159	0.012	8.6900	0.15
12	2.0185	0.010	8.6686	0.10
13	1.9979	0.008	8.9456	0.05
14	2.0251	0.010	9.0335	0.10

Specific volume of Hg at 25 °C = 0.0738888 ml/g.

TABLE XXXII

Calibration of Hamilton 10 λ Micro-Syringe
Measurements at 25 °C

Trial Number	Weight 4 λ Hg, gms.	Average weight 4 λ Hg.
1	0.0525	
2	0.0530	
3	0.0522	
4	0.0520	
5	0.0517	
6	0.0526	

0.05233 \pm .0004

Specific volume of Hg at 25 °C = 0.0738888 ml/g.

4 λ volume of micro-syringe = 3.866 \pm .03

TABLE XXXIII

Viscosities of Solutions

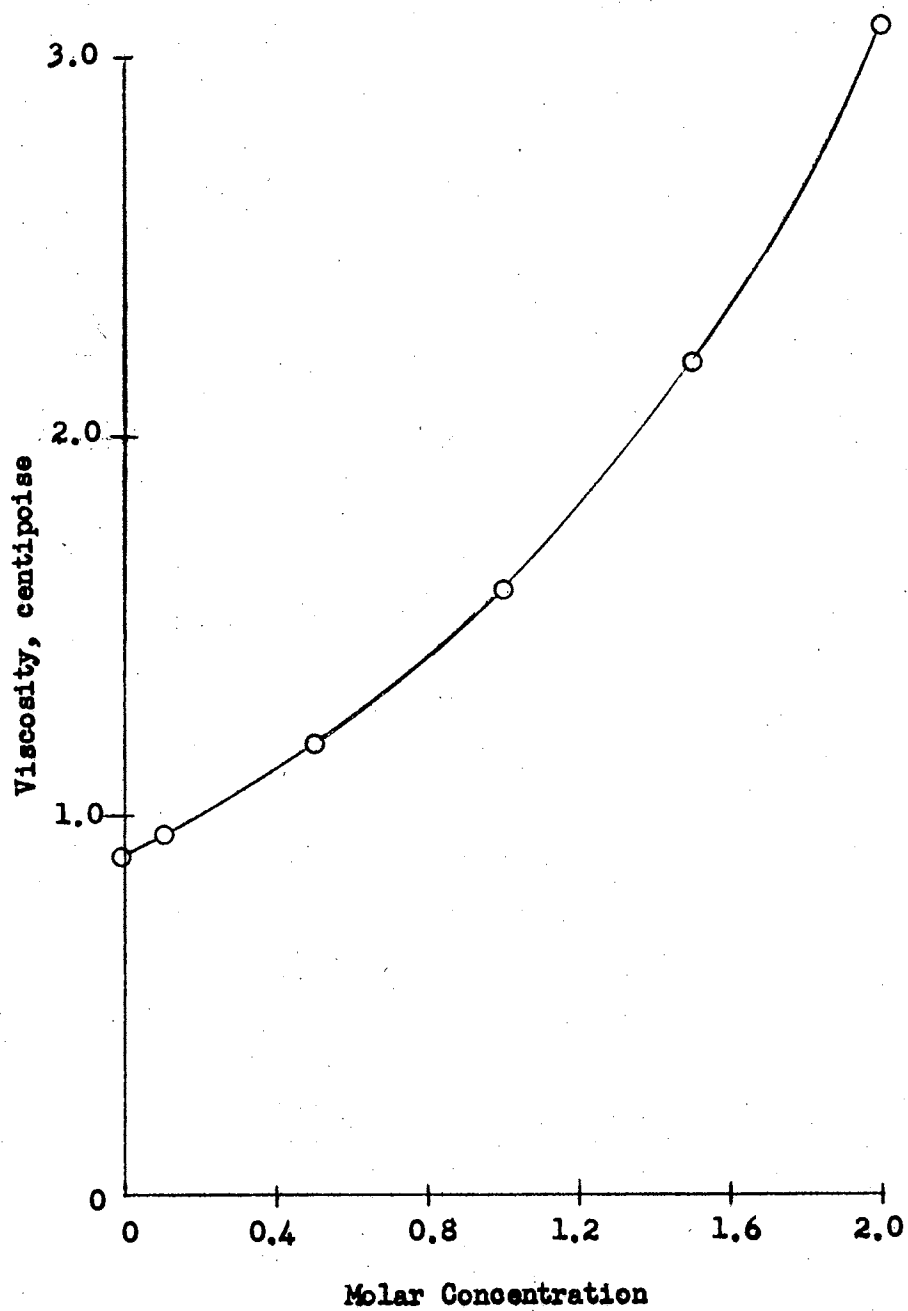
Temp. = 25 °C

Solution	Ostwald Tube No.	Number of Determinations	Average Flow Time, Sec.	Deviation, %	Viscosity, Centipoise
Distilled water	1	4	97.8	0.15	0.8937
Distilled water	2	4	104.0	0.06	0.8937
0.1 M $\text{UO}_2(\text{NO}_3)_2$	1	5	101.3	0.73	0.955
0.5 M $\text{UO}_2(\text{NO}_3)_2$	2	5	119.9	0.11	1.197
1.0 M $\text{UO}_2(\text{NO}_3)_2$	1	5	132.3	0.09	1.602
1.5 M $\text{UO}_2(\text{NO}_3)_2$	2	5	172.4	0.07	2.205
2.0 M $\text{UO}_2(\text{NO}_3)_2$	1	5	205.2	0.09	3.090
0.1 M HNO_3	1	5	97.8	0.12	0.899
0.5 M HNO_3	2	5	104.5	0.18	0.919
1.0 M HNO_3	1	5	97.4	0.02	0.927
1.5 M HNO_3	2	5	104.3	0.05	0.947
2.0 M HNO_3	2	5	98.6	0.17	0.968
4.0 M HNO_3	1	5	96.9	0.10	0.996

TABLE XXXIII (Continued)

Solution	Ostwald Tube No.	Number of Determinations	Average Flow Time, Sec.	Deviation, %	Viscosity, Centipoise
30% TBP-Amsco (Water Saturated)	2	5	261.8	0.28	1.835
0.454 M $\text{UO}_2(\text{NO}_3)_2$ 30% TBP-Amsco	1	3	395.4	0.26	3.483

Figure 19
Viscosity as a Function of
Concentration
(Uranyl Nitrate)



APPENDIX C

TABLE XXXIV

Data for Least Mean Square Regression of Liquid Scintillation
Integral Counting Rate as a Function of Uranium Concentration

Spectrophotometer Determination of Uranium Conc., Molar	Liquid Scintillation Integral Count Rate CPM	Average Scintillation Count Rate CPM	Average Count Rate Standard Error, Per cent	Regression Model			
				Y = A + BX		Y = BX	
				Calculated Count Rate	Deviation from Average	Calc. Count Rate	Deviation from Average
0.00	44.0	43.5	2.83	20.43	- 7.14		
0.00	43.0						
0.00	42.6						
0.00	44.0						
0.05	75.4	77.6	2.83	103.74	+33.69	64.68	-16.65
0.05	79.8						
0.1042	147.9	148.3	0.90	172.37	+16.23	134.79	- 9.11
0.1042	146.9						
0.1042	145.1						
0.1042	145.5						
0.1042	150.9						
0.1042	153.5						
0.2500	325.0	325.0	0.0	356.99		323.40	- 0.49
0.2500	325.0						
0.5056	683.2	670.0	1.12	680.64	+ 1.59	654.05	- 238
0.5056	648.6						
0.5056	644.9						
0.5056	644.2						
0.5056	679.6						

TABLE XXXIV (Continued)

Spectrophotometer Determination of Uranium Conc., Molar	Liquid Scintillation Integral Count Rate CPM	Average Scintillation Count Rate CPM	Average Count Rate Standard Error, Per cent	Regression Model			
				Y = A + BX		Y = BX	
				Calculated Count Rate	Deviation from Average	Calc. Count Rate	Deviation from Average
0.5056	692.8						
0.5056	671.8						
0.5056	694.7						
1.006	1342.4	1345.5	1.11	1314.2	-2.33	1301.3	- 3.29
1.006	1331.1						
1.006	129.2						
1.006	1339.0						
1.006	1397.1						
1.006	1373.3						
1.042	1421.3	1367.3	2.61	1359.8	-0.55	1367.3	- 1.42
1.042	1380.7						
1.042	1299.8						
1.091	1507.8	1432.1	2.98	1421.9	-0.71	1411.3	- 1.45
1.091	1503.1						
1.091	1371.1						
1.091	1346.4						
1.133	1525.0	1514.1	0.72	1475.0	-2.58	1465.6	- 3.20
1.133	1503.1						
1.243	1666.9	1640.9	0.87	1614.3	-1.62	1607.9	- 2.01
1.243	1587.6						
1.243	1636.0						
1.243	1707.5						
1.243	1638.8						

TABLE XXXIV (Continued)

Spectrophotometer Determination of Uranium Conc., Molar	Liquid Scintillation Integral Count GPM	Average Scintillation Count Rate GPM	Average Count Rate Standard Error, Per cent	Regression Model			
				Y = A + BX		Y = BX	
				Calculated Count Rate	Deviation from Average	Calc. Count Rate	Deviation from Average
1.243	1621.7						
1.243	1627.5						
1.415	1794.1	1808.6	0.99	1832.1	+ 1.36	183.4	+ 1.21
1.415	1792.5						
1.415	1788.6						
1.415	1855.5						
1.415	1788.7						
1.415	1870.9						
1.415	1770.2						
1.553	1955.3	2076.8	1.74	2006.9	- 3.37	2008.9	- 3.27
1.553	2311.7						
1.553	2269.1						
1.553	2055.1						
1.553	1958.7						
1.553	2219.7						
1.553	1979.3						
1.553	2049.0						
1.553	1976.4						
1.553	2107.0						
1.553	1987.2						
1.553	2052.8						
1.883	2343.7	2329.4	0.60	2424.7	+ 4.09	2435.8	+ 4.57
1.883	2296.0						
1.883	2295.1						

TABLE XXXIV (Continued)

Spectrophotometer Determination of Uranium Conc., Molar	Liquid Scintillation Integral Count Rate CPM	Average Scintillation Count Rate CPM	Average Count Rate Standard Error, Per cent	Regression Model			
				Y = A + BX		Y = BX	
				Calculated Count Rate	Deviation from Average	Calc. Count Rate	Deviation from Average
1.883	2352.1						
1.883	2281.7						
1.883	2337.3						
1.883	2303.7						
1.883	2288.2						
1.883	2359.4						
1.883	2323.4						
1.883	2442.4						
2.087	2743.7	2732.2	1.02	2683.1	- 1.80	2699.7	- 1.19
2.087	2801.5						
2.087	2714.8						
2.087	2668.8						

TABLE XXXV

Uranyl Nitrate Activity Coefficients Conversions

Density (Gm/CC)	Molar	Gamma (Molar)	Molal	Gamma (Molal)	Activity
1.03152	0.09923	0.54715	0.10000	0.54300	0.05429
1.06258	0.19699	0.51981	0.20000	0.51200	0.10239
1.09317	0.29328	0.52168	0.30000	0.51000	0.15299
1.12331	0.38813	0.53382	0.40000	0.51800	0.20719
1.15300	0.48159	0.55440	0.50000	0.53400	0.26699
1.18225	0.57368	0.58046	0.60000	0.55500	0.33299
1.21110	0.66449	0.60888	0.70000	0.57800	0.40459
1.23953	0.75395	0.64513	0.80000	0.60800	0.48639
1.29516	0.92905	0.73084	1.00000	0.67900	0.67899
1.34924	1.09929	0.83071	1.20000	0.76100	0.91319
1.40182	1.26479	0.94640	1.40000	0.85500	1.19699
1.45300	1.42587	1.05815	1.60000	0.94300	1.50879
1.50278	1.58256	1.23179	1.80000	1.08300	1.94939
1.55124	1.73509	1.40395	2.00000	1.21800	2.43599
1.66698	2.09942	1.90766	2.50000	1.60200	4.00499
1.77550	2.44100	2.45799	3.00000	2.00000	5.99999
1.87753	2.76216	3.00308	3.50000	2.37000	8.29499
1.97356	3.06440	3.44601	4.00000	2.64000	10.55999
2.06418	3.34963	3.82877	4.50000	2.85000	12.82499
2.14974	3.61897	4.15863	5.00000	3.01000	15.04999
2.23071	3.87382	4.54331	5.50000	3.20000	17.59999

Figure 20

Activity and Activity Coefficient of
Uranyl Nitrate as a Function
of Molar Concentration

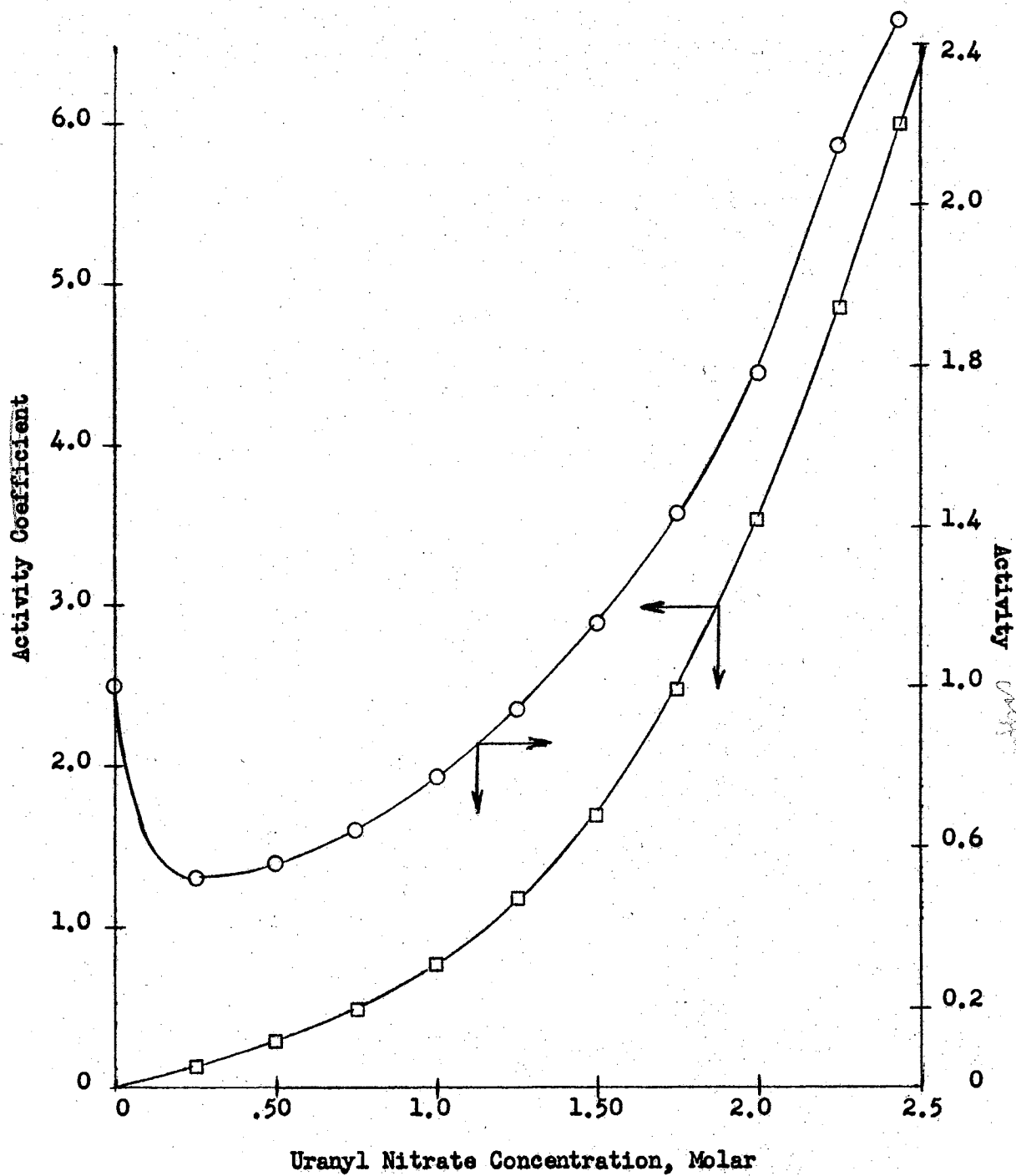


TABLE XXXVI

Thermodynamic Correction Factor
as a
Function of Uranyl Nitrate Concentration
(Coarse Grid)

Molar Concentration	Thermodynamic Correction Factor
0.20000	0.96418
0.30000	1.05105
0.40000	1.14437
0.50000	1.22217
0.60000	1.34381
0.70000	1.44646
0.80000	1.53571
0.90000	1.66850
1.00000	1.77274
1.10000	1.85289
1.20000	1.96974
1.30000	2.08861
1.40000	2.14473
1.50000	2.22589
1.60000	2.37770
1.70000	2.48200
1.80000	2.56656
1.90000	2.61522
2.00000	2.57628
2.10000	2.63712
2.20000	2.64644
2.30000	2.60870

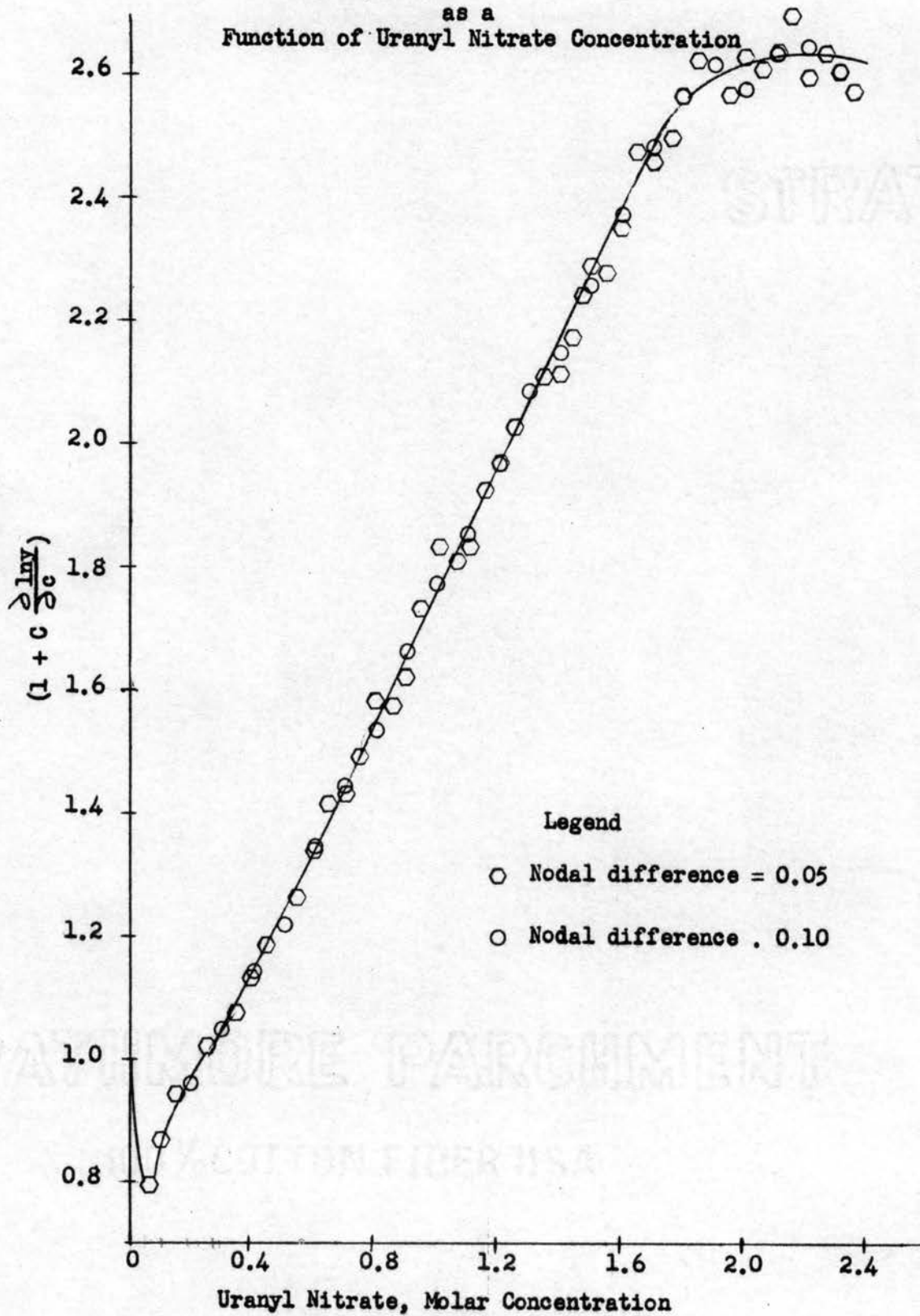
TABLE XXXVII

Thermodynamic Correction Factor
as a
Function of Uranyl Nitrate Concentration
(Fine Grid)

Concentration, Molar	Thermodynamic Correction Factor	Concentration, Molar	Thermodynamic Correction Factor
0.00000	1.00000	1.20000	1.95414
0.05000	0.79191	1.25000	2.03123
0.10000	0.87027	1.30000	2.09775
0.15000	0.94338	1.35000	2.11742
0.20000	0.96554	1.40000	2.15534
0.25000	1.02392	1.45000	2.17103
0.30000	1.05736	1.50000	2.29390
0.35000	1.07909	1.50000	2.28172
0.40000	1.14871	1.60000	2.35577
0.45000	1.18872	1.65000	2.47710
0.50000	1.21431	1.70000	2.45874
0.55000	1.26834	1.75000	2.48455
0.60000	1.33653	1.80000	2.56097
0.65000	1.41742	1.85000	2.62820
0.70000	1.42641	1.90000	2.62790
0.75000	1.49748	1.95000	2.56632
0.80000	1.58752	2.00000	2.63241
0.85000	1.57628	2.05000	2.60975
0.90000	1.62786	2.10000	2.63719
0.95000	1.73897	2.15000	2.70023
1.00000	1.83974	2.20000	2.59105
1.05000	1.80809	2.25000	2.63879
1.10000	1.82686	2.30000	2.60109
1.15000	1.92366	2.35000	2.57572

Figure 21

Thermodynamic-Correction Factor
as a
Function of Uranyl Nitrate Concentration



Calculation of Nernst Limiting Values

Harned and Owen (22) discuss the method of obtaining a limiting equation for the diffusion coefficients of a single salt. From the Onsager-Fuoss theory for dilute solution it is shown that the limiting equation is

$$D = D_0 - \mathcal{S}_{(D)} \sqrt{C}$$

where

$$\mathcal{S}_{(D)} = \frac{1.3273 \times 10^{-3} (\sum v_i z_i^2)^{3/2}}{D^{3/2} T^{1/2}} \frac{v_1 |z_1|}{\left[\frac{\lambda_1^{\circ} \lambda_2^{\circ}}{\Lambda^{\circ}} \right]} + \frac{2.604 \times 10^8 (\sum v_i z_i^2)^{1/2}}{\eta_0 D^{1/2} T^{-1/2}} \frac{|z_2| \lambda_1^{\circ} - |z_1| \lambda_2^{\circ}}{\left[\frac{|z_1| \lambda_2^{\circ}}{\Lambda^{\circ}} \right]^2}$$

and

$$D_0 = 8.936 \times 10^{-10} T \frac{(v_1 + v_2)}{v_1 |z_1|} \left[\frac{\lambda_1^{\circ} \lambda_2^{\circ}}{\Lambda^{\circ}} \right]$$

The quantities in the equation are:

v_i = number of cations, anions produced by disassociation of one molecule of electrolyte.

z_i = valences of ions indicated (carry sign of charge)

λ_i° = limiting equivalent conductances of ions indicated at infinite dilution.

Λ° = limiting equivalent conductance of electrolyte at infinite dilution

η_0 = viscosity of solvent

D = dielectric constant of solution

Designating the nitrate ion as 1 and the uranyl ion as 2, the values for uranyl nitrate are found to be:

$$V_1 = 1.0$$

$$V_2 = 2.0$$

$$Z_1 = 2.0$$

$$\lambda_1^{\circ} = \frac{30.9 + 32.0}{2} = 31.45 \quad (15,19)$$

$$\lambda_2^{\circ} = 71.44$$

$$\Lambda^{\circ} = \lambda_1^{\circ} + \lambda_2^{\circ} = 31.45 + 71.44 = 102.89$$

$$T = 25 \text{ }^{\circ}\text{C} = 298 \text{ }^{\circ}\text{K}$$

$$D = 80 - 0.4(t - 20^{\circ}) = 80 - 0.4(25-20) = 80 - 2.0 = 78.0 \quad (48)$$

$$\eta_0 = .008903 \text{ poise}$$

$$D_0 = 8.936 \times 10^{-10} (298) \frac{3}{2.0} \frac{(31.45)(71.44)}{102.89}$$

$$= 8.936 \times 10^{-10} (9.761 \times 10^3) = 8.722 \times 10^{-6}$$

$$D_0 = 8.722 \times 10^{-6} \text{ cm}^2 \text{ sec}^{-1}$$

thus:

$$\begin{aligned} \mathcal{S}_{(D)} &= \frac{1.3273 \times 10^{-3}}{(78)^{3/2} (298)^{1/2}} \frac{[(1.0)(4.0) + (2.0)(1.0)]^{3/2}}{(1.0)(2.0)} \frac{[(31.45)(71.44)]}{102.89} \\ &+ \frac{2.604 \times 10^{-8}}{(.8903)(78)^{1/2} (298)^{-1/2}} \frac{(6.0)^{1/2}}{2.0} \frac{[(1.0)(31.45) - (2.0)(71.44)]^2}{102.89} \\ &= 8.2024 \times 10^7 (21.815) + 7.002 \times 10^{-8} (1.082) \end{aligned}$$

$$\mathcal{S}_{(D)} = 17.968 \times 10^{-6}$$

and finally the limiting expression for a dilute solution of uranyl nitrate

is

$$D = 8.722 \times 10^{-6} - 17.968 \times 10^{-6} \sqrt{C}$$

These calculated values may vary, somewhat, depending on the data source of the limiting conductance values chosen for the ions.

Computer Program for Formal Solution to
Fick's Second Law

Equation 6, the formal solution of Fick's Second Law with the boundary conditions for the capillary method may be simplified to

$$\frac{C_{Av.}}{C_0} = \frac{8}{\pi^2} \left[\sum_{n=0}^{\infty} \frac{e^{-(2n+1)^2 \theta}}{(2n+1)^2} \right]$$

where $\theta = \frac{\pi^2 D t}{4L^2}$

Expanding this expression to eight terms gives

$$\frac{C_{Av.}}{C_0} = \frac{8}{\pi^2} \left[\frac{e^{-1\theta}}{1} + \frac{e^{-9\theta}}{9} + \frac{e^{-25\theta}}{25} + \frac{e^{-49\theta}}{49} \right. \\ \left. + \frac{e^{-81\theta}}{81} + \frac{e^{-121\theta}}{121} + \frac{e^{-169\theta}}{169} + \frac{e^{-225\theta}}{225} \right]$$

The program was designed to calculate $C_{Av.}/C_0$ as a function of θ , employing up to eight terms or until the difference between two successive terms was 0.0001 or less. The argument, θ , was incremented by 0.0001 units and a table was made of C/C_0 for each value of θ . The symbols used in the programming were as follows:

ARG = argument, θ

KK = total number of arguments desired

DA = argument incrementation

R = C/C_0

TERM = exponential function common to each series term

CONV = convergence of series

IBM 650 Source Program of a
Formal Solution of Fick's Second Law

```
000000READ, ARG, KK, DA
000000DIMENSIONR(2,3)
000020D044J=1, KK
000460D043K=1, 3
000030ARG=ARG+DA
000040TERMO=EXPEF(-ARG)
000050TERM1=(TERMO**9)/9.0
000060CONV1=TERMO+TERM1
000070IF(ABSF(TERMO-CONV1)-.0001)8,
0000718, 10
000080CONVT=CONV1
000090GOTO47
000100TERM2=(TERMO**25)/25.0
000110CONV2=CONV1+TERM2
000120IF(ABSF(CONV2-CONV1)-.0001)13
000121, 13, 15
000130CONVT=CONV2
000140GOTO47
000150TERM3=(TERMO**49)/49.0
000160CONV3=CONV2+TERM3
000170IF(ABSF(CONV3-CONV2)-.0001)18
000171, 18, 20
000180CONVT=CONV3
000190GOTO47
000200TERM4=(TERMO**81)/81.0
000210CONV4=CONV3+TERM4
000220IF(ABSF(CONV4-CONV3)-.0001)23
000221, 23, 25
000230CONVT=CONV4
000240GOTO47
000250TERM5=(TERMO**121)/121.0
000260CONV5=CONV4+TERM5
000270IF(ABSF(CONV5-CONV4)-.0001)28
000271, 28, 30
000280CONVT=CONV5
000290GOTO47
000300TERM6=(TERMO**169)/169.0
000310CONV6=CONV5+TERM6
000320IF(ABSF(CONV6-CONV5)-.0001)33
000321, 33, 35
000330CONVT=CONV6
000340GOTO47
000350TERM7=(TERMO**225)/225.0
000360CONV7=CONV6+TERM7
000370IF(ABSF(CONV7-CONV6)-.0001)38
000371, 38, 40
000380CONVT=CONV7
000390GOTO47
000400TERM8=(TERMO**289)/289.0
000410CONV8=CONV7+TERM8
000420CONVT=CONV8
```

IBM 650 Source Program (Continued)

```
000470R(2,K)=ARG
000430R(1,K)=CONVT*(8.00/3.1416**2)
000440PUNCH,R(1,1),R(2,1),R(1,2),R(
0004412,2),R(1,3),R(2,3)
000450END
```

TABLE XXXVIII

Sample of Formal Solution Output Table

C/C_0	θ	C/C_0	θ	C/C_0	θ
.41002033	.68200000	.40997919	.68210000	.40993803	.68220000
.40989688	.68230000	.40985574	.68240000	.40981460	.68250000
.40977347	.68260000	.40973234	.68270000	.40969121	.68280000
.40965009	.68290000	.40960898	.68300000	.40956786	.68310000
.40952675	.68320000	.40948564	.68330000	.40944454	.68340000
.40940345	.68350000	.40936236	.68360000	.40932127	.68370000
.40928018	.68380000	.40923912	.68390000	.40919804	.68400000
.40915697	.68410000	.40911589	.68420000	.40907484	.68430000
.40903378	.68440000	.40899273	.68450000	.40895167	.68460000
.40891064	.68470000	.40886959	.68480000	.40882855	.68490000
.40878752	.68500000	.40874649	.68510000	.40870546	.68520000
.40866444	.68530000	.40862344	.68540000	.40858242	.68550000
.40854141	.68560000	.40850042	.68570000	.40845942	.68580000
.40841842	.68590000	.40837743	.68600000	.40833645	.68610000
.40829546	.68620000	.40825449	.68630000	.40821352	.68640000
.40817254	.68650000	.40813158	.68660000	.40809062	.68670000
.40804966	.68680000	.40800870	.68690000	.40796776	.68700000
.40792682	.68710000	.40788588	.68720000	.40784494	.68730000
.40780401	.68740000	.40776308	.68750000	.40772217	.68760000
.40768125	.68770000	.40764033	.68780000	.40759943	.68790000
.40755852	.68800000	.40751762	.68810000	.40747672	.68820000
.40743583	.68830000	.40739494	.68840000	.40735405	.68850000
.40731317	.68860000	.40727230	.68870000	.40723143	.68880000
.40719056	.68890000	.40714970	.68900000	.40710883	.69810000
.40706798	.68920000	.40702713	.68930000	.40698630	.68940000
.40694545	.68950000	.40690461	.68960000	.40686378	.68970000
.40782294	.68980000	.40678212	.68990000	.40674130	.69000000
.40670048	.69010000	.40665967	.69020000	.40661887	.69030000
.40657806	.69040000	.40653726	.69050000	.40649646	.69060000
.40645567	.69070000	.40641488	.69080000	.40637410	.69090000
.40633332	.69100000	.40629254	.69110000	.40625178	.69120000
.40621101	.69130000	.40617025	.69140000	.40612950	.69150000
.40608874	.69160000	.40604798	.69170000	.40600724	.69180000
.40596650	.69190000	.40592577	.69200000	.40588503	.69210000
.40584430	.69220000	.40580357	.69230000	.40576286	.69230000
.40572214	.69250000	.40568143	.69260000	.40564072	.69270000
.40560001	.69280000	.40555932	.69290000	.40551863	.69300000
.40547794	.69310000	.40543725	.69320000	.40539657	.69330000
.40535589	.69340000	.40531522	.69350000	.40527454	.69360000
.40523388	.69370000	.40519321	.69380000	.40515256	.69390000
.40511190	.69400000	.40507125	.69410000	.40503061	.69420000
.40498997	.69430000	.40494934	.69440000	.40490870	.69450000
.40486807	.69460000	.40482744	.69470000	.40478684	.69480000
.40474622	.69490000	.40470561	.69500000	.40466500	.69510000
.40462440	.69520000	.40458380	.69530000	.40454321	.69540000

Sample Calculation of Diffusion Coefficient
Employing Formal Solution

As an example of the method employed, consider the data obtained from a typical experimental run.

Run No. 26
 Temp. = 25 °C, ± .01 °C
 Diffusion time = 40 hrs = 1.44 x 10⁵ sec
 Solute = Uranyl Nitrate
 Solvent = Water

Capillary No.	Capillary Volume.	Capillary Length, cm.	Standard Initial Solute, CPM	Final Capillary Solute CPM	Nominal Initial Conc., Molar
1B	9.0514	2.0559	617.8	611.7	0.5
4B	9.0809	2.0538	1329.2	1241.4	1.0
5B	9.2065	2.0444	1888.8	1685.6	1.5
7B	9.2065	2.0439	2562.8	2300.0	2.0

Volume of standard sample = 3.866 lambda

$$R_{1B} = \frac{(611.7)(3.866)}{(617.8)(9.0514)} = 0.42289$$

$$R_{4B} = \frac{(1241.4)(3.866)}{(1329.2)(9.0809)} = 0.39760$$

$$R_{5B} = \frac{(1685.6)(3.866)}{(1888.8)(9.2065)} = 0.37474$$

$$R_{7B} = \frac{(2300.0)(3.866)}{(2562.8)(9.2065)} = 0.37685$$

Consult the table of R as a function of θ for each calculated value ratio.

$$\theta = \frac{\pi^2 Dt}{4l^2}$$

then

$$D = \frac{0.49^2}{\pi^2 t}$$

thus for

$$R_{1B}, \theta_{1B} = 0.6512$$

$$R_{4B}, \theta_{4B} = 0.7126$$

$$R_{5B}, \theta_{5B} = 0.7717$$

$$R_{7B}, \theta_{7B} = 0.7661$$

and

$$D_{1B} = \frac{(0.6512)(0.40529)(4.2267)}{1.44 \times 10^5} = 7.747 \times 10^{-6}$$

$$D_{4B} = \frac{(0.7126)(0.40529)(4.2181)}{1.44 \times 10^5} = 8.460 \times 10^{-6}$$

$$D_{5B} = \frac{(0.7717)(0.40529)(4.1796)}{1.44 \times 10^5} = 0.078 \times 10^{-6}$$

$$D_{7B} = \frac{(0.7661)(0.40529)(4.1775)}{1.44 \times 10^5} = 9.007 \times 10^{-6}$$

Numerical Method Solution of
Fick's Second Law

In binary systems, under circumstances that would lead to the conclusion that the diffusivity of the system would be concentration dependent, Fick's Second Law (Equation 4) is

$$\frac{\partial C}{\partial t} = \frac{\partial}{\partial x} \left[D \frac{\partial C}{\partial x} \right]$$

In order to adequately express the dependence of D on concentration, the following general expression for D was assumed,

$$D = A + BC^P + EC^Q + UC^R + VC^S$$

The quantity A was taken as the Nernst limiting diffusion coefficient for dilute solutions, while the exponent P was to be taken as 0.5. The other coefficients and exponents to be determined by the results of the numerical solution agreeing with the experimentally measured final concentration in the capillaries.

The following substitutions were made:

$$D = D_0 (1 - bC^P + eC^Q - uC^R + vC^S)$$

$$D_0 = A$$

$$b = \frac{B}{A}$$

$$u = \frac{U}{A}$$

$$e = \frac{E}{A}$$

$$v = \frac{V}{A}$$

$$C' = \frac{C}{C_0}$$

$$X' = \frac{X}{L}, \text{ where } L = \text{capillary length, cm.}$$

$$T = \frac{D_o t}{L^2}, \text{ where } t = \text{diffusion time, sec.}$$

Making these substitutions in the above equation yields the result

$$\frac{C_o \partial C'}{L^2/D_o \partial T} = \frac{\partial}{L \partial X'} D_o (1 - bC'^P C_o^P + eC'^Q C_o^Q - uC'^R C_o^R + vC'^S C_o^S) \left(\frac{C_o \partial C'}{L \partial X'} \right)$$

Simplifying and, since the transformation is complete, dropping the prime notation, then

$$\frac{\partial C}{\partial T} = \frac{\partial}{\partial X} (1 - bC^P C_o^P + eC^Q C_o^Q - uC^R C_o^R + vC^S C_o^S) \left(\frac{\partial C}{\partial X} \right)$$

Performing the indicated partial differential yields

$$\begin{aligned} \frac{\partial C}{\partial T} = & (1 - bC^P C_o^P + eC^Q C_o^Q - uC^R C_o^R + vC^S C_o^S) \left(\frac{\partial^2 C}{\partial X^2} \right) \\ & - (PbC^{P-1} C_o^P + QeC^{Q-1} C_o^Q - uRC^{R-1} C_o^R + vSC^{S-1} C_o^S) \left(\frac{\partial C}{\partial X} \right)^2 \end{aligned}$$

In order to make the equation a little more amenable to programming for a digital computer, the following substitutions were made

$$\begin{aligned} F &= bC_o^P = \frac{B}{A} C_o^P & H &= uC_o^R = \frac{U}{A} C_o^R \\ G &= eC_o^Q = \frac{E}{A} C_o^Q & W &= vC_o^S = \frac{V}{A} C_o^S \end{aligned}$$

and the equation becomes

$$\begin{aligned} \frac{\partial C}{\partial T} = & (1 - FC^P + GC^Q + HC^R + WC^S) \left(\frac{\partial^2 C}{\partial X^2} \right) \\ & - (PFC^{P-1} + QGC^{Q-1} - HRC^{R-1} + WSC^{S-1}) \left(\frac{\partial C}{\partial X} \right)^2 \end{aligned}$$

Finite difference methods were applied to this equation by employing

forward differences for the derivatives with respect to T and central differences for the derivatives with respect to distance.

Denoting the increment in distance as i and the increment in time as j, the following difference expressions were used:

$$\left(\frac{\partial C}{\partial X}\right)^2 = \frac{C_{i+1,j}^2 - 2C_{i+1,j}C_{i-j} + C_{i-1,j}^2}{4(\Delta X)^2}$$

$$\frac{\partial^2 C}{\partial X^2} = \frac{C_{i+1,j} - 2C_{i,j} + C_{i-1,j}}{(\Delta X)^2}$$

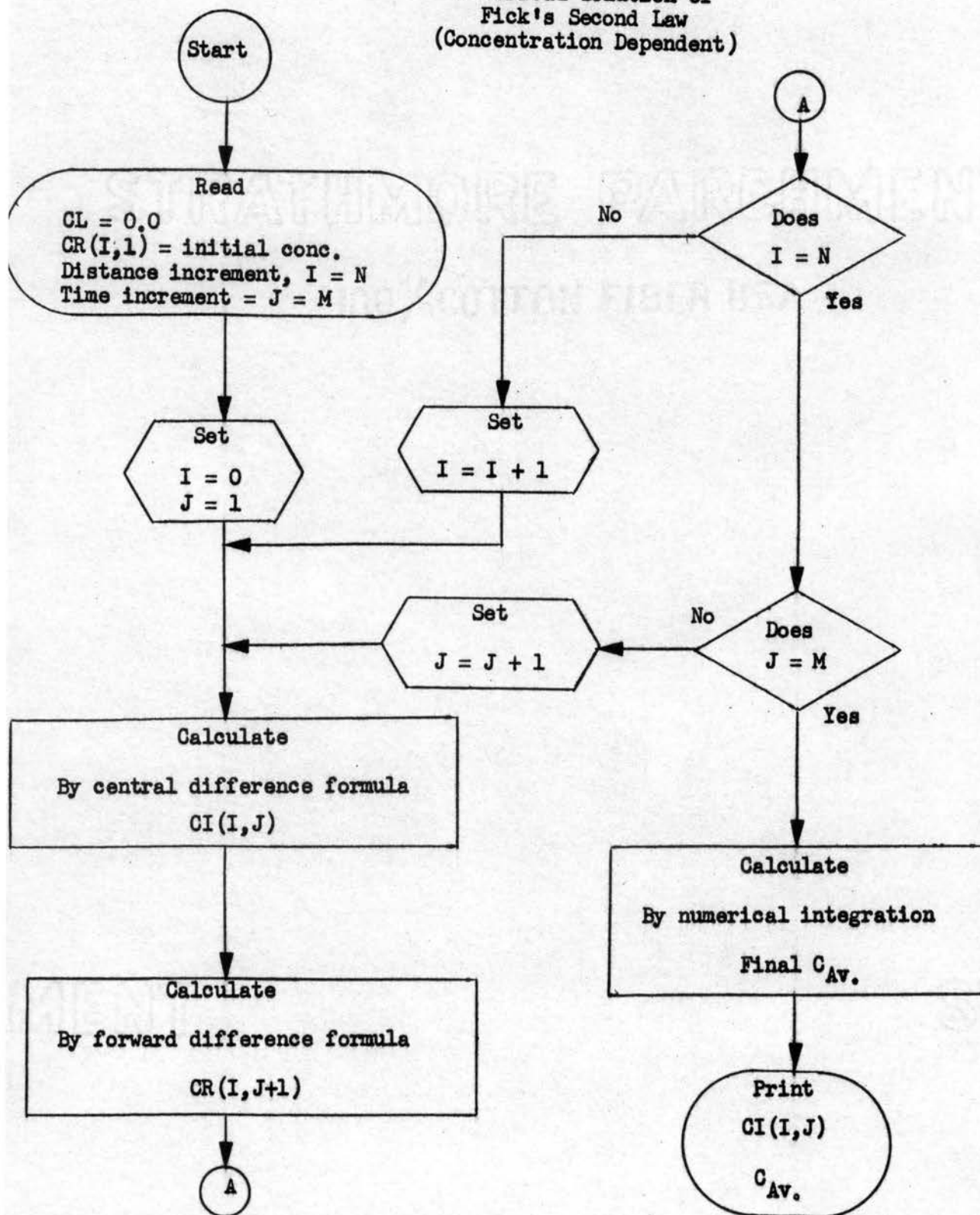
Substituting these expressions into and solving for the concentration of the i, j+1 increment results in

$$C_{i,j+1} = \frac{\Delta T}{(\Delta X)^2} \left[(1 - FC^P + GC^Q - HC^R + WC^S)(C_{i+1,j} - 2C_{i,j} + C_{i-1,j}) \right. \\ \left. - (PFC_i^{P-1} + QGC_i^{Q-L} - HRC_i^{R-1} + WSC_i^{S-1}) \right. \\ \left. \frac{(C_{i+1,j}^2 - 2C_{i+1,j}C_{i-1,j} + C_{i-1,j}^2)}{4} \right] + C_{i,j}$$

This is the equation that was programmed to obtain the final concentration distribution across the length of the capillary.

Figure 22

Flow Diagram
Numerical Solution of
Fick's Second Law
(Concentration Dependent)



Computer Program for the Numerical
Solution of Fick's Second Law

In programming the numerical solution of Fick's Second Law, the following symbols were used:

CL = preceding concentration increment

CI = central concentration increment

CR = proceeding concentration increment

N = number of distance increments

M = number of time increments

L = length of capillary, cm.

CO = initial capillary concentration

DELX = length increment

P = first concentration term exponent

Q = second concentration term exponent

R = third concentration term exponent

S = fourth concentration term exponent

DELT = time increment = $D_0 t / L^2$

A = first term coefficient in D

B = second term coefficient in D

E = third term coefficient in D

U = fourth term coefficient in D

V = fifth term coefficient in D

The numerical solution calculated a concentration profile across the capillary by central differences for an increment of time, set these values as preceding values and obtained the next time increment values by forward difference. Thus, the program was two dimensional -

one in distance, the other dimension was time. The final calculated concentration distribution was used to obtain an average value by numerical integration. The mathematical model for D was varied until the calculated average concentrations over the range of concentrations studied agreed with the experimentally measured concentrations.

IBM 7090 Source Program for Numerical Solution of Fick's Second Law With a Concentration Dependent Diffusion Coefficient

```

*      XEQ
*      LIST 8
*      LABEL
CFIX  NUMERICAL SOLUTION OF FICKS 2ND LAW
      DIMENSION CL(52), CI(52), CR(52)
      READ INPUT TAPE 5, 77, NCASE
77    FORMAT(14)
      DO 100 IXX=1, NCASE
      READ INPUT TAPE 5, 1, N, M, L
1     FORMAT(13, 14, 13)
      READ INPUT TAPE 5, 25, CO, DELX, P, Q, R, S
25    FORMAT(F10.5, F10.5, F10.5, F10.5, F10.5, F10.5)
      READ INPUT TAPE 5, 26, DELT, A, B
26    FORMAT(E15.5, E15.5, E15.5)
      READ INPUT TAPE 5, 26, E, U, V
      WRITE OUTPUT TAPE 6, 102, N, M, L
102   FORMAT(1H, 13, 14, 13)
      WRITE OUTPUT TAPE 6, 103, CO, DELX, P, Q, R, S
103   FORMAT(1H, F10.5, F10.5, F10.5, F10.5, F10.5, F10.5)
      WRITE OUTPUT TAPE 6, 106, DELT, A, B
106   FORMAT(1H, E15.5, E15.5, E15.5)
      WRITE OUTPUT TAPE 6, 107, E, U, V
107   FORMAT(1H, E15.5, E15.5, E15.5/))
      CI(1) = 0.0
      NM = N+1
      NN = N+2
      DO 2 I = 2, NN
2     CI(1) = 1.0
      F=B*CO**P/A
      G=E*CO**Q/A
      H=U*CO**R/A
      W=V*CO**S/A
      CONST = DELT/(DELX**2)
      DO 9 J = 1, M
      DO 3 I = 2, NM
      X=(1.+F*CI(I)**P+G*CI(I)**Q+H*CI(I)**R+W*CI(I)**S)
      X=X*(CI(I+1)-2.0*CI(I)+CI(I-1))
      Y=(P*F*CI(I)**(P-1.)+Q*G*CI(I)**(Q-1.))
      Y=Y+(H*R*CI(I)**(R-1.)+W*S*CI(I)**(S-1.))
      Y=Y*(CI(I+1)**2-2.*CI(I+1)*CI(I-1)+CI(I-1)**2)/4.
3     CR(I)=CONST*(X+Y)+CI(I)
      CI(NN)=CI(N)
      DO 9 I = 2, NM
9     CI(I) = CR(I)
      DO 11 I = 2, NM
      K = I-1
      CL(I) = CR(I)*CO
11    WRITE OUTPUT TAPE 6, 104, K, CL(I)
104   FORMAT(1H, 2HC(,13,4H) = ,F10.5)
      A=0.0
      J=NM-2

```

IBM 7090 Source Program (Continued)

```
DO 15 I=3,J,2
15 A=4.*CL(I)+2.*CL(I+1)+A
  A=(A+CL(2)+CL(NM))*DELX/3.
  WRITE OUTPUT TAPE 6, 105, A
105 FORMAT(//,1H ,16HAVERAGE CONC. = ,F8.5,1H1)
100 CONTINUE
21 CALL EXIT
  END
  DATA
```

*
@

VITA

John Browning Finley

Candidate for the Degree of

Doctor of Philosophy

Thesis: DIFFUSION IN CONCENTRATED URANYL NITRATE SOLUTIONS

Major Field: Chemical Engineering

Biographical:

Personal Data: Born in Crowley, Louisiana, July 18, 1919, the son of John A. and Bess B. Finley. Married Katherine B. Finley of San Antonio, Texas in 1943. The couple has a family consisting of two boys and two girls.

Education: Attended grade school in Crowley, Louisiana; graduated in 1936 from Crowley High School; received the Bachelor of Science degree from the University of Southwestern Louisiana, with a major in Chemistry, in May, 1941; received the Bachelor of Science in Chemical Engineering from the University of Southwestern Louisiana in May, 1942; received the Master of Science degree from the University of Southwestern Louisiana, with a major in Chemical Engineering in May, 1960; completed the requirements for the Doctor of Philosophy degree in May, 1964.

Professional experience: A total of 16 years experience comprised of four years in chemical engineering research and development work for Humble Oil and Refining Company, two years of private practice in chemical engineering consulting, and ten years in various managerial capacities. Taught college-level courses in Chemical Engineering and General Engineering. At present, an associate professor in Chemical Engineering at the Texas College of Arts and Industries, Kingsville, Texas.